# Characterization of the Interferon αβ receptor knockout mouse model of Crimean-Congo hemorrhagic fever (CCHF) and assessment of Adenovirus based CCHF virus vaccine efficacy and correlates of protection

By

Marko Zivcec

A thesis submitted to the Faculty of Graduate Studies of

The University of Manitoba

in partial fulfilment of the requirements of the degree of

DOCTOR OF PHILOSOPHY

Department of Medical Microbiology

University of Manitoba

Winnipeg

ABSTRACT

Crimean-Congo hemorrhagic fever (CCHF) is an inflammatory disease caused by the tick-borne pathogen CCHF virus (CCHFV). CCHFV is widely distributed with a endemic area including central and western Asia, the Middle East, southeastern Europe and the African continent, and can be transmitted to humans directly by tick bite or by contact with body fluids of infected animals or people. Most animals, while susceptible to CCHFV infection, do not display disease signs following infection, therefore, the development of CCHF disease models has been severely hampered. The lack of disease models has resulted in a lack of characterization of disease progression and lack of evaluated clinical countermeasures. The aims of this study were to further characterize a recently reported small animal model, the interferon alpha/beta receptor knockout ($IFNAR^{-/-}$) mouse model of CCHF and to utilize this model to evaluate the protective efficacy of Adenovirus (Ad) vaccines as well as mechanisms of protection. To achieve the goals of the study hematological, coagulation, virological, pathological and cytokine/chemokine parameters of $IFNAR^{-/-}$ mice were assessed chronologically following CCHFV challenge. Vaccines were developed by construction of Ad expressing CCHFV nucleocapsid protein (Ad-NP) and glycoproteins (complete glycoprotein precursor Ad-GPC, and mature glycoproteins Ad-$G_N$ and Ad-$G_C$). $IFNAR^{-/-}$ mice were then evaluated for adaptive immune responses following Ad vaccination and then challenged with a lethal dose of CCHFV and monitored for survival. To determine the roles of humoral and cell mediated adaptive immune responses in protection against CCHFV, experiments using adoptive transfers of Ad vaccinated $IFNAR^{-/-}$ mice to naïve $IFNAR^{-/-}$ mice and depletion of B- and/or T-cells were undertaken. The results demonstrate that $IFNAR^{-/-}$ mice develop an inflammatory, lethal disease following CCHFV challenge that resembles human CCHF; Ad-NP and Ad-NP/Ad-GPC vaccinated $IFNAR^{-/-}$ mice are protected from CCHFV

challenge; and that humoral responses are essential for protection from CCHFV while T-cell responses are dispensable, at least in this vaccine platform, in this animal model. These studies provide the basis for more detailed work in vivo and suggest which mechanisms of protection may be important for subsequent advances in CCHFV vaccinology.

**ACKNOWLEDGEMENTS**

I am grateful to my supervisor, Dr. Heinz Feldmann, for providing an excellent opportunity to work on this interesting project. Heinz's mentorship style allowed me to learn how to conduct research independently and work with other world class investigators. I would also like to especially thank Drs. David Safronetz and Hideki Ebihara. Hideki was an important influence and source of knowledge and help prior to and initially during my graduate studies and helped me develop essential molecular biology skills. David was instrumental in efforts during the latter stages of my graduate work helping with all of my animal studies and, in combination with Heinz, improving my writing abilities by being an excellent editor.

I would like to thank Drs. Gary Kobinger and Darwyn Kobasa for funding and lab space during the first year of research. A special thanks goes out to everyone at Special Pathogens branch at the National Microbiology Lab for all their help, you guys are great.

To the department of Medical Microbiology, thank you for your support over the years and especially to Angela Nelson for all her help with all the administrative issues.

To everyone at the Laboratory of Virology at Rocky Mountain Labs (RML), thank you for helping so much over the years, both in and out of the lab. I would especially like to thank RML vet branch for teaching me animal handling and taking care of the animals; Dr. Shelly Robertson for her assistance with everything flow cytometry; Dr. Dana Scott for all the assistance with the pathology work; Kay Menk and Joyce Walczynski for their help with all things administrative, and Ricki Feldmann for the BSL-4 training and assistance.

Thanks to my committee Drs. Xi Yang and Daniel Gietz for their assistance and recommendations over the years, and for reading the thesis. Lastly, I would like thank Dr. Ali Mirazimi for serving as the external reviewer on my thesis.

DEDICATION

This thesis is dedicated to my family and friends who have been a constant encouragement to me throughout the years. Thanks for all your support and advice in all types of matters.

TABLE OF CONTENTS

LIST OF TABLES

LIST OF FIGURES

LIST OF COPYRIGHTED MATERIAL FOR WHICH PERMISSION WAS OBTAINED

Figure 3. Carter S D et al. J. Virol. 2012;86:10914-10923. ASM authorizes an advanced degree candidate to republish the requested material in his/her doctoral thesis or dissertation. (open access)

Figure 5. from Anagnostou & Papa Infect Genet Evol. 2009 Sep;9(5):948-54
License number 3255430322268

Figure 8. Ergonul 2006 Lancet Infect Dis. 2006 Apr;6(4):203-14 License Number 3253890856607
Zakhashvili et al 2009 Emerg Infect Dis. 2010 Aug;16(8):1326-8. doi: 10.3201/eid1608.100097. (open access)

Figure 9. Nemerow et al Virology. 2009 Feb 20;384(2):380-8. doi: 10.1016/j.virol.2008.10.016 (open access)
Giberson et al Nucleic Acids Res. 2012 Mar;40(6):2369-76. doi: 10.1093/nar/gkr1076
License Number 3253880703947

Figure 19-24, 26-29, and 32 all from Zivcec et al J Infect Dis. 2013 Jun 15;207(12):1909-21. doi: 10.1093/infdis/jit061. Epub 2013 Feb 15.
License Number 3253871443140

## 1. INTRODUCTION

### 1.1 History of Crimean-Congo hemorrhagic fever

The first reports of Crimean-Congo hemorrhagic fever (CCHF) are thought to be from 12$^{th}$ century physicians from what is present-day Tajikistan [1]. The symptoms of disease were described as presence of blood in vomit, sputum and feces, and hemorrhage from the gums, urinary and gastrointestinal tract. The disease was reportedly associated with "bite of a small tough arthropod related to a tick or louse, and was sometimes resistant to treatment with the available medicine." Since the 1100s CCHF has been described several times by populations of southern Uzbekistan, however the disease was not characterized clinically until an outbreak in the Crimean peninsula in 1944-1945.

Following the outbreak, the disease, termed Crimean hemorrhagic fever, was suspected to be of viral origin and transmitted by ticks common to the area. The etiologic agent of disease could not be cultured in available tissue culture and animals, and thus was not isolated. Over the following 20 years outbreaks of a similar disease were reported in Bulgaria, the former USSR republics, central Asia and western, eastern and central Africa [1-3]. In 1956, in the current day Democratic Republic of Congo, CCHF virus (CCHFV) was first isolated following inoculation into suckling mice and named Congo virus [1]. By 1970 the etiologic agent of Crimean hemorrhagic fever was isolated and following electron microscopic, physiochemical and serological classification was found to be identical to Congo virus thus renaming the disease to CCHF and the etiologic agent to CCHF virus (CCHFV) [3]. Since then yearly outbreaks have occurred across central Asia, Africa and Eastern Europe (Figure 1).

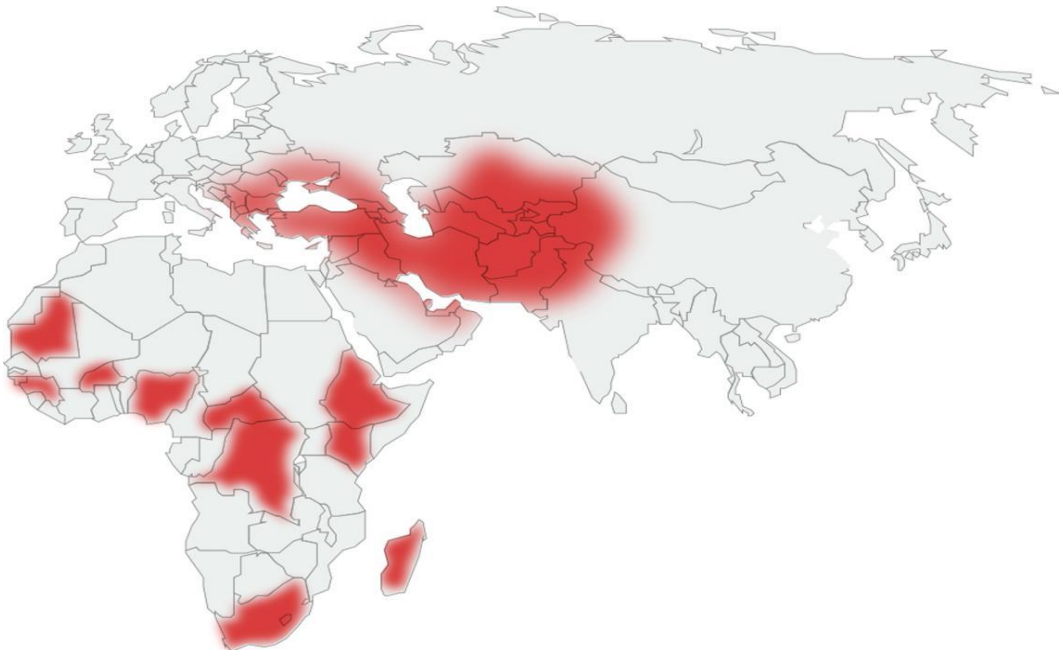

Figure 1. Distribution of human CCHF cases. Red denotes areas where confirmed human cases have been recorded from 1940-2013. Adapted from Zivcec et al. *Pathogens* **2013**, *2*, 402-421.

**1.2 Virus structure**

CCHFV is an enveloped, roughly spherical particle with a negative sense single-stranded, tri-segmented RNA genome. The 3 genome segments, named the large segment (L segment), the medium segment (M segment) and the small segment (S segment), encode 3 open reading frames: the viral RNA-dependent RNA polymerase (L protein), the glycoprotein precursor (GPC protein) and the nucleoprotein (NP), respectively (Figure 2a). CCHFV is thought to produce at least 4 viral structural proteins, NP, L and the processed glycoproteins $G_N$ and $G_C$ (formed from post-translational processing of GPC; formerly referred to as G1 and G2, Figure 2) as well as 3-4 non-structural proteins, GP38, the mucin-like domain, GP85/GP160 (unprocessed GP38/mucin-like domain), and $NS_M$ which are derived from post-translational processing of GPC [4-8].

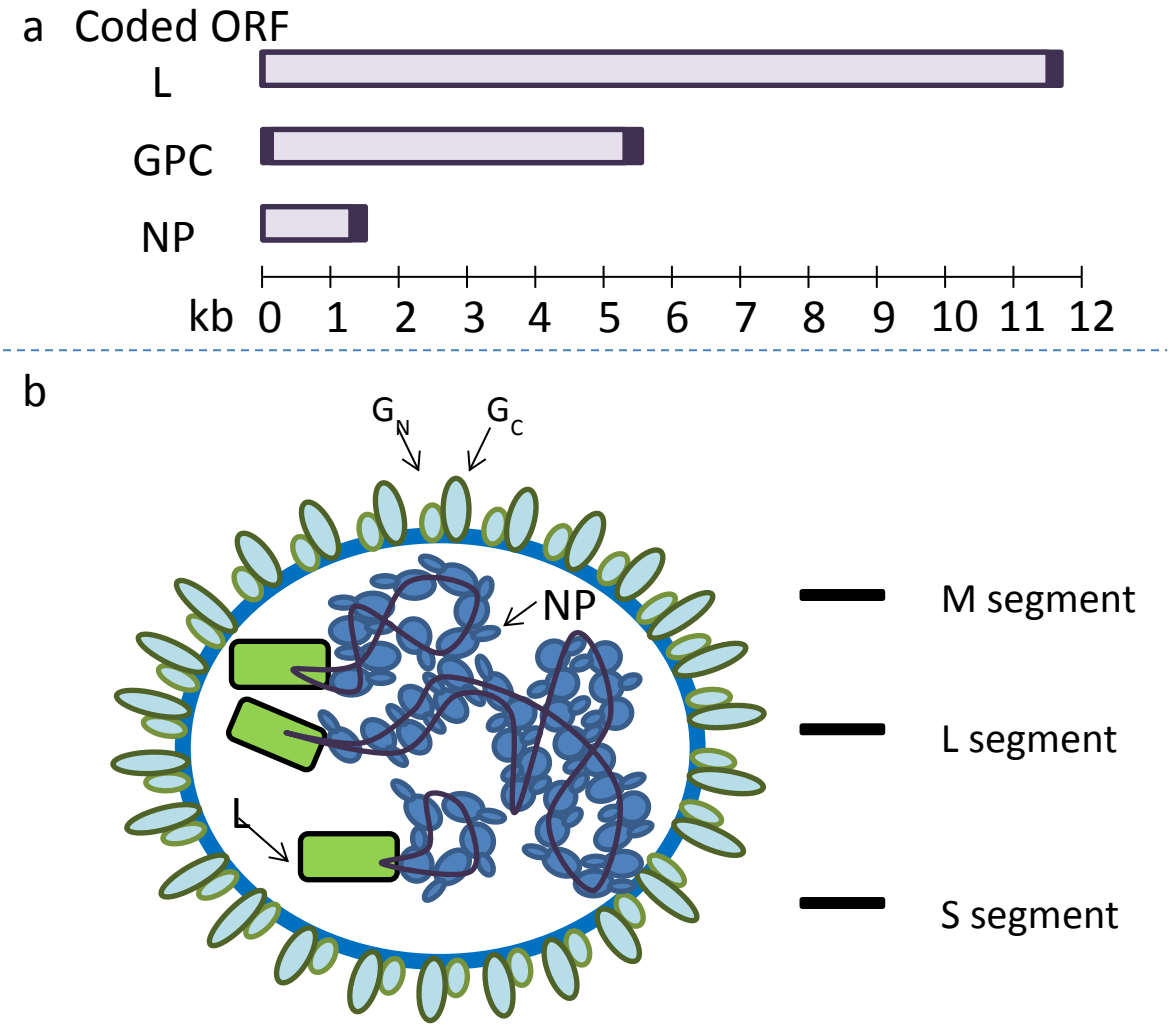


Figure 2. Schematic of CCHFV genome and virion. (a) CCHFV contains a tri-segmented, negative sense genome; the S (~1.5kb), M (~5.5kb) and L (~12kb) encoding NP, GPC and L, respectively. Dark purple represents non-coding RNA which are thought to act as transcriptional initiators/terminators and light purple represents coding RNA. (b) Schematic of the proposed virion composition. The viral RNA strands are bound to NP and the ends form a "panhandle" which is thought to be bound by the L. Mature $G_N$ and $G_C$ are thought to be viral attachment factors and are present on the viral membrane. NP = nucleoprotein, GPC = glycoprotein precursor, $G_N$ = mature glycoprotein N terminal, $G_C$ = mature glycoprotein C terminal, L = RNA-dependent-RNA polymerase

The NP is approximately 500 amino acids (aa) long and is a major component of the viral capsid however its complete role in the viral life cycle has not been determined. Based on studies of other bunyaviruses, the NP is thought to encapsidate viral RNA, act as a cap-snatching and transcriptional activator protein, and may act as a matrix protein for the CCHFV virion [9-12]. The interaction of NP with nucleic acids is poorly understood, but it is thought to bind to RNA with low affinity and to DNA as an endonuclease [13]. During CCHFV infection and *in vitro* expression NP is targeted, by cellular actin, to the perinuclear region, rather than Golgi [14]. While this targeting is important for viral replication the function of this remains unknown but may suggest that CCHFV virions can bud from the plasma membrane. Recently the crystal structure of this protein has been solved revealing 2 distinct "head" and "stalk" domains, which is more reminiscent of Arenavirus nucleoproteins (Figure 3) instead of other Bunyavirus NPs [13, 15]. CCHFV NP is also one of the major targets of both adaptive and innate immune responses and is often used in assays to detect previous infection [16-19]. CCHFV NP is often regarded as one of the primary targets of antibodies in mammals; is known to be a major target of the type I IFN response as it is target by the IFN stimulated gene MxA and of caspase-3 during cellular apoptosis [17, 20-23].

The GPC is unusually long (~1700aa) compared to most related viruses and is more extensively processed than other bunyaviruses resulting in up to 7-8 separate proteins [7] (Figure 4). GPC is either post- or co-translationally modified by furin, SKI-1, and SKI-1 like protease to yield $PreG_{N,}$ $PreG_{C,}$ mature $G_N$ and $G_{C,}$ GP85/GP160, mucin, GP38 and $NS_M$ [4-8]. The function of GP85/GP160, mucin, GP38, $G_N/NS_M$ and $NS_M$ are unknown, however significant amount of mucin and GP85/GP160 are secreted by infected cells [4-8]. Mature $G_N$ and $G_C$ are thought to be the

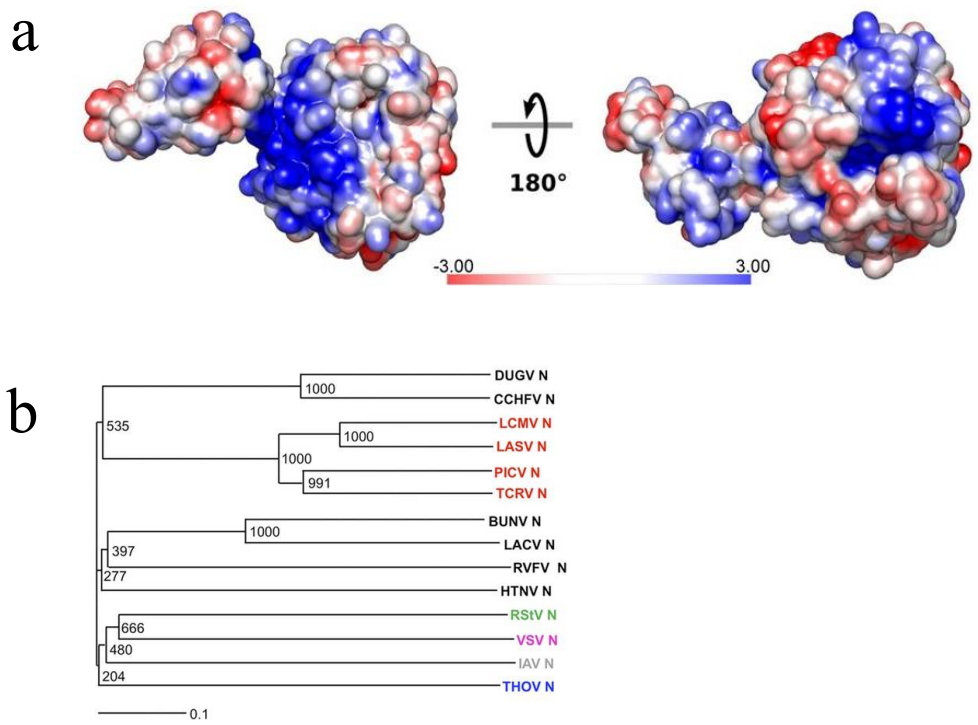


Figure 3. Structure CCHFV NP and a phylogenetic analysis of the NP of segmented negative-strand RNA viruses. (a) A space filling model of CCHFV NP. (b) The amino acid sequences of 14 viral NP as aligned by ClustalW. Included are bunyaviruses (black text) and arenaviruses (red text). Virus species abbreviations (GenBank accession numbers) are as follows: DUGV, Dugbe virus (P15190.1); CCHFV, Crimean-Congo hemorrhagic fever virus (AAB48503.1); LCMV, lymphocytic choriomeningitis virus (AAX49342.1); LASV, Lassa virus (ADY11071.1); PICV, Pichinde virus (AAC32282.1); TCRV, Tacaribe virus (AAA47903.1); BUNV, Bunyamwera virus (P16495.1); LACV, La Crosse virus (AAM94389.1); RVFV, Rift Valley fever virus (ABP88854.1); HTNV, Hantaan virus (AFA36178.1); RStV; rice stripe virus (P68559.2); VSV, vesicular stomatitis virus (AAA48470.1); IAV, influenza A virus (VHIVX1); and THOV, Thogoto virus (YP_145809.1). Adapted from J. Virol. 2012;86:10914-10923.

primary receptor binding molecules of CCHFV, however how the glycoproteins interact with various host cells is unknown [24]. Following translation and processing $G_N$ and $G_C$ are targeted to the Golgi for processing and budding [8, 25]. The localization of the mature glycoproteins has been attributed to the N terminal of the $G_N$ and is thought to be associated with N linked glycosylation as $G_C$ alone is not targeted to the Golgi [8, 25]. Whether the glycoproteins or the NP mediate CCHF egress are unknown but like other Bunyaviruses, CCHFV is thought to bud through the Golgi to which $G_N$ and $G_C$, have been shown to localize [26]. The receptor(s) of

CCHFV is(are) unknown, however recent reports suggest that human surface nucleolin binds $G_c$ and may therefore be an entry factor for CCHFV [27]. The binding has not been confirmed with whole CCHFV particles.

The L of CCHFV is significantly larger than most RNA-dependent RNA polymerases with a total size of ~3900-4000 aa. The entire protein is not known to be post-translationally modified and contains a ovarian tumor (OTU)-like protease motif, followed by zinc fingers, helicase and the bunyaviral RNA-dependent RNA polymerase motifs [28-33]. The OTU domain, due to its ability to deconjugate ubiquitin (Ub) and the Ub-like interferon-simulated gene 15 (ISG15), is currently considered one of the innate immune evasion mechanisms of CCHFV, however the potential of this domain to enhance or augment virulence of CCHFV is unknown. The OTU domain is capable of deconjugating Ub and ISG15 from many proteins and has been reported to be dispensable for virus replication [28-30, 32, 34, 35].

**1.3 Virus taxonomy**

CCHFV belongs to the Nairovirus genus of the Bunyaviridae family [24, 28]. CCHFV isolates often show significantly different sequences and are usually grouped based on the S segment. Currently there are 7 reported clades of CCHFV based on S segment classification (Figure 5a). The clade Europe 1 comprises of strains first isolated in the Balkans and southern Russia; Europe 2 clade was first isolated from Greece and is the only clade of CCHFV thought to be naturally attenuated; Africa 1 clade is predominantly isolated from western Africa; Africa 2 clade is predominantly isolated from central and eastern Africa; Africa 3 clade isolates predominantly are found in western and southern Africa; Asia 1 clade is predominantly isolated from the middle East and Asia 2 clade are mainly isolated from western Asia and former Soviet republics. Despite the classical view of the geographic distribution of strains considerable overlap between

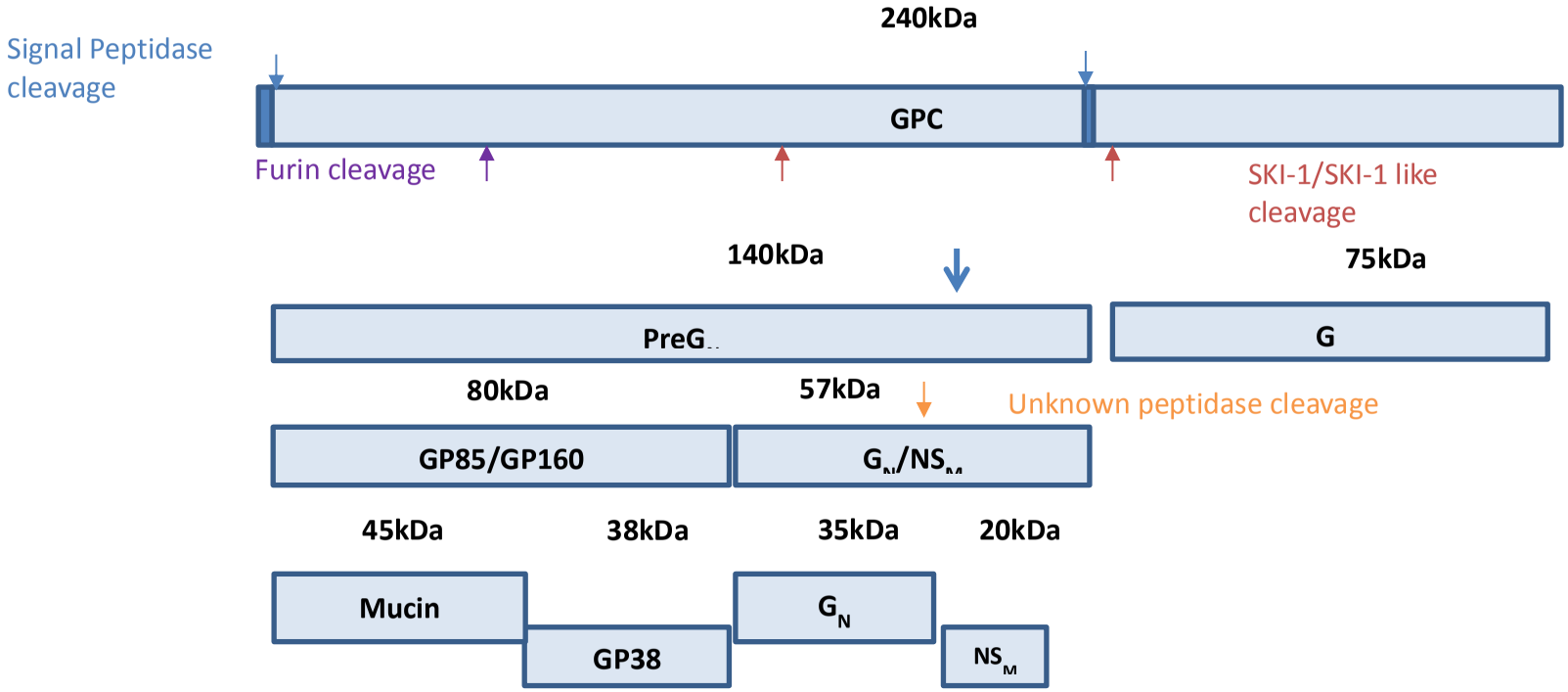


Figure 4. Schematic of the post- or co-translational processing of CCHFV GPC. At some point during processing GPC is processed into up to 8 separate proteins by a combination of signal peptidase, Furin, SKI-1, and SKI-1 like proteases. The order of processing and the function of GP85/GP160, mucin, GP38, $G_N/NS_M$, $NS_M$ and $PreG_N$ are unknown. Mature $G_N$ and $G_C$ constitute the viral surface glycoproteins and are thought to be the proteins that mediate entry into cells.

clades of CCHFV occur in several endemic areas [28-31]. As sequencing efforts have expanded phylogenetic trees based on M and L segments have been generated. M segment sequences can be grouped in 5 to 6 clades depending on the similarity criteria requirements with M segment sequences of CCHFV isolated from often distant geographic locations e.g. M segments isolated from some Asian outbreaks group more closely together with M segments isolated from some African outbreaks than with other Asian isolates M segments (Figure 5b). L segment sequences may be grouped into 5 or 6 clades and, much like S segment sequences, group closely with isolates from similar geographic isolations e.g. L segments isolated from Africa group into clades with other African strains (Figure 5c) [32-34]. However due to the large size of L and M segments (~12000 and ~5500 bp, respectively), and the more limited sequencing data available CCHFV strains will be classified based on CCHFV S segments.

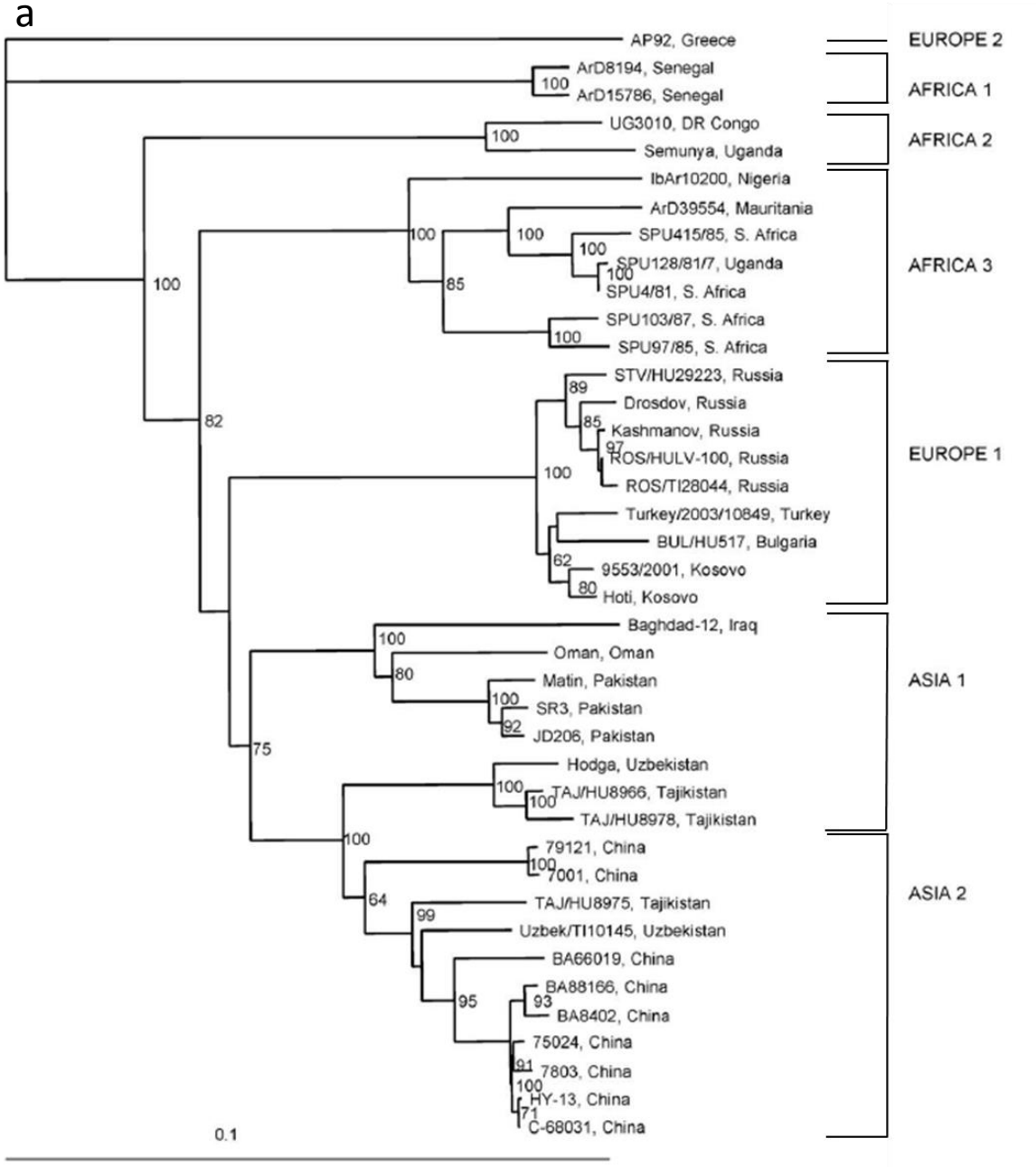
a
AP92, Greece
ArD8194, Senegal
ArD15786, Senegal
UG3010, DR Congo
Semunya, Uganda
IbAr10200, Nigeria
ArD39554, Mauritania
SPU415/85, S. Africa
SPU128/81/7, Uganda
SPU4/81, S. Africa
SPU103/87, S. Africa
SPU97/85, S. Africa
STV/HU29223, Russia
Drosdov, Russia
Kashmanov, Russia
ROS/HULV-100, Russia
ROS/TI28044, Russia
Turkey/2003/10849, Turkey
BUL/HU517, Bulgaria
9553/2001, Kosovo
Hoti, Kosovo
Baghdad-12, Iraq
Oman, Oman
Matin, Pakistan
SR3, Pakistan
JD206, Pakistan
Hodga, Uzbekistan
TAJ/HU8966, Tajikistan
TAJ/HU8978, Tajikistan
79121, China
7001, China
TAJ/HU8975, Tajikistan
Uzbek/TI10145, Uzbekistan
BA66019, China
BA88166, China
BA8402, China
75024, China
7803, China
HY-13, China
C-68031, China
0.1
EUROPE 2
AFRICA 1
AFRICA 2
AFRICA 3
EUROPE 1
ASIA 1
ASIA 2

b

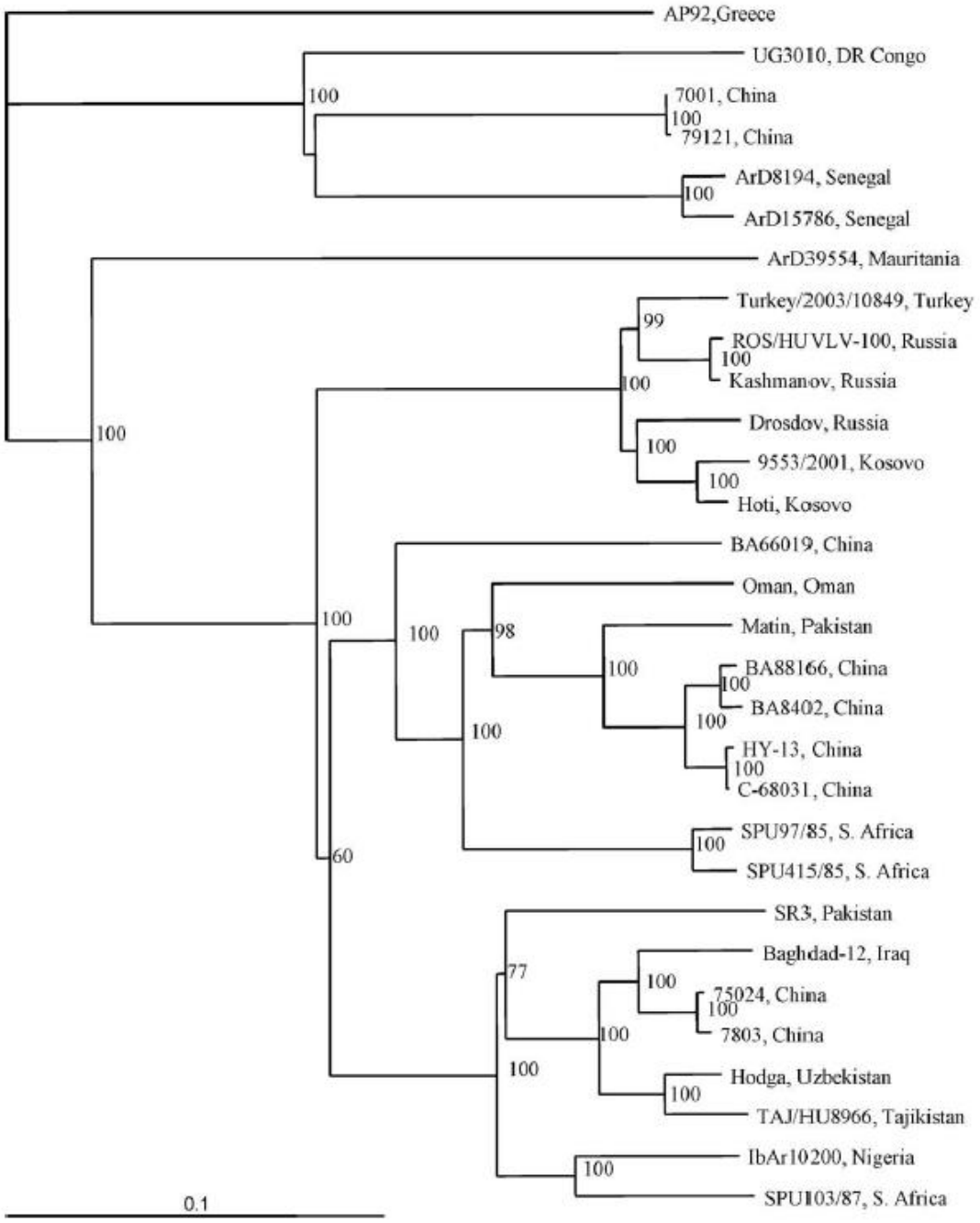
AP92,Greece
UG3010, DR Congo
100
7001, China
100
79121, China
ArD8194, Senegal
100
ArD15786, Senegal
ArD39554, Mauritania
Turkey/2003/10849, Turkey
99
ROS/HUVLV-100, Russia
100
Kashmanov, Russia
100
Drosdov, Russia
100
9553/2001, Kosovo
100
Hoti, Kosovo
100
BA66019, China
Oman, Oman
100
100
98
Matin, Pakistan
100
BA88166, China
100
BA8402, China
100
100
HY-13, China
100
C-68031, China
SPU97/85, S. Africa
100
60
SPU415/85, S. Africa
SR3, Pakistan
77
Baghdad-12, Iraq
100
75024, China
100
100
7803, China
100
Hodga, Uzbekistan
100
TAJ/HU8966, Tajikistan
IbAr10200, Nigeria
100
SPU103/87, S. Africa
0.1

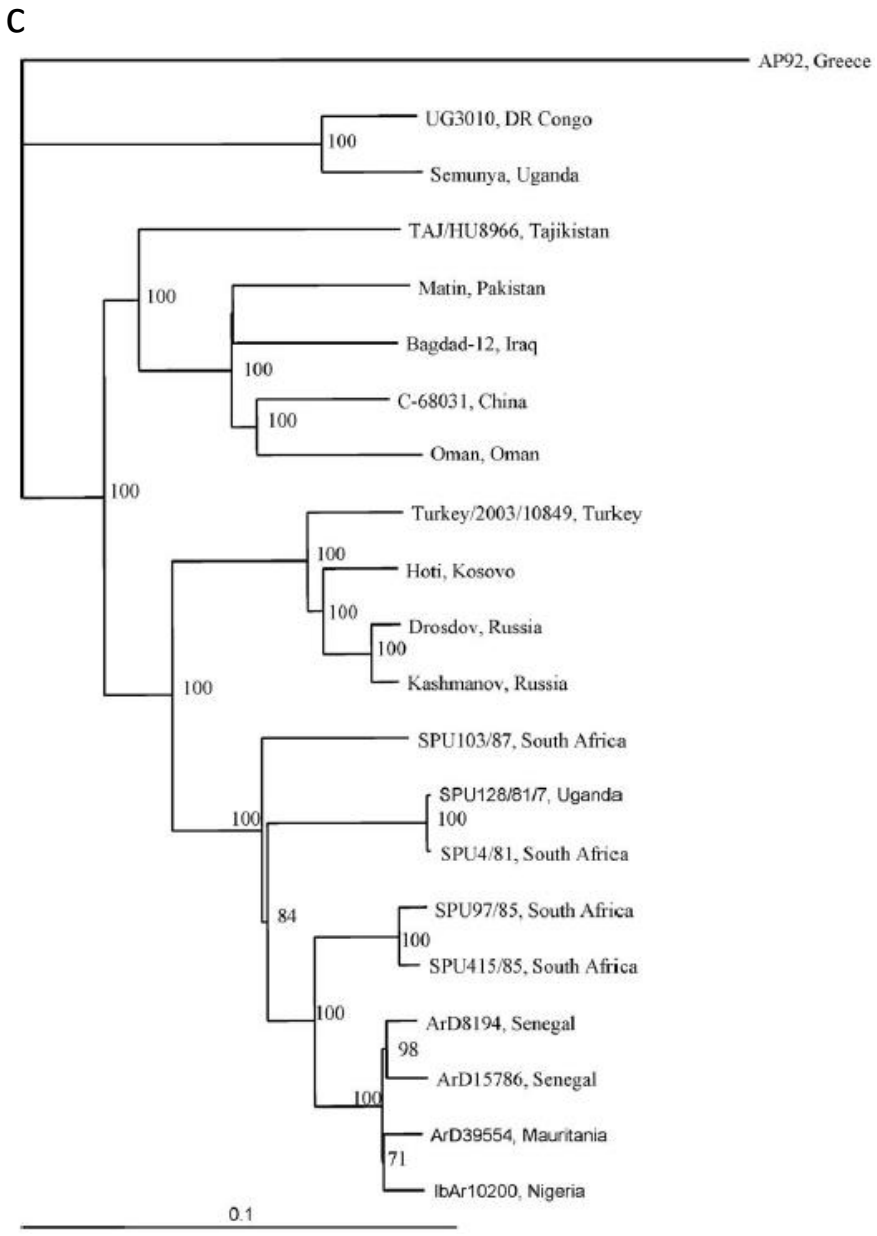


Figure 5. Maximum-likelihood phylogenetic trees based on the full length coding regions of CCHFV. (a) S (1446 coding base pairs), (b) M (5121 coding base pairs) and (c) L (11836 coding base pairs) segments of CCHFV. Names corresponded to 'strain name, country'. Bootstrap values were shown on the key nodes of the trees with bars representing 0.1 as indicated. All comparisons done on single isolates and contain sequence data of 38 (a), 30(b), and 21(c) isolates. Adapted from Anagnostou & Papa Infect Genet Evol. 2009 Sep;9(5):948-54.

### 1.4 Life cycle of CCHFV vectors

In the environment CCHFV is predominantly maintained by hard-body ticks of the genus *Hyalomma*. Tick species from the genera *Amblyomma, Boophilus, Dermacentor, Haemaphysalis,* and *Rhipicephalus,* may harbor or even experimentally transmit CCHF, however there is little evidence of the involvement of these other tick species in natural, both enzootic and zoonotic, transmission or maintenance of CCHFV foci [35].

Ticks feeding on mammals may pass on CCHFV to other ticks by co-feeding in close proximity on an animal, by feeding on a viremic animal, through direct sexual contact with another tick or from female ticks to their offspring [36-41]. *Hyalomma* ticks are persistently infected and can transmit CCHFV at any life stage. Therefore, CCHFV circulates by an enzootic cycle predominantly between ticks, mammals and birds.

#### 1.4.1 Feeding cycle

Hard-body ticks, like *Hyalomma* genus ticks, have 3 life stages: larvae, nymph and adult. *Hyalomma* genus ticks actively pursue their potential hosts by crawling onto the host skin and attaching with their mouthparts. The mouthparts then become cemented onto the skin of the host with tick saliva and the tick proceeds to break the dermal capillary blood vessels to form a feeding lesion for feeding on blood and lymph that is released into the lesion. Tick feeding is slow as the body wall needs to expand prior to ingesting the large blood meal. Depending on whether the ticks have 2 or 3 host life cycles (see below) the ticks will either detach from their host and drop to ground to molt to their next life cycle or molt on the host following their feeding (Figure 6). To fully engorge with a blood meal larvae require 3 to 5 days, while nymphs

require 4 to 8 days and adult females 5 to 20 days. Adult male ticks do not become fully engorged like the females and only feed enough for their reproductive organs to mature [42].

### 1.4.2 Reproduction cycle

Adult males, of the *Hyalomma* genus, will remain on the host and will attempt to mate with multiple females during feeding while females will mate only once just prior to being fully engorged. Following feeding and mating, adult females will detach and lay a large amount of eggs (2000-20000) in a single batch in the environment. Following mating adult males die while adult females die following deposition of eggs [42].

a

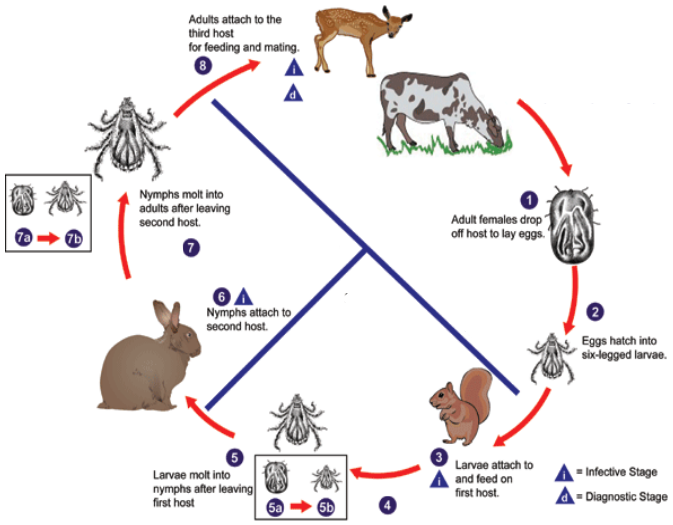


b

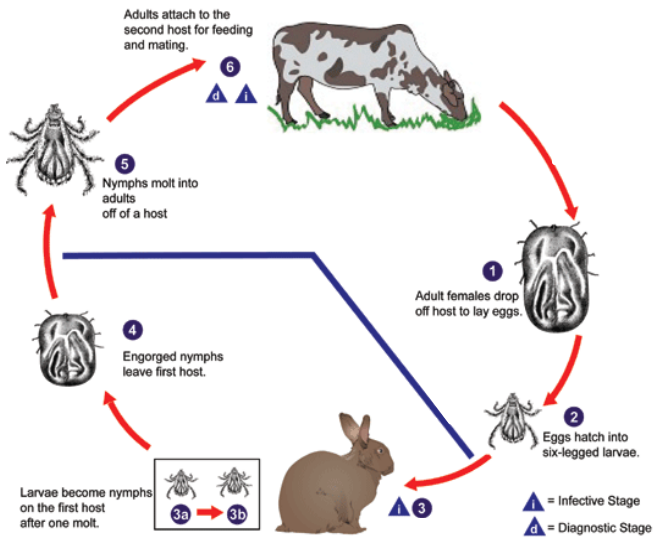


Figure 6. Life cycle of three and two host ticks. (a) Following birthing the first winter, larvae attach to first host, usually small mammals and ground birds and obtain a blood meal over the course of a few days. Following the detachment the larvae will molt into nymphs and overwinter prior to attaching to a second host which are usually small to moderate size mammals or birds and molt into adults during their final winter. The adults will then feed on larger mammals such as cattle and humans and mate to produce thousands of eggs. (b) Two host ticks have a more rapid life cycle usually requiring only 2 winters prior to reaching their adult stage. Following birth and overwintering larvae will feed on moderate to large mammals without attacking birds (group A) or small to moderate size mammals and birds (group b). Two host ticks will then molt into the nymph stage while on the host prior to taking a second blood meal and detaching to molt into their adult stage and overwinter. Following the second overwinter the adult tick will feed once more on large mammals, mate and then detach to release its eggs. Adapted from http://www.dpd.cdc.gov.

### 1.4.3 Multiple host life cycles

Some *Hyalomma* genus members such as *H. marginatum* and *H. detritum* are 2 host ticks, other such as *H. impeltatum* and *H. lusitanicum* are 3 host ticks, and some members such as *H. dromedarii* and H. *anatolicum*, can be either 2 or 3 host ticks.

2 host ticks are hatched in the environment and quest for hosts. Following attachment and feeding the larvae remain attached to the host and molt into nymphs. The nymphs then feed on the same host as the larvae and detach following feeding to molt into adults in the environment. The adult species will then seek out an additional host to feed and mate (Figure 6). 2 host ticks may be further subdivided into 2 groups; those which feed on similar hosts during both immature and adult stages (group A) and those, which feed on dissimilar hosts between immature and adult stages (group B) [1]. 2 host ticks belonging to group A generally parasitize medium to large mammals usually without parasitizing birds during both immature and adult stages. In contrast, group B 2 host ticks parasitize ground birds and small mammals during their immature stages and larger wild and domestic mammals, including humans, and occasionally large birds such as ostriches, during their adult stages [1]. The 2 host life cycle is more rapid lasting from 3 to 18 months to complete [42].

3 host ticks, like 2 host ticks, are born in the environment and quest for hosts. After the first feeding a 3 host larvae will detach from the host and molt into a nymph in the environment followed by attachment to a new host. The nymphs will then feed, detach and molt into adults. Adults attach to their final hosts, mate and then die. 3 host *Hyalomma* members prefer to feed on small mammals during their immature stages and on moderate to large mammals, including humans, during their adult stages [1]. The 3 host ticks have a slower life cycle lasting from 6 months to more than 24 months [42].

**1.5 CCHFV in mammals**

The distribution of *Hyalomma* genus ticks is broad and includes diverse environments stretching from western Asia and throughout southern Europe and throughout Africa (Figure 7). Therefore, numerous transmission cycles with many hosts have been reported.

Figure 7. Global distribution of *Hyalomma* genus ticks. Red denotes areas with confirmed captures of ticks. Adapted from Zivcec et al. *Pathogens* **2013**, *2*, 402-421.

There is no evidence that CCHFV causes disease in mammals aside from humans [24]. Natural CCHFV infection, as evidenced by seroconversion against CCHFV, has been demonstrated among small wild mammals, such as rodents and hares, large wild mammals, such as giraffe, zebra, buffalo goats, sheep, and domestic mammals, such as dogs, goats, sheep, camel, and cattle [43, 44]. Antibodies specific for CCHFV are also found among several species of birds such as guinea fowl, starling and ostrich [43, 45, 46], however birds are usually considered refractory to infection with CCHFV [1]. Despite the numerous animals capable of supporting CCHFV

replication, hares, sheep, goats, ostriches, and/or cattle are required for sustained transmission of CCHFV within an geographic location [1, 43, 45-49].

Due to the lack of disease symptoms and the broad range of animals capable of transmitting CCHFV to humans the risk of acquiring infection is significant to individuals in close contact with animals in endemic areas. Furthermore medical staff are at increased risk of acquiring CCHFV from a viremic patient as a result of misdiagnosis or prior to diagnosis. Therefore, it is not surprising that abattoir workers, farmers, veterinary staff, nurses, and medical doctors are the most likely individuals to be infected with CCHFV [24].

**1.6 Human clinical disease**

Severe human CCHF usually can be separated into by 4 distinct phases: incubation, pre-hemorrhagic, hemorrhagic and convalescence (Figure 8a). The incubation lasts between 1 - 7 days post infection, although more recently incubations of >13 days have been documented [24, 50, 51]. The pre-hemorrhagic phase is usually between 3 - 7 days in length and begins with rapid onset of fever (>39.0 °C), fatigue, cephalalgia, dizziness, photophobia and myalgia, but often accompanied by nausea, vomiting and diarrhea [24, 50-53]. Severe CCHF cases progress to the hemorrhagic phase which lasts between 2 – 3 days and is characterized by petechiae, ecchymosis, epistaxis, and gingival hemorrhage, but can often include gastrointestinal and cerebral hemorrhage (Figure 8b). It is during the hemorrhagic phase that patients succumb to disease with the predictors of fatal outcome being high viremia ($\geq 10^8$ viral copies/mL blood), increased serum aspartate and alanine aminotransferase, lactate dehydrogenase, creatine phosphokinase, thrombocytopenia (<20,000/mL), increased clotting times, increased serum levels of tumor necrosis factor-α (TNFα), interleukin (IL)-6, hyaluronic acid, intercellular adhesion molecule-1 (ICAM1), vascular cell adhesion molecule-1 (VCAM1), vascular endothelial

growth factor-A (VEGFA), interferon-γ (IFNγ), low antibody titers and presence of melena [54-72]. Infection kinetics are unknown in humans and currently there is no data describing the order in which cell types are infected nor how this is altered during the course of disease. The main targets of virus infection in humans are mononuclear phagocytes, endothelial cells and hepatocytes [73, 74]. Severe liver necrosis, shock and subsequent multiorgan failure are the main causes of death [24, 50, 51, 73]. The case fatality is approximately 30% [24, 50, 51, 75], however case fatality varies between CCHFV strains and geographic regions with an overall case fatality of approximately 5% in the Turkish outbreaks [68] to 70% in the United Arab Emirates outbreak [76-79]. Convalescence occurs between 10-20 days post symptom onset and may include clinical symptoms such as tachycardia, polyneuritis, breathing impairment, poor vision, loss of hearing, and loss of memory [24, 50, 51, 53]. Mild CCHF cases will rapidly recover following the onset of disease, without need for hospitalization, and will bypass the hemorrhagic phase without complications [80]; up to 88% of CCHFV infections may lead to subclinical disease [80]. Despite a wide distribution, the pathogenesis of CCHF remains poorly understood due to limited human pathology data and the need for high containment to handle CCHFV infected specimens. Furthermore, there is currently no data linking severity of disease to CCHFV strains. Thus, the question whether a higher pathogenicity observed in some CCHFV strains is due to host responses or CCHFV genetic variability has not been addressed.

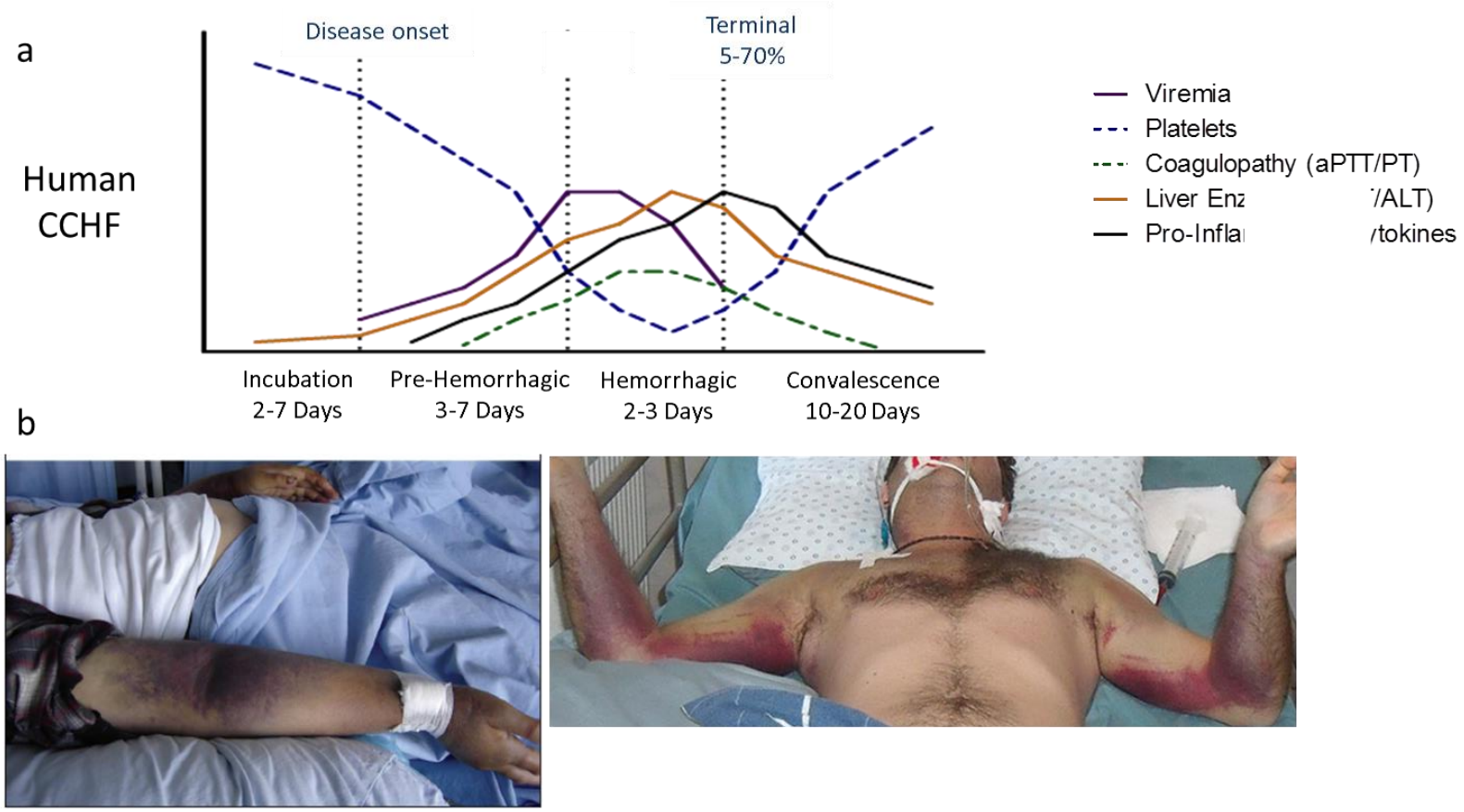


Figure 8. Clinical presentation of CCHF. Following short incubation period of 2-7 days patients have rapid onset of non-specific flu like symptoms which persist for 3-7 days. During this time viremia is detectable, and liver enzymes alanine aminotransferase (ALT) and asparatate aminotransferase (AST) increase. Following the pre-hemorrhagic phase, severe cases will experience a rapid drop in platelets and coagulopathy as measured by increases in activated partial thromboplastin time (aPTT) and prothrombin time (PT), and will experience hemorrhagic manifestations (b) such as ecchymosis (bottom left) and petechiae (bottom right). Approximately 6-70% of the severe cases succumb to infection during the hemorrhagic phase. Adapted from Ergonul 2006, and Zakhashvili et al 2009.

### 1.7 Animal models of CCHFV

Mice, rats, hamsters, guinea pigs, rabbits, ostriches, cattle, sheep, goats, calves, donkeys, horses, and non-human primates have been experimentally infected with CCHFV as demonstrated by presence of antibodies. However, only suckling mice and rats, and adult signal transducer and activator of transcription 1 (STAT1) knockout ($STAT1^{-/-}$) and interferon α/β receptor (IFNAR) knockout ($IFNAR^{-/-}$) mice developed overt disease following inoculation [47, 49, 81-86].

#### 1.7.1 Suckling mouse

Following CCHFV inoculation suckling mice develop a fatal disease [81, 83]. The disease course has variable kinetics, based on amount of CCHFV inoculated and route of infection, with a time to terminal disease of approximately 8 days post infection (p.i.) [83]. Suckling mice are sensitive to the intraperitoneal (i.p.) and intracranial (i.c.) routes of infection and display weight loss, or lack of weight gain, ruffled fur and neurologic symptoms. CCHFV initially infects the liver and spleen of suckling mice prior to spreading systemically (infectious virus isolated from heart, brain and serum). Main targets of CCHFV replication in this model are cells of liver morphologically consistent with Kupffer cells, followed by clusters of hepatocytes and sometimes tissue macrophages [81, 83]. This animal species, while useful for isolation and propagation of CCHFV and antiviral testing, does not mimic human disease [83].

#### 1.7.2 $STAT1^{-/-}$ mouse

$STAT1^{-/-}$ mice develop a severe, inflammatory disease following CCHFV infection [84]. Only the i.p. route of CCHFV infection was reported. Disease onset is dependent on inoculation dose,

with higher doses resulting in faster infection kinetics and occurs over a period of 3 to 5 days p.i.. STAT1$^{-/-}$ mice develop disease signs which include lethargy, ruffled fur, hunched posture, temperature change (initially fever followed by hypothermia prior to death/euthanasia) and weight loss starting at day 3 p.i. and deteriorate rapidly. CCHFV genomic RNA was detected by RT-PCR at 1 day p.i. in the blood of animals; was detected in blood, liver, spleen and lung of animals by day 2 p.i.; and was detected in all tissues (blood, brain, kidney, liver, lung, spleen) by day 3 p.i.. Main targets of CCHFV replication are hepatocytes and occasionally Kupffer cells and pathological changes occur in the liver and spleen. Liver damage is reflected by an increase in serum alanine aminotransferase (ALT), which is detected following disease onset. The pathological changes occur with an increase in T-cell activation and increases in serum interferon-α (IFNα), interferon-β (IFNβ), interferon-γ (IFNγ), tumor necrosis factor-α (TNFα), interleukin (IL)-1β, IL-6, IL-10, and monocyte chemotactic protein 1 (CCL2). In addition, STAT1$^{-/-}$ mice develop a transient thrombocytopenia, which is resolved prior to terminal stages of infection. This model has been utilized to test the efficacy of ribavirin treatment and concludes that it is effective when low doses of CCHFV (2.5 times the lethal dose 50% [$LD_{50}$]) are used for inoculation[84]. Therefore, this model recapitulates several hallmarks of human CCHF; however, due to the severe impairments in its type I and II IFN responses, this model has limitations in its use as a model of CCHF disease kinetics and evaluation of CCHFV countermeasures.

### 1.7.3 IFNAR$^{-/-}$ mouse

IFNAR$^{-/-}$ mice, much like STAT1$^{-/-}$ mice, are essentially unresponsive to type I IFN signaling; unlike STAT1$^{-/-}$ mice, however, IFNAR$^{-/-}$ mice still have intact type II IFN signaling which is more slowly induced due to the absence of type I IFN signaling [87]. The IFNAR$^{-/-}$ mouse model is susceptible to lethal CCHFV infection by the i.p. route [85]. IFNAR$^{-/-}$ mice disease onset is inversely

dependent on inoculation dose with disease course lasting between 2 to 4 days following inoculation with the highest to lowest CCHFV dose, respectively. CCHFV genomic RNA was detected by RT-PCR in the blood, brain, heart, liver, and spleen starting at 2 days p.i. until terminal stage of disease. Disease signs were noted starting at 42 hours p.i. and included labored breathing and purple discoloration of the facial features. The only noted pathological changes were liver congestion with hemorrhagic areas [85]. The initial description of this model did not include detailed description of pathology, blood chemistry or immune responses following CCHFV infection. Addressing these parameters is a major focus of this thesis.

### 1.8 Prevention and countermeasures

#### 1.8.1 Prevention of CCHFV infection

In addition to tick bite or unprotected crushing of an engorged tick, during the viremic phase animals or humans may transmit CCHFV to others. Therefore, avoidance of tick bite, treatment with acaricide and quarantine of animals prior to slaughter or barrier nursing of patients or during veterinary examination should be conducted.

To prevent tick bite infection avoid tick attack by not spending significant time in areas infested with ticks, and wearing protective clothing and applying DEET or Permethrin insect repellent if venturing into tick infested areas [88]. Ticks of the *Hyalomma* genus are slow feeders allowing individuals, who are victims of tick attack, several hours to remove a tick prior to becoming bitten. It is advised to take a bath or shower, or have the body inspected following activities in tick infested areas. Tick removal should be accomplished by using fine tweezers followed by washing of the affected skin area with soap and water or a disinfecting agent such as alcohol [88].

As humans may become infected following close contact with fluids of animals, most likely due to contact with CCHFV infected blood, it is essential to make sure animals are not viremic prior to high risk activities with animals such as slaughter. Currently data on safety equipment during invasive veterinary inspection of animals is lacking, but presumably proper use of gloves and protective clothing is advised. Another method to prevent transmission between animal and human is to de-tick and quarantine animals against tick attack for 2 weeks prior to high risk activities such as slaughter [47].

Health care workers are the second group of people at higher risk for acquisition of CCHFV infection, however, nosocomial spread can be effectively stopped by implementation of proper barrier nursing of all patients with hemorrhagic syndromes [24, 50, 89]. In case of accidental nosocomial exposure immediate administration of oral ribavirin may be considered; however, the efficacy of ribavirin against CCHFV is still controversial [24, 90-94].

### 1.8.2 CCHFV vaccines

As animals do not readily display disease signs, development and evaluation of the protective efficacy of CCHFV vaccines has been severely hampered. To date a single vaccine has been developed and safety tested in humans [95, 96]. The vaccine was developed by chemical and heat inactivation of CCHFV infected suckling mouse brains in the former Soviet Union in 1970 and is only licensed for use in Bulgaria [95, 96]. In its current formulation the vaccine is based on CCHFV strain V42/81 which was isolated from a patient in 1981[95]. The vaccine has not been clinically tested for efficacy; however, following vaccination of at risk individuals, the incidence rate decreased from 1105 cases over 20 years (1953-1974) to 279 over 20 years (1975-1996) [95]. Individuals receiving the vaccine develop a T cell response to CCHFV NP (100-fold increase in reactive T-cells), seroconvert to CCHFV NP and develop a weak neutralizing

response following vaccination (up to 1:128 serum dilution in order to achieve >50% CCHFV neutralization), and the efficacy of both T-cell and antibody immunity appears to increase with higher number of boosters [96].

To date 2 experimental vaccines have been proposed [97, 98]. Following DNA vaccination, approximately half of the tested mice developed a weakly neutralizing antibody response (plaque reduction/neutralization of >50% of CCHFV was achieved with serum titers of 1:40-1:160), while vaccination with tobacco expressed recombinant glycoprotein was only reported to induce antibodies against CCHFV glycoprotein. Neither of these vaccination approaches has been evaluated for safety in humans nor for efficacy in a disease model.

Therefore evaluation of vaccine efficacy is of paramount importance and must be addressed to mitigate the negative impact CCHFV infection has on global public health. Furthermore, vaccines must demonstrate the ability to protect against several CCHFV clades concurrently due to the potential of novel strains to become introduced into endemic areas. Since prophylactic vaccines are not evaluated, the majority of endemic regions have relied exclusively on barrier approaches to prevent infection.

Therefore, currently with the exception of physical barriers there are no agreed upon mechanisms of preventing CCHFV infection in humans. This is mostly due to a lack of CCHF animal models.

**1.9 Vaccine design approaches**

Effective replication incompetent or non-infectious vaccines consist of at least 2 components: an antigen or antigenic sequence and an immune-activating adjuvant. Antigen presenting cells (APCs) are essential in generating and orchestrating an effective antiviral immune response. The

APCs should process the desired antigen for subsequent presentation to virus specific T- and B-cells. In order to process and present antigens, APCs must first be activated by various stimuli such as cytokines or pathogen associated molecular patterns (PAMPs). Following activation, APCs simultaneously upregulate necessary co-stimulatory molecules and migrate to immune tissues where they stimulate helper (Th) and cytotoxic T cells (CTLs) which then give rise to both primary and memory B- and T-cell responses [99]. Traditional vaccines have focused on delivery of an antigen with inactivated viral particles, viral subunits or antigenic viral sequences and have relied on either chemical adjuvants or immunogenicity of the molecules to activate APCs and generate effective immune responses [95, 97, 98]. Viral vectors can efficiently infect specific cell types and trigger their activation [100]. Therefore carefully designed viral vectors act as both antigen and adjuvant and are often superior to other vaccine platforms.

Adenovirus (Ad) vectors are icosahedral nonenveloped DNA viruses with a 80- to 100-nm diameter [101]. Ad infection is common in humans and generally manifests as a mild, usually respiratory disease. Following attachment to its receptors Coxsackie-Adenovirus receptor or CD46, Ad is transported from the plasma membrane to the nucleus by microtubules where it persists as an episome (Figure 9, top panel)[26, 102]. Regardless of whether or not the Ad genome is integrated into the host genome the Ad genome is transcribed and translated by Ad and the host machinery. Primary activation of Ad transcription requires the early activation of the E1a gene of Ad and deletion of the E1 genes renders Ad vectors replication deficient and increases the genomic carrying capacity of Ad [26, 102] (Figure 9 lower panel). Ad E3 proteins act further to subvert innate immune responses and prevent effective clearance of Ad. To prevent this subversion and maximize immune stimulation recombinant Ad vectors often have their E3 gene deleted. To express genes of interest, such as viral antigens, the gene of interest followed by a transcriptional terminator is cloned under the control of a constitutively

expressing promoter in the Ad genome. The final Ad vector will infect cells, be transported to the nucleus and the mammalian promoter will be recognized and transcribed by the host machinery. Ad vectors can stably carry and express large genes, can transduce both dividing and non-dividing cells, generate robust T- and B- cell responses, are efficiently grown *in vitro*, and are as safe as inactivated or subunit vaccines [100]. For all these reasons this vaccination platform was selected to be used in protection studies.

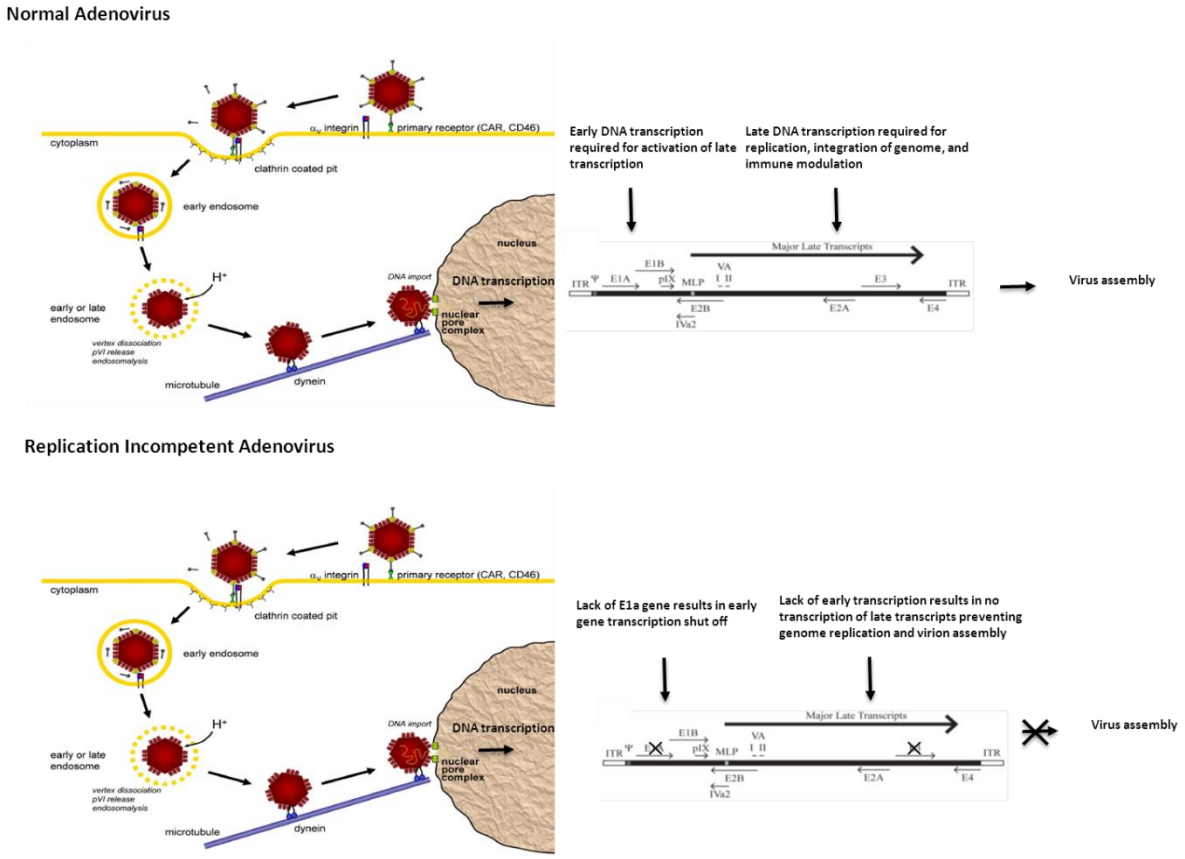


Figure 9. Schematic of life cycles of normal and replication incompetent Adenovirus (Ad). Normal Ad enters by binding to its receptors and enters the cell by clathrin coated pits. The virion escapes the endosome following acidification and is brought to the nucleus. After arrival at the nucleus the Ad genome undergoes early transcription which provides it with proteins required for activation of late transcription. Late transcription supplies Ad proteins required to integrate into the genome of the host, replicate its genome, and undergo viral particle assembly. The entry steps of replication incompetent Ad are similar; however, replication incompetent Ad lacks E1a gene required for activation of early and late transcription. Adapted from Nemerow et al 2009 virology, and Giberson et al 2011 nucleic acids research.

## 1.10 Objectives, rationale and hypothesis

### 1.10.1 Rationale of animal model and vaccine development, and evaluation of immune response to vaccination

As no adult animal models of disease existed for CCHF at the beginning of this work, animal modeling was an attractive venue of research especially with the recent expansion in the availability of knockout mouse strains. Without an available adult animal disease model it would be impossible to assess vaccine efficacy and mechanisms of protection upon vaccination. At the time, unpublished data supported only the development of the $STAT1^{-/-}$ mouse model of CCHFV. However, this animal model contained several impairments in immune functions, which would make it difficult, if not impossible, to evaluate vaccine candidates due to a total lack of STAT1 signaling. A report published soon after the start of this work described an alternate CCHF animal model, which lacked only STAT1 signaling by type I IFN, but had intact alternate STAT1 signaling pathways.

Following the assessment of the $IFNAR^{-/-}$ mouse model of CCHF, further experiments observing the efficacy of Ad vectors as vaccine platforms against CCHFV were undertaken. The goal of these experiments was to find a protective vaccine regimen or eliminate this platform as a vaccine candidate.

$IFNAR^{-/-}$ mice are severely compromised in their ability to fight off intracellular pathogens due to an inability to respond to type I IFN. Therefore, a vaccine which is to be successful in this model must be replication incompetent, and induce a strong, multifaceted adaptive immune response which is capable of overcoming the inability of this model to develop a non-specific antiviral response.

Following the success of this vaccine platform to protect IFNAR$^{-/-}$ mice from lethal CCHFV challenge evaluation of the protective immune response was the next logical step. It was assumed that since IFNAR$^{-/-}$ mice do not respond to a type I IFN response, which is critical in controlling CCHFV replication in immunocompetent mice, the adaptive immune responses following vaccination are responsible for protection against lethal CCHFV challenge. It has been reported that antibody responses are important for survival in human CCHF [24, 68] and this model would allow for evaluation of this observation in controlled studies. To assess the role of humoral responses and cell mediated responses gain of function experiments were undertaken to assess the protective efficacy of antibody and/or immune cell transfer for the ability to protect against lethal CCHFV.

### 1.10.2 Hypotheses and Objectives

It was hypothesized that the lethal disease which results from CCHFV infection of IFNAR$^{-/-}$ mice mimics human CCHF and can be used for the evaluation of vaccine efficacy and for elucidation of the mechanisms of protection.

Furthermore, it was hypothesized that IFNAR$^{-/-}$ mice could be protected from lethal CCHFV infection by vaccination with replication incompetent Adenoviruses expressing CCHFV antigens.

Finally, as most of the data from human cases of CCHF infection implicated antibody responses as key for favorable outcome, it was hypothesized that antibody responses were essential for protection from lethal CCHFV infection in IFNAR$^{-/-}$ mice.

Objectives:

1) Characterize a new animal model for CCHF
2) Develop effective prophylactic vaccines which prevent lethal CCHFV infection
3) Characterize the mechanisms of protection in the new animal model

### 1.10.3 Significance

CCHF remains understudied as assessment of countermeasures can only be performed on human patients due to a lack of animal models. This has significantly impaired development of specific treatments or prophylaxis. Therefore, development of new animal models which mimic human CCHF is of paramount importance for the evaluation of potential countermeasures. The characterization of this animal model will build a strong foundation upon which other research can be conducted to observe disease progression and evaluate novel countermeasures.

To date, due to a lack of animal models, there have been no efficacy studies of any vaccine platform in a disease model. The Ad work is, therefore, the first attempt to evaluate the protective efficacy a potential vaccine against CCHFV and the first to observe the difference between essential and non-essential or detrimental immune responses following vaccination.

## 2. MATERIALS AND METHODS

### 2.1 Maintenance of tissue culture

SW-13 (human adrenal gland carcinoma) cells (obtained from ATCC, Manassas, VA, USA) were maintained in Leibovitz's L-15 medium (ATCC) supplemented with 10% heat-inactivated (30 minutes at 56°C) fetal bovine serum (FBS), 1mM L-glutamine, 0.5U/mL penicillin and 0.5µg/mL streptomycin (Life Technologies Corp., Carlsbad, CA, USA) at 37°C in an environment not enriched in $CO_2$.

HEK 293 (human embryonic kidney) cells (obtained from Sonia Best, Rocky Mountain Laboratories (RML), Hamilton, MT, USA) Vero (Macaque kidney) cells (ATCC) and baby hamster kidney (BHK) cells stably expressing T7 polymerase (obtained from Hideki Ebihara RML, Hamilton, MT, USA) were maintained in Dulbecco's modified Eagle medium (DMEM) supplemented with 10% FBS 2mM L-Glu, 0.5U/mL penicillin and 0.5µg/mL streptomycin (Life Technologies Corp.) at 37°C in a 5% $CO_2$ environment.

**2.2 Virus infections and infectivity assays**

**2.2.1 CCHFV infection**

All infectious CCHFV work was performed in BSL4 facilities at RML according to standard operating procedures (SOPs). CCHFV strain IbAr10200 (obtained from Michael Holbrook, University of Texas Medical Branch, Galveston, TX, USA) was used in all experiments and propagated in SW-13 cells. To propagate CCHFV, T150 flasks were inoculated with 3 mL of CCHFV ($2x10^5$ $TCID_{50}$ total per flask, multiplicity of infection [MOI] of 0.01) in L-15 medium (ATCC) supplemented with 2% FBS for 1 hour with occasional rocking. Following infection 27 mL of L-15 medium supplemented with 2% FBS was added to the flasks and the flasks were observed for cytopathic effect (CPE) for 6-7 days. Following appearance of CPE, supernatants were collected, centrifuged at 1500 RPM for 5 minutes, aliquoted, and frozen at -80 °C. Viral titers were determined by the tissue culture infectious dose 50% ($TCID_{50}$) assay (see section 2.2.2) and are expressed as $TCID_{50}$/mL or $TCID_{50}$/g. All viral stocks were stored in liquid nitrogen and were used immediately after thawing; all thawed and leftover virus stock was immediately destroyed according to RML SOPs.

**2.2.2 CCHFV titration**

Approximately $1.5x10^4$ SW-13 cells were seeded in 96-well tissue culture plates (Thermo Fisher Scientific Inc., Rockford, IL USA) overnight in L-15 medium supplemented with 10% FBS. The following day CCHFV titrations were performed on 10-fold serial dilutions (prepared in L-15 media supplemented with 2% FBS) of tissue (10% w/v solution), blood (10% v/v solution) or tissue culture supernatant (10% v/v solution) to form a dilution range of $10^{-1}$ to $10^{-7}$. The L-15 medium containing 10% FBS was removed from SW-13 cells and replaced with 100µL of CCHFV diluted in L-15 media supplemented with 2% FBS. The cells were incubated for 6 days at 37°C without increased $CO_2$, and wells were scored for CPE. Virus titres were calculated using the Reed-Münch formula [103] (Figure 10) and expressed as $TCID_{50}$ per gram of tissue or mL of blood/supernatant.

(i) Proportionate Distance (PD) = $\frac{(\%\ CPE\ at\ dilution\ above\ 50\%) - 50\%}{(\%\ CPE\ at\ dilution\ above\ 50\%) - (\%\ CPE\ at\ dilution\ below\ 50\%)}$

(ii) $-\text{Log}_{(\text{fold dilution})}$(dilution interval) = dilution above 50% CPE in replicates;
e.g. 10-fold dilutions and 5 dilution steps or wells with >50% of the wells containing CPE = $-\text{Log}(10^5) = -5$

(iii) $TCID_{50} = 10^{-(\text{Log(dilution interval)-PD})}$

(iiii) $TCID_{50}/mL = \frac{TCID_{50}}{starting\ volume}$

e.g.

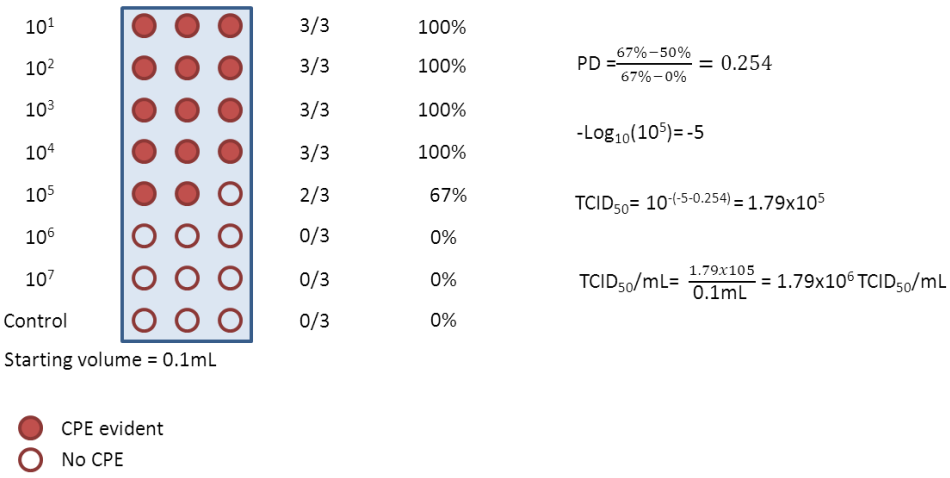


Figure 10. Reed-Muench Formula for calculation of $TCID_{50}$ of CCHFV stock. An example is shown to illustrate how a dilution series conducted in series is interpreted.

### 2.2.3 Quantitative reverse transcription polymerase chain reaction of CCHFV

To detect CCHFV level and sites of replication quantitative RT-PCR (qRT-PCR) was employed in addition to viral isolation. All qRT-PCR were performed on the Rotor-Gene 6000 thermal cycler (Qiagen) using the QuantiFast Probe RT-PCR Kit (Qiagen). CCHFV S segment specific primers CCHFSF and CCHFSR (Table 1) and probe CCHFSPr (Table 1) were designed and synthesized by TIB MOLBIOL (Adelphia, NJ, USA). RNA from whole blood or tissue culture supernatant was extracted as described in section 2.3.1.1. 5µL of extracted RNA was mixed with 12.5µL 2x QuantiFast probe RT-PCR master mix (1x final concentration), 0.5µL of 20mM primer/ 10 mM probe mix (final concentration of 0.4µM of each CCHFSF and CCHFSR and 0.2µM of CCHFSPr), 0.25µL of QuantiFast RT mix and 6.75µL of DEPC water. The reaction was incubated at 50°C for 10 minutes followed by incubation at 95°C for 5 minutes followed by 40 cycles of 95°C for 5s followed by 60°C for 10s.

Table 1. Primer sequences, melting temperatures and target sequence length. All cloning primers (white background) were obtained from Integrated DNA technologies (Coralville, IA, USA) and quantitative RT-PCR primers (grey background) from TIB Molbiol (Adelphia, NJ, USA).

| Name | Sequence | $Tm_{co}$ (°C) | $Tm_{tot}$ (°C) | Size (kb) |
|---|---|---|---|---|
| pCNPF | GCTAGAATTCCACCATGGAAAACAAGATCGAGGTGAA | 54.5 | 63.4 | 1.6 |
| pCNPR | CGATAGATCTCTATTAAATGATGTTAGCACTGGTGGCA | 57 | 61.4 | 1.6 |
| pCGPCF | CGATCTGTTTACGCGTCACCATGCATATATCATTAATGTATG CAATCC | 56.5 | 64.3 | 5.5 |
| pCGPCR | GAGTTACTTTCCTAGGCTAGCCAATGTGTGTTTTTGTAGAG AA | 55.6 | 63.4 | 5.5 |
| pAdGnF | GTAACTATAACGGTCCACCATGTCAGAAGAACCCAGTGAT GAC | 54.2 | 65.1 | 1 |
| pAdGnR | ATTACCTCTTTCTCCTTACTACAACAGCTTTCTTACAACCCA | 56.3 | 63 | 1 |
| pAdGcF | GTAACTATAACGGTCCACCATGTTCCTAGATAGTACAGCTA AAGG | 50.9 | 63.3 | 2.5 |
| pAdGcR | ATTACCTCTTTCTCCTTACTAGCCAATGTGTGTTTTTGTAGA | 53.5 | 62.2 | 2.5/5.5 |
| pAdPreG nF | GTAACTATAACGGTCCACCATGCACAATGAAACTAGACACA ATAA | 53.1 | 63 | 5.5 |
| pAdNPF | GTAACTATAACGGTCCACCATGGAAAACAAGATCGAGGTG | 52.9 | 63.9 | 1.6 |
| pAdNPR | ATTACCTCTTTCTCCCTATTAAATGATGTTAGCACTGGTGG | 53.3 | 62.4 | 1.6 |
| pVSVGP CF | CGATCTGTTTACGCGTCACCATGCACAATGAAACTAGACAC AATAA | 55.6 | 63.4 | 5.5 |
| pVSVGP CR | GAGTTACTTTCCTAGGCTAGCCAATGTGTGTTTTTGTAGAG AA | 54.6 | 65.5 | 5.5 |
| CCHFSF | TGGACTTGTGGACACCTTCAC | 57 | 57 | 0.2 |
| CCHFSR | CAATGCCAGTGGAGCTAACC | 56 | 56 | 0.2 |
| CCHFSPr | 6FAM-TGCCTCCACCAGAGCAGATGCGT—BBQ | 65 | 65 | N/A |

### 2.2.4 Adenovirus infection

All infectious Ad work was performed in BSL2 facilities at RML according to RML SOPs. The Human Ad5 strain, (rescued from Clontech AdenoX systems 3 kit see section 2.3, Clontech Laboratories Inc., Mountain View, CA, USA) was used in all experiments and propagated in HEK 293 cells. Following extensive CPE (>50% of cells rounded and detached), HEK 293 cells and media were collected in 50 mL conical falcon tubes; centrifuged at 1500xg for 5 minutes; the supernatant aspirated and the cell pellet resuspended in a small volume of PBS (approximately 1mL per $2x10^7$ cells). Ad was recovered from cells by a series of 3 freeze-thaw cycles (freeze at -80°C for 30 minutes followed by a 2-5 minute thaw at 37°C) and cellular debris was removed by low speed centrifugation (1500xg for 5 minutes). Viral titers were determined by the AdenoX Rapid Titer Kit (Clontech Laboratories Inc.) (see below) and are expressed as infectious units (ifu)/mL.

### 2.2.5 Ad titration

Approximately $2.5x10^5$ HEK 293 cells were seeded in 24-well tissue culture plates (Thermo Fisher Scientific Inc.) in 500µL of DMEM supplemented with 10% FBS for <2 hours. Immediately following HEK 293 seeding, 10-fold serial dilutions (prepared in sterile phosphate buffered saline (PBS)) from infected, lysed HEK 293 cells were prepared to form a dilution range of $10^{-3}$ to $10^{-8}$. 100µL of diluted Ad was added to each well and the cells were incubated for 2 days at 37°C in a 5% $CO_2$ environment. Following 2 days, DMEM was aspirated, the cells were dried (~5 minutes) and 500µL of ice cold methanol was added to each well and the plates were incubated for 10 minutes at -20°C to fix and permeabilize the cells. Following fixation the cells were washed twice with PBS containing 1% w/v bovine serum albumin (BSA) (PBSB) and either stored in PBSB overnight at 4°C or stained immediately. Fixed 293 cells were incubated with a mouse anti-Ad

hexon antibody diluted 1:1000 in PBSB for 1 hour at 37°C; washed 3 times with PBSB; incubated with a rat anti-mouse horseradish peroxidase (HRP) conjugated antibody diluted 1:500 in PBSB for 1 hour 37°C; washed 3 times with PBSB; stained with 3,3'-Diaminobenzidine (DAB) and the stained cells were counted with a microscope (antibodies and DAB from Clontech Laboratories Inc.). Virus concentration was calculated by averaging the number of infected cells in 3 fields of a 24-well plate well, multiplying by the number of fields/well and dividing it by the volume of virus multiplied by the dilution factor, i.e. $\frac{\frac{infected\ cells}{field}\ x\ \frac{fields}{well}}{Volume\ virus\ (mL)\ x\ dilution}$ =ifu/mL. For example, if average number of infected cells is 67 from a 24-well plate well infected with 100µL at a dilution of $10^{-5}$ from virus stock observed at 200x total magnification the ifu/mL is equal to $\frac{67\frac{infectedcells}{field}\ x\ 313\ \frac{fields}{well}}{(0.1mL)x\ 10^{-5}\ dilution}$ = 2.1x$10^{10}$ ifu/mL.

**2.2.6 VSV-GPC titration**

VSV-GPC recombinant virus was titrated on vero cells 48-well plates. Briefly, in 48-well plates vero cells were seeded at a density of greater than 90%. 10-fold dilutions of VSV-GPC from $10^{-2}$ to $10^{-8}$ were made in DMEM which was not supplemented with FBS. The media was removed from Vero cells and in each well was placed 200µL of the diluted VSV-GPC. The wells were incubated at 37°C for 2 hours with occasional rocking. Following incubation the infectious supernatant was removed, washed 3 times with 200 µL of plain DMEM and the vero cells overlaid with 200µL of 1.4% carboxymethylcellulose ( CMC, 50:50 2.8% CMC in PBS:2xMEM supplemented with 5% FBS). All samples were done in triplicate. The plaques were developed for 8 days, stained with crystal violet stain (0.2% crystal violet w/v, 4% formalin, Sigma-Aldrich) overnight and the number of plaques at each dilution counted by eye. VSV-GPC concentration (plaque forming units/mL or pfu/mL) was calculated by averaging the number of plaques per

well from the 3 wells and dividing it by the volume of virus multiplied by the dilution factor, i.e. $\frac{\frac{number\ of\ plaques}{wells\ counted}\ or\ (average\ plaque\ number)}{Volume\ virus\ (mL)\ x\ dilution}$ =pfu/mL. For example, if average number of infected cells is 67 from 3 wells, i.e. 201 total plaques from 3 wells, infected with 200µL at a dilution of $10^{-5}$ from virus stock the pfu/mL is equal to $\frac{\frac{201\ total\ plaques}{3\ wells}}{(0.2mL)x10^{-5}\ dilution}$ = 3.4x$10^{7}$ pfu/mL.

2.2.7 VSV-GPC neutralization assay

Recombinant VSV-GPC (200 pfu, MOI≈$10^{-4}$) was incubated with serial dilutions (1:100 to 1:3200, 2-fold dilutions) of DMEM, and sera of mock vaccinated, Ad-GPC/Ad-NP vaccinated or Ad-GPC/Ad-NP vaccinated and CCHFV challenged IFNAR$^{-/-}$ mice in DMEM not supplemented with FBS and incubated for 1 hour at 37 °C. Following incubation, the VSV-GPC and antibody mixture was applied to 6-well plate of Vero cells, in triplicate. The cells were incubated for 2 hours with occasional rocking. Following incubation the neutralization supernatants were removed, washed 3 times with 1000 µL of plain DMEM and the Vero cells overlaid with 1000µL of 1.4% CMC (50:50 2.8% CMC in PBS:2xMEM supplemented with 5% FBS, 2.5% final FBS concentration). VSV concentration was determined as described in section 2.2.5 and the percent inhibition was determined by dividing the calculated pfu following incubation with sera with pfu without incubation with sera i.e. $\frac{Sera\ pfu}{Mock\ pfu}\ x\ 100\%$. ≥50% inhibition was considered to be positive for neutralization at a given dilution of sera, e.g the VSV-GPC pfu/mL for untreated VSV-GPC is 200, at 1:100 dilution of Ad-GPC/Ad-NP vaccinated sera the VSV-GPC pfu/mL is 100, whereas at the 1:200 dilution of Ad-GPC/Ad-NP vaccinated sera the VSV-GPC pfu/mL is 200. Therefore a neutralizing response of ≥50% is last seen at a dilution of 1:100.

## 2.3 Construction of CCHFV proteins expression vectors

### 2.3.1 Isolation of CCHFV RNA and DNA

#### 2.3.1.1 RNA extraction

SW-13 cells were infected with CCHFV (MOI 0.01) as described in section 2.2.1 and CCHFV RNA was isolated using the QIAamp Viral RNA kit (All contents from Qiagen, Valencia, CA, USA, unless otherwise indicated). At 4 to 6 days post infection (p.i.) 140µL of CCHFV infected SW-13 supernatant was mixed with 560µL of Buffer AVL and either frozen at -80°C or processed immediately. Immediately prior to processing supernatant was incubated in AVL for 10 minutes and transferred into a new tube containing 560µL of 100% ethanol (Sigma-Aldrich, St. Louis, MO, USA). The samples were then removed from BSL-4 and immediately applied to a RNA binding column and spun at 6000xg for 1 minute. The columns were washed with 500µL of buffer AW1 and centrifugation at 6000xg for 1 minute; 500µL of buffer AW2 following by centrifugation at 15000xg for 3 minutes; and dried by centrifugation at 15000xg for 1 minute over an empty collection tube. Total RNA was eluted, by addition of 60µL of RNase-free water followed by centrifugation at 15000xg for 1 minute (RNase-free water, buffers and columns from Qiagen); aliquoted and frozen at -80°C until use.

#### 2.3.1.2 Agarose gel DNA extraction

Following polymerase chain reaction (PCR) or restriction endonuclease (REN) digestion samples were resolved on a 1% agarose gel (1% agarose in TAE buffer, ~1 hour at 100V). The correct size band was excised and DNA was purified using the QIAquick gel extraction kit (Qiagen). Briefly, the excised band was dissolved in 3 times the volume of GC buffer at 50°C with gentle shaking (~400 rotation per minute); the DNA was precipitated with 1 volume of 100% isopropanol (Sigma); the solution loaded onto a extraction kit column and centrifuged at ≥8000xg for 15

seconds; the column was washed with 500µL GC buffer and 700µL PE buffer (10mM Tris-HCl, 80% ethanol), dried by centrifugation at 15000xg for 60s and eluted in 50µL of deionized water (DW).

2.3.1.3 Gel-free DNA extraction

Following PCR or REN digestion if gel extraction was unnecessary due to highly specific PCR, serial digestion or over-digestion, QIAquick PCR purification kit (Qiagen) was used to purify DNA. Briefly, the reaction was diluted in 5 volumes of PB buffer; the diluted solution was loaded onto a DNA binding column and centrifuged at ≥8000xg for 15 seconds; the column was washed with 700µL of PE buffer, dried by centrifugation at 15000xg for 60s and eluted in 50µL of DW.

2.3.1.4 Column miniprep plasmid extraction

Small scale DNA extraction was accomplished using QIAprep Spin Miniprep kit ~1.5mL of overnight bacterial culture was pelleted by centrifugation at 15000xg for 20-40 seconds; the bacterial pellet was resuspended in 250µL P1 buffer (50 mM Tris hydrochloride, pH 8.0; 10 mM EDTA; 100µg/mL RNase A) by gentle agitation, lysed by addition of 250µL of P2 buffer (200 mM sodium hydroxide; 1% sodium dodecyl sulfate w/v) and neutralized with 350µL of N3 (4.2 M guanidine-HCl; 0.9 M potassium acetate; pH 4.8) buffer; majority of cellular protein and membranes were removed from the DNA containing supernatant by centrifugation at 15000xg for 10 minutes. The supernatant was transferred to a DNA binding column and centrifuged at 15000xg for 15-60s; the DNA washed with 500µL of buffer PB and 700µL of buffer PE; the column was dried by centrifugation at 15000xg for 60s and DNA was eluted in 50µL of DW.

2.3.1.5 Crude miniprep plasmid extraction

The crude miniprep procedure used ~1.5mL of overnight bacterial culture which was pelleted by centrifugation at 15000xg for 20-40 seconds; the bacterial pellet was resuspended in 200µL P1 buffer (see section 2.3.1.4) by gentle agitation, lysed by addition of 200µL of P2 buffer (see section 2.3.1.4) and neutralized with 200µL of cold P3 buffer (3.0 M potassium acetate); majority of cellular debris were removed from the DNA containing supernatant by centrifugation at 15000xg for 10 minutes. The supernatant was removed to a new tube and the DNA precipitated with 500µL of 100% isopropanol (Sigma-Aldrich) followed by centrifugation at 15000xg for 15 minutes to pellet the DNA. The DNA pellet was washed twice with 1mL of 70% ethanol in DW solution (70% EtOH) followed by centrifugation at 15000xg for 5 minutes. The 70% EtOH was removed, the pellet dried for ≥12 minutes using the SpeedVac instrument (Thermo Scientific) and resuspended in 50µL of DW water.

2.3.1.6 Maxiprep plasmid extraction

DNA maxipreps were carried out using QIAGEN Plasmid Plus Maxi Kit (Qiagen). Briefly, 200mL of overnight bacterial culture was pelleted by centrifugation at 3500xg for 30 minutes; resuspended in 10mL of P1 buffer (see section 2.3.1.4) by pipetting, lysed by addition of 10mL of P2 buffer (see section 2.3.1.4) and neutralized with 10mL of cold P3 buffer (see section 2.3.1.5). To remove bacterial debris, the neutralized solution was briefly centrifuged (~5 minutes at 3500xg). During centrifugation the DNA binding column was equilibrated with 10mL QBT buffer (750 mM sodium chloride; 50 mM 3-(N-morpholino)propanesulfonic acid pH 7.0; 15% 2-propanol; 0.15% Triton X-100). The clarified supernatant was filtered into the DNA binding column, washed twice with a total volume of 60mL of QC buffer (1.0 M sodium chloride; 50 mM 3-(N-morpholino)propanesulfonic acid pH 7.0; 15% 2-propanol), and eluted with 15mL of QF

buffer (1.25 M sodium chloride; 50mM Tris hydrochloride pH 8.5; 15% 2-propanol). The eluted DNA was precipitated with 10.5mL of 100% isopropanol (Sigma-Aldrich) and centrifuged at 15000xg for 30 minutes. The precipitated DNA was washed twice with 2mL of 70% EtOH followed by centrifugation at 15000xg for 5 minutes. The 70% EtOH was removed, the pellet dried for ≥12 minutes using the SpeedVac instrument (Thermo Scientific) and resuspended in 500µL of DW water. The concentration of plasmid DNA was determined using a Nanodrop 8000 instrument (Thermo Scientific) and adjusted as needed.

### 2.3.2 RT-PCR of CCHFV

#### 2.3.2.1 RT of CCHFV RNA

Extracted RNA was reverse-transcribed using SuperScriptIII reverse transcriptase (RT) (Life Technologies). 2µL of total RNA (40-500µg total RNA) was incubated with 200ng of random hexamers (in 2µL), and 1µL of 10mM dNTP mix (10mM of each dATP, dTTP, dCTP, dGTP) and 8µL of RNase-free water were mixed and incubated at 65°C for 5 minutes. Following the high temperature incubation the mixture was incubated on ice for 2-5 minutes, briefly centrifuged and 4 µL of 5X First-Strand Buffer (250 mM Tris-HCl (pH 8.3 at room temperature), 375 mM KCl, 15 mM MgCl2), 1 µL of 0.1 M Dithiothreitol, 1 µl of 40 U/µL RNaseOUT™ Recombinant RNase Inhibitor and 1 µL of 200U/µL SuperScript™ III RT. The complete RT mixture was incubated at room temperature for 5 minutes followed by 50°C for 1 hour to generate complementary DNA (cDNA) and the reaction stopped by heating to 70°C for 15 minutes followed by cooling to 4°C. Following stoppage 1µL RNase H (2U/µL) was added to the mixture and incubated at 37°C for 20 minutes. The cDNA was immediately used as a PCR template or frozen at -20°C.

2.3.2.2 PCR to amplify target cDNA

cDNA generated as described above or plasmid DNA were used at templates for CCHFV specific PCRs. iProof polymerase (Bio-rad Laboratories, Hercules, CA, USA) was used for all PCRs according to manufacturer's instructions. Briefly, 1µL of CCHFV cDNA was mixed in a reaction containing 0.8mM of a NP, GPC, $G_N$ or Gc specific primers (Table 1), 0.3mM dNTPs, 1x HF buffer, 3% DMSO and 1U of iProof polymerase in a 50µL reaction (Table 2). The reaction was conducted in a DNA Engine Tetrad® 2 Thermal Cycler (Bio-Rad) using cycling conditions as outline in Tables 1 and 3. Briefly, double stranded DNA (dsDNA) dissociation, or melting, into single stranded DNA (ssDNA) is accomplished by an initial heating to 98°C; followed by 4 cycles of melting (98°C for 15s), annealing (3°C higher than primer complimentary sequence melting temperature (Tm) for 25s) and extension (72°C for 20s per 1000 bases (1kb)); followed by 31 cycles of melting (98°C for 15s), annealing (3°C higher than primer total sequence Tm for 25s) and extension (72°C per 1kb); finishing off with a final extension (72°C for 600s). Tm was calculated using OligoAnalyzer3.1 (Integrated DNA Technologies, Inc, Coralville, IA, USA). The PCR is divided into 2 steps to insure the absolutely highest possible annealing temperature was used to avoid non-specific annealing and extension. The primers almost always contain non-sequence complimentary region (usually between 20-40% of the total primer length, marked in red in Table 3) and therefore the complimentary annealing temperature is used during initial 4 cycles of the PCR; once 4 cycles have passed the amount of template containing the full primer sequence (newly synthesized DNA in the first 4 cycles) becomes the dominant template in the reaction (~90% of total template DNA) and the higher annealing temperature ($T_m$ total) is used for the remaining 31 cycles. For example, from Table 1 pCNPF and pCNPR have a Tm complementary of 54.5°C and 57°C, respectively; a Tm total of 63.4°C and 61.4°C respectively; and are used to amplify the NP gene which is 1.6kb. Therefore following the steps from Tables 1

and 2 the extension time is 20s/kb x 1.6kb = 32s for all extension cycles. As the lowest Tm complementary is 54.5°C the Anneal 1 temperature is 54.5°C + 3°C = 57.5°C. Following the initial 4 cycles, the annealing temperature is raised to 64.4°C (the lowest Tm total is 61.4 + 3 =66.4°C) and the reaction is allowed to proceed for 31 additional cycles (35 cycles total) of a total PCR.

Table 2. Generic PCR components and final concentrations

| Component | Volume (µL) [final concentration, if applicable] |
|---|---|
| Template | 1 [1-5ng/µL] |
| Forward primer (10mM) | 4 [0.8mM] |
| Reverse primer (10mM) | 4 [0.8mM] |
| dNTPs (10mM of each dATP, dTTP, dCTP, dGTP) | 1.5 [0.3mM] |
| 5x Buffer HF with 7.5mM $MgCl_2$ | 10 [1xBuffer HF, 1.5mM $MgCl_2$] |
| 100% Dimethyl Sulfoxide | 1.5 [3% v/v] |
| iProof 2U/µL | 0.5 [1U] |
| DNA-free water | 28 |
| Total | 50 |

Table 3. General thermal cycler program for PCR

| Order | Number of cycles | Step name | Time (s) | Temperature (°C) |
|---|---|---|---|---|
| 1 | X1 | Initial melt | 120 | 98 |
| 2 | x4 | Melt | 15 | 98 |
| 3 | | Anneal 1 | 25 | Lowest Tm complementary[a] + 3 |
| 4 | | Extension | 20 per 1000 bases (kb) | 72 |
| 5 | x31 | Melt | 15 | 98 |
| 6 | | Anneal 2 | 25 | Lowest Tm total[a] + 3 |
| 7 | | Extension | 20 per kb | 72 |
| 8 | X1 | Final extension | 600 | 72 |

[a] =refer to Table 1; Tm = melting temperature of primer, calculated using OligoAnalyzer 3.1, (Integrated DNA Technologies)

### 2.3.3 DNA cloning

#### 2.3.3.1 Expression plasmid constructions for CCHFV proteins

Insert DNA was generated by PCR with pCNPF/pCNPR and pCGPCF/pCGPCR for NP and GPC insert DNA for pCAGGS (Figure 11), respectively. The amplified DNA (NP or GPC insert DNA) was gel purified and inserted into the expression vector pCAGGS with the appropriate enzymes (FastDigest EcoRI, BglII for NP, and FastDigest MluI, AvrII for GPC, Thermo Scientific Molecular Biology). Briefly 6.5µL of 10x FastDigest buffer (1x final concentration) and 100mM (10mM final concentration) BSA were added to 48µL of eluted DNA and 2µL each of the appropriate enzymes were added to the reaction. 2µg of pCAGGS vector were digested with the identical enzymes. Digestions were carried out at 37°C for approximately 3 hours. Following digestion the DNAs were purified using the QIAquick PCR purification kit. Briefly, the DNA was diluted in 5x volume of buffer PB and loaded onto a DNA affinity column, washed once with 700µL buffer PE, dried by centrifugation at 15000xg for 60s and eluted in 50µL of DW. The concentrations of insert and vector DNAs were quantified using a Nanodrop 8000 instrument (Thermo Scientific) and the final concentrations of both were adjusted to 30 µg/µL. A ratio of 3:1 insert:vector were ligated with T4 DNA ligase (Life Sciences) in a total reaction volume of 15µL overnight at 14°C. Following overnight ligation the mixture was used to transform chemically competent *Escherichia coli (*One Shot® TOP10 Chemically Competent E. coli (Life Technologies)).

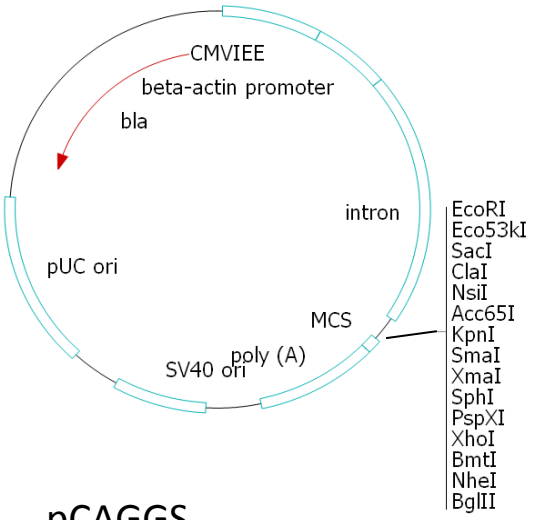


pCAGGS
4735 bp

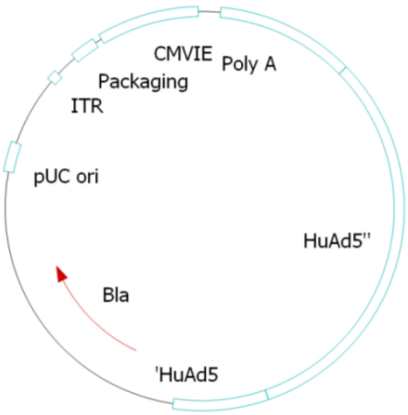


pAdenoX
34209 bp

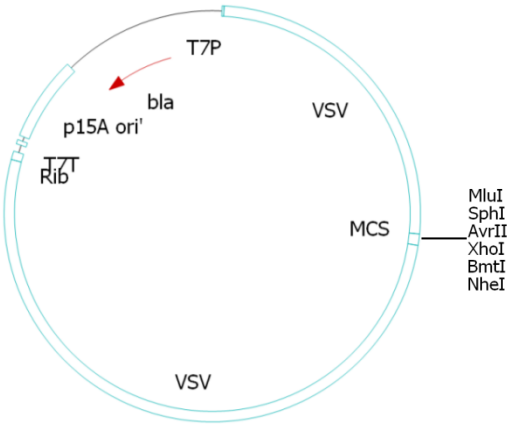


pAK15-VSV
12443 bp

Figure 11. Vector maps and sizes of pCAGGS, pAdenoX, pAK15-VSV plasmids. Unique restriction endonuclease digestion sites which may be used for cloning are shown for pCAGGS and pAK15-VSV. Due to a lack of unique restriction endonuclease digestion sites in pAdenoX none are shown. pAdenoX features are not to scale in order to demonstrate the features more clearly. MCS: multiple cloning site; pUC/p15A ori: plasmid bacterial origin of replication; SV40 ori: plasmid mammalian origin of replication; CMVIEE/CMVIEE: cytomegalovirus promoter; T7P: T7 promoter; T7T: T7 terminator; bla: beta-lactamase; Poly A: poly adenylation site; Rib: Hepatitis D ribozyme; Packaging: Adenovirus packaging signal; HuAd5: human Adenovirus 5 genome; VSV: vesicular stomatitis virus genome.

#### 2.3.3.2 pAdenoX plasmid expression of CCHFV proteins

The In-Fusion system was used to clone CCHFV proteins into the pAdenoX vector (Figure 11) utilizes an exonuclease and PCR imparted complementary sequence to generate very long (15 nucleotide) complementary overhangs and thus bypasses the need to perform restriction endonuclease digestion (Figure 12). To obtain insert DNA, GPC, $G_N$, $G_C$, and NP were amplified from corresponding pCAGGS plasmids using the pAdPreGn/pAdGcR, pAdGnF/pAdGnR, pAdGcF/pAdGnR and pAdNPF/pAdNPR (Table 1), respectively. Following extraction, insert DNA was simultaneously digested and ligated into the pAdenoX plasmid using the In-Fusion cloning system (Clontech). Briefly, 2 µL of insert DNA (100µg total) were mixed with 1µL linearized pAdenoX (200µg total) and 2µL 5x In-Fusion HD enzyme premix (1x total) in a 10µL total reaction and incubated for 15 minutes at 50°C. Following incubation the reaction was cooled on ice for ~ 5 minutes and used immediately to transform chemically competent *E. coli* (Stellar™ Competent Cells see section 2.3.3.4 Bacterial transformation (Clontech).

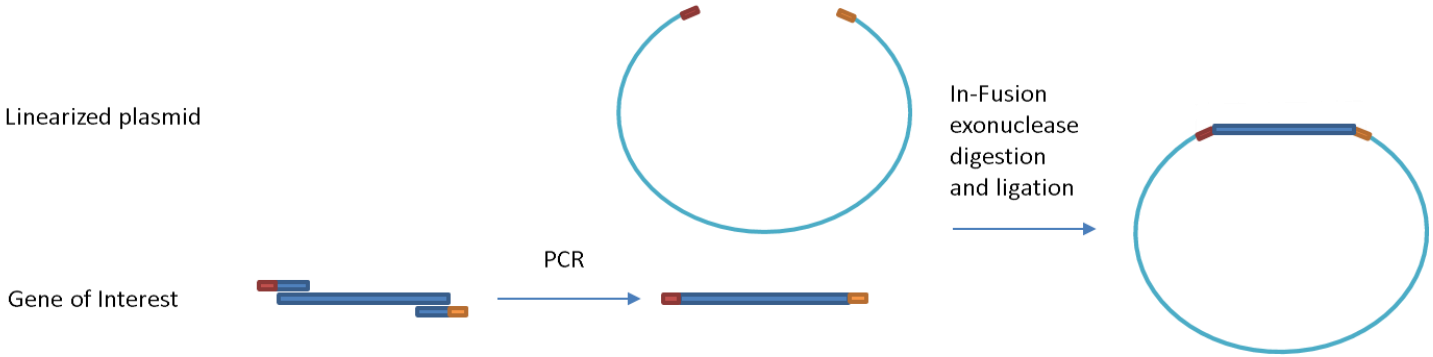


Figure 12. Schematic of an In-Fusion Reaction. Primers are designed with a 15 nucleotide stretch in the 5' to 3' orientation complementary to a linearized vector. The primers are then used to amplify the sequence of interest and the vector is linearized. The purified insert and vector are then incubated in the presence of In-Fusion exonuclease. The 5' terminal 15 nucleotides are removed by the In-Fusion exonuclease on both the vector and insert and the ligation occurs concurrently. The ligation mixture may then used immediately to transform competent cells.

#### 2.3.3.3 pAK-VSVΔG plasmid expression of CCHFV proteins

GPC DNA was amplified by PCR using the pVSVGPCF/pVSVGPCR primers (Table 1). Following extraction, CCHFV GPC DNA was simultaneously digested and ligated into pAK-VSVΔG digested with AvrII and KpnI using the In-Fusion cloning system (Clontech). Briefly, 2 µL of insert DNA (100µg total) were mixed with 1µL linearized pAdenoX (200µg total) and 2µL 5x In-Fusion HD enzyme premix (1x total) in a 10µL total reaction, incubated and used to transform competent bacteria as described in section 2.3.3.4.

#### 2.3.3.4 Bacterial transformation

2 commercially available E. coli strains were used for all transformation experiments, One Shot® TOP10 Chemically Competent E. coli (Life Technologies) and Stellar™ Competent Cells (Clontech) for pCAGGS and pAdenoX vector cloning, respectively. 7µL of pCAGGS or 1.5µL of pAdenoX ligation mixtures were used for all transformation reactions and the same incubation conditions were used for all transformation procedures. 50µL of competent *E. coli* were added to the bottom of a 15mL conical falcon tube and incubated on ice; the appropriate amount of ligation mixture was added to the tube and the reaction was incubated on ice for 30 minutes. Following the incubation transformed *E. coli* were heat shocked at 42°C for 45s followed by a brief incubation on ice (3-5 minutes). 900µL of 37°C SOC medium (2% tryptone, 0.5% yeast extract, 10 mM sodium chloride, 2.5 mM potassium chloride, 10 mM magnesium chloride, 10 mM magnesium sulfate and 20 mM glucose) was added to the mixture and the cells were incubated at 37°C with shaking (250-300 rpm) for approximately 1 hour. Following incubation 100µL of the incubation mixture was spread on a 37°C LB agar plate supplemented with ampicillin (100µg/mL). The remainder of the bacterial cells was centrifuged at 4000xg for 2 minutes,

resuspended in 100µL of 37°C SOC media and spread on a 37°C LB agar plate supplemented with ampicillin. All plates were incubated overnight (≥16 hours) at 37°C.

#### 2.3.3.5 Screening bacterial clones

Selected bacterial clones were cultured in ~2mL of LB broth supplemented with 100µg/mL of ampicillin for overnight at 37°C with shaking. Following culturing the clones were extracted either via QIAprep Spin Miniprep Kit (Qiagen) or "crude" DNA miniprep method as described in sections 2.3.1.4 and 2.3.1.5. The extracted DNA was screened by REN digestion according to the recipe outlined in Table 4 and digested for 30-60 minutes at 37°C. Following digestion the clones were screen by agarose gel electrophoresis as described previously. Clones which contained expected migration patterns following agarose gel electrophoresis were sequence confirmed.

Table 4. Restriction endonuclease reaction for screening plasmids

| Component | Volume (µL) |
|---|---|
| Plasmid DNA | 5 |
| Fermentas 10X Buffer | 1 |
| BSA (100mM) | 1 |
| REN 1 | 0.2 |
| REN 2 | 0.2 |
| DW | 2.6 |
| Total | 10 |

#### 2.3.3.6 DNA sequencing

Gel positive clones were sequenced by an in-house sequencing core BigDye Terminator v3.1 Cycle Sequencing Kit on an ABI DNA Analyzer 3730xl according to manufacturer's instructions (Life Technologies).

### 2.3.4 Rescue of recombinant viruses expressing CCHFV proteins

#### 2.3.4.1 Rescue of recombinant Ad

Seqeunce confirmed pAdenoX constructs were digested with PacI. The reaction was combined as outlined in Table 5.

Table 5. Reaction input for PacI digestion of pAdenoX constructs for rescue of replication incompetent Adenovirus

| Reagent | Volume |
|---|---|
| pAdenoX construct (500ng/µL) | 10 |
| Fermentas buffer | 4 |
| BSA (100mM) | 4 |
| PacI FastDigest (10U/µL) | 2 |
| DW | 20 |
| Total | 40 |

The reaction was incubated at 37°C for 2 hours without shaking. Following digestion the reaction volume was brought up to 100µL with DW; 100µL of phenol:chloroform:isoamyl alcohol (25:24:1) (Life Technologies) was added to the mixture; the mixture was agitated gently and then centrifuged at ≤15000xg for 5 minutes resulting in the appearance of an aqueous phase on top of the solution; the top layer of the solution was carefully removed to a new tube and 400µL of 100% EtOH and 10µL of 3M sodium acetate were added to the tube; the tube was incubated at -20°C for 15 minutes and centrifuged at ≥15000xg for 5 minutes; the supernatant was discarded and the DNA pellet washed with 300µ of 70% EtOH followed by centrifugation at 15000xg for 5 minutes; the EtOH was removed, the DNA pellet air dried for 10-15 minutes in a biological safety cabinet and resuspended in 10µL of DW. 10µL of digested, purified pAdenoX DNA was mixed with 209µL of DW and 31µL of 2M calcium solution; 250µL of 2x HEPES buffered saline were added drop-wise to a DNA mixture undergoing constant shaking; the mixture was incubated for 15 minutes at room temperature and added drop-wise to a 60mm dish of ~50-70% 293 cells and incubated for 12-16 hours at 37°C. Following the 12-16 hour incubation the

medium was replaced with fresh culture medium. 293 cells were observed for CPE for 6-14 days post transfection. The cells were collected by scraping into medium and lysed by 3 freeze-thaw cycles. The cellular debris was removed from adenovirus by centrifugation at 1500xg for 5 minutes. Adenovirus was propagated as described in section 2.2.4.

#### 2.3.4.2 Rescue of VSV expressing CCHFV glycoproteins

pAK-VSVΔG CCHFV GPC were selected for virus rescue following sequence confirmation. A day prior to rescue approximately $5x10^5$ BHK-T7 cells per well were plated in 5 6-well plates. To rescue recombinant VSV CCHFV GPC (VSV-GPC) the helper plasmids expressing VSV nucleoprotein (pCAGGS-N), VSV RNA dependent RNA polymerase (pCAGGS-L), and VSV phosphoprotein (pCAGGS-P) were purified by standard maxiprep (all constructs obtained from Andrea Marzi and Josh Marceau, RML, Hamilton, MT, USA). 2.0µg of VSV-GPC was mixed with 0.5µg of pCAGGS-N, 0.25µg pCAGGS-L, and 1.25µg of pCAGGS-P per rescue well. 100µL of OptiMEM (Life Technologies) and then 12µl of LT1 transfection reagent (Mirus Bio LLC, Madison, WI, USA) were added to the tube, mixed and incubated at room temperature for 30 minutes. During the incubation period BHK-T7 cells were prepared for transfection by removing previous media and replacing it with fresh, warm (37°C) DMEM containing 5% FBS. Approximately 120µL of the transfection mixture was added drop-wise to each well of BHK-T7 cells and the cells were placed back into the incubator overnight. The transfected cells were kept for approximately 2 weeks following transfection. Every 3 to 4 days following transfection (day 3, 7, and 14), or when the BHK-T7 cells showed significant CPE (>50% of cells rounded and/or floating) the wells were blind passaged onto Vero cells and media were replaced onto the initial transfection wells.

In order to blind passage the recombinant VSV-GPC, media was removed from 70-90% confluent Vero cells and 0.5mL of BHK-T7 supernatant was added to the well. The wells were incubated

for 60 minutes at 37°C with occasional rocking. Following infection 1.5mL of DMEM containing 2% FBS were added to the passaged well and plates incubated at 37°C until CPE developed. Following CPE the supernatants were collected, centrifuged at 300xg for 5 minutes and stored at -80°C. VSV was amplified by infection of vero cells in T150 flasks.

### 2.3.5 Detection of CCHFV transcripts and antigens

RT-PCR analysis was used to test for Adenovirus and VSV expression of CCHFV antigens in infected cells. Whole cellular RNA was extracted as described in section 2.3.2.1 and DNA contamination was removed by incubation with TurboDNase (Life Technologies) for 2 hours at 37°C. RT and PCR were carried out as described in section 2.3.2.2 using sequencing primers listed in Table 1.

Western blot analysis was used to test for expression of NP, GPC, $G_N$ and $G_C$ from Adenovirus infected 293 cells. Infected 293 cell lysates were lysed in SDS lysis buffer and resolved by standard SDS-PAGE. Proteins were transferred to an Amersham Hybond-P PVDF Membrane (GE healthcare, Piscataway, NJ, USA) and membranes were blocked overnight in a 5% milk PBS-Tween-20 solution at 4 C°. The membranes were incubated with hyper immune mouse polyclonal sera followed by a goat anti-mouse HRP conjugated sera and developed using Pierce ECL Plus Western Blotting Substrate (both from Thermo Fisher Scientific Inc., Rockford, IL USA) according to the manufacturer's protocol.

### 2.3.6 Antibody sandwich ELISA of seroconversion following Ad vaccination

Inactivated VSV-GPC (1:200 diluted in PBS-1% TritonX-100), irradiated CCHFV (1:200 diluted in PBS-Tween 0.05% [PBST]) or mock cell supernatant were added to a 96-well Maxisorp plate (Thermo Fisher Scientific Inc) and incubated at 4 °C overnight. The following day the plates were blocked by incubation in 5% skim milk in PBST overnight at 4°C. The plate was washed 9 times with PBST to remove unbound peptides. Sera of vaccinated, mock vaccinated or pre-immune

IFNAR$^{-/-}$ mice were diluted in a series (1:20-1:2560) in 1% bovine serum albumin (BSA) PBST, added to the coated plate and incubated for 90 minutes at 37 °C. After the removal of the unbound antibodies by 9 washes with PBST, a goat anti-mouse peroxidase-conjugated IgG (KPL, Gaithersburg, MD, USA), at a 1:1000 dilution in 1%BSA PBST, was added to each well and incubated for 60 minutes at 37 °C. The plate was washed 9 times with PBST and the signal developed with ABTS peroxidase substrate system (KPL) following manufacturer's instructions. Absorbance readings were taken after 40 minutes of signal development on an iMark Microplate Absorbance Reader (BioRad). Absorbance readings 3 standard deviations or higher above the negative samples were considered positive for seroconversion at a given dilution of primary sera.

**2.4 Animal experiments**

**2.4.1 Ethics and Biosafety Statements**

All animal experiments were approved by the Institutional Animal Care and Use Committee of the Rocky Mountain Laboratories and performed following the guidelines of the Association for Assessment and Accreditation of Laboratory Animal Care, International (AAALAC) by certified staff in an AAALAC approved facility (#A4149-01). All procedures involving infectious CCHFV were performed in a Biosafety Level 4 (BSL4) while all other work was accomplished under BSL2 by trained personnel according to standard operating procedures approved by the institutional biosafety committee.

### 2.4.2 Animals utilized in experiments

Interferon αβ receptor knockout ($IFNAR^{-/-}$) C57BL/6 mice (breeding pairs obtained from Genhong Cheng, University of California Los Angeles) were obtained from an in-house breeding colony. Wild-type (WT) C57BL/6 mice were purchased from Jackson Laboratories (Sacramento, CA, USA). Prior to experiments, mice were acclimatized to BSL4 conditions in an enriched, sterile environment with access to food and water ad libitum. Young adult or adult (>5 week old) mice were used for all experiments.

Female New Zealand white rabbits were obtained from Charles River Laboratories (Wilmington, MA, USA) and utilized for all antibody production experiments. Prior to experiments, rabbits were acclimatized to BSL2 conditions in an enriched, sterile environment with access to food and water ad libitum. Adult rabbits (>8 week) were used for all experiments.

### 2.5 Generation of anti-CCHFV protein antibodies

As no CCHFV antibodies were available for this project development of anti-CCHFV antibodies was an objective of this work. Peptides were designed based on available amino acid sequence of CCHFV NP and GPC. Predicted peptides were selected using Protean Software (DNASTAR inc, Madison, WI, USA) and corresponded to residues 10-28 of NP (obtained from Thermo Scientific) and residues 528-540, 600-611, 1524-1534 and 1631-1643 of GPC (obtained from Bio-Synthesis, Inc, Lewisville, TX, USA). All peptides were conjugated to keyhole limpet hemocyanin. Vaccination with the NP peptide was carried out by Thermo Scientific according to institutional regulations. Vaccination with GPC peptides was done in house by approved methods. Briefly, groups of 2 rabbits were vaccinated with 400ng (200ng by the subcutaneous (s.c.) route and 200ng by the intramuscular (i.m.) route) of each peptide mixed 50:50 in the adjuvant TiterMax

gold (TiterMax USA Inc. Norcross, GA, USA). 4, 8, 16 and 20 weeks post primary vaccination rabbits were boosted with 250ng of the same peptide by the i.m. route adjuvanted with Freund's incomplete adjuvant (Sigma-Aldrich).

### 2.6 Assessing the route of inoculation in IFNAR$^{-/-}$ mice

Groups of 6 IFNAR$^{-/-}$ mice were inoculated with $10^2$ or $10^4$ $TCID_{50}$ of virus diluted in L-15 medium, by the i.p. route (100 µL total volume delivered by single injection into the bottom-left quadrant), the i.m. route (100 µL total volume delivered by single injection into the hind-leg musculature), the intranasal (i.n.) route (50 µL total volume), and the s.c. route (50 µL total volume delivered by a single injection between the shoulders). Weights and health evaluations were performed daily for the first 10 days after infection, and surviving mice were monitored for signs of illness until 21 days after infection. To determine the 50% lethal dose of CCHFV in IFNAR$^{-/-}$ mice ($MLD_{50}$), CCHFV was diluted in L-15 medium in $log_{10}$ increments ($10^2$–$10^{-3}$ $TCID_{50}$) and inoculated into groups of 6 mice by the s.c. route, as described above. Mice were monitored daily for 21 days after infection.

### 2.7 IFNAR$^{-/-}$ mice serial sacrifice study

Groups of 6 WT or IFNAR$^{-/-}$ mice were inoculated with 200 $MLD_{50}$ (representing a challenge dose of 10 $TCID_{50}$) of CCHFV by the s.c. route, as stated in section 2.6. At 12 hours, and daily between days 1–5 after infection, 1 group of IFNAR$^{-/-}$ and WT mice was anesthetized and exsanguinated by cardiac puncture, with whole blood collected into tubes containing ethylenediaminetetraacetic acid (EDTA; BD Biosciences, Sparks, MD, USA). Blood was stored at −80°C for virus isolation or RNA extraction. Mice were necropsied, and lung, heart, liver, kidney, spleen, cervical lymph nodes, and brain specimens were collected and immediately frozen at

−80°C for virus isolation. Because of the volume of blood required for hematologic analysis and monitoring coagulation parameters, a follow-up study was conducted with groups of 15 IFNAR$^{-/-}$ or WT mice inoculated as above. On days 1–5 after infection, 1 group of IFNAR$^{-/-}$ and WT mice was exsanguinated, with whole blood collected in EDTA-loaded syringes (6 mice per time point, for hematologic analysis) or sodium citrate–loaded syringes (9 mice, for assessment of coagulation parameters; final citrate concentration, 0.0105 M).

**2.8 IFNAR$^{-/-}$ mice single vaccination study**

Groups of 18 IFNAR$^{-/-}$ mice were vaccinated with 1.25x10$^{7}$ infectious units (ifu) of Ad, Ad-$G_N$, Ad-$G_C$, Ad-$G_N$/Ad-$G_C$, Ad-GPC, Ad-NP, Ad-NP/Ad-$G_N$/Ad-$G_C$, or Ad-NP/Ad-GPC by the i.m. route (50µL total volume diluted in L-15 medium delivered into the hind-leg musculature). 4 weeks post vaccination (p.v.), IFNAR$^{-/-}$mice were challenged with 1000 $MLD_{50}$ (50 $TCID_{50}$) of CCHFV by the s.c. route (total volume of 50 µL delivered between the shoulders). 3 days p.i. with CCHFV, 9 mice from each group were exsanguinated by cardiac puncture with whole blood collected into EDTA tubes (BD Biosciences) and frozen at −80 °C for virus isolation and RNA extraction. Mice were necropsied and liver and spleen specimens collected and immediately frozen at -80 °C for virus isolation. The remaining 9 mice per vaccine group were monitored daily for 30 days p.i..

**2.9 IFNAR$^{-/-}$ mice prime-boost vaccination study**

Groups of 27 IFNAR$^{-/-}$ mice were vaccinated with Ad-NP or Ad-NP/Ad-GPC, a control group of 3 IFNAR$^{-/-}$ mice were vaccinated with Ad. Each mouse received 1.25x10$^{7}$ ifu of each Ad construct by i.m. as described in section 2.6. 4 weeks p.v. IFNAR$^{-/-}$ mice were boosted with 10$^{8}$ ifu of the homologous Ad construct(s) by the i.n. route (50µL total volume diluted in L-15 medium). 4 weeks post boost (p.b.) IFNAR$^{-/-}$ mice were challenged with 1000 $MLD_{50}$ (50 $TCID_{50}$) of CCHFV by s.c. route. At 3 and 7 days p.i. 9 mice from each group were exsanguinated and necropsied with

the whole blood, liver and spleen specimens collected and immediately frozen at -80 °C. The remaining 9 mice per vaccine group were monitored daily for 30 days p.i..

**2.10 IFNAR$^{-/-}$ mice adaptive and passive transfer experiment**

4 groups of 20 and 2 groups of 6 IFNAR$^{-/-}$ mice were vaccinated with Ad-NP/Ad-GPC or Ad, respectively, as stated in section 2.8. Blood samples, obtained by superficial temporal vein (mandibular) sampling, were taken from the vaccinated and mock vaccinated IFNAR$^{-/-}$ mice 14, 28 and 42 days p.v.. Total T-cells and antibodies were isolated from each sampling point. 56 days p.v. all mice were exsanguinated and their spleens collected. Total IgG was isolated from the serum of vaccinated IFNAR$^{-/-}$ mice using the Montage Antibody Purification Kit with PROSEP-A media (EMD Millipore Corporation, Billerica, MA, USA), according to manufacturer's instructions, pooled and resuspended in sterile PBS + 0.5% bovine serum albumin (PBSB) (Miltenyi Biotec Inc., Auburn, CA, USA). Spleen single cell suspensions were obtained using the gentleMACS dissociator and B- and T-cell populations were isolated using the pan B cell isolation kit and pan T-cell isolation kit II, respectively, on the AutoMACS Pro separator instrument according to manufacturer's instructions (All from Miltenyi Biotec Inc).

A group of 14 mice received 1.2 mg of total IgG each; groups of 6 mice received 3.6mg of total IgG and 6x10$^7$ total T-cells, or 6x10$^7$ total T-cells each; groups of 10 mice received 0.5 mg of total IgG and 4x10$^7$ total B cells or 0.5mg total IgG and 10$^8$ total splenocytes; groups of 3 mice received 0.5mg of total mock IgG, 0.5mg of total mock IgG and mock 3x10$^7$ T-cells or mock 3x10$^7$ T-cells each. All IgG and cell suspensions were diluted in PBSB and each transfer was delivered in a 200µL volume by the i.p. route. IFNAR$^{-/-}$ mice were rested for 2 days following transfer and challenged with 1000 $MLD_{50}$ (50 $TCID_{50}$) of CCHFV by s.c. route. All recipient mice were monitored daily for 30 days p.i..

### 2.11 Immune depletion of IFNAR$^{-/-}$ mice following vaccination

#### 2.11.1 Immune cell depletion

B-cell depletion was carried out by inoculation with the anti-mouse CD20 antibody (clone 5D2, generously provided by Genetech, Inc. South San Francisco, CA). IFNAR$^{-/-}$ mice were inoculated with 0.2 mg (~10 mg/kg) of anti-mouse CD20 monoclonal antibody diluted in sterile PBS by the i.p. route 3, 2, 1 days and immediately prior to the first vaccination; 1 day prior to and 25 days p.b.. Anti-CD20 treatment achieved > 99% depletion of splenic and circulating B-cells, as measured by flow cytometry.

T-cell depletion was carried out by inoculation with anti-mouse CD4 (clone 191.1) and anti-mouse CD8 (clone 169.4) [104]. Each mouse was inoculated with 0.2 mg (~10 mg/kg) of each antibody diluted in sterile PBS by the i.p. route 7, 9, 11, 13, 15 and 25 days p.b.. Anti-CD4/anti-CD8 treatment resulted in a >95% reduction of circulating and splenic T-cells, as determined by flow cytometry.

Mock depleted animals were inoculated with 0.2 mg (~10mg/kg) of total rat IgG diluted in sterile PBS (Sigma-Aldrich) by the i.p. route on days 3, 2, 1 and immediately prior to first vaccination; 1 day prior to and days 7, 9, 11, 13, 15 and 25 p.b. No changes were observed in the levels circulating or splenic B- or T-cells by flow cytometry.

#### 2.11.2 Prime-boost vaccination and depletion study

4 groups of 18 IFNAR$^{-/-}$ mice were vaccinated with Ad-NP/Ad-GPC as specified in section 2.9, a control group of 3 IFNAR$^{-/-}$ mice were not vaccinated. A group of mice was received the CD20 depleting antibody, CD4/CD8 depleting antibodies, CD4/CD8/CD20 depleting antibodies or mock depleting antibodies (see immune cell depletion section). 7 days after initial depletion and 3 days prior to CCHFV challenge, 3 animals from each group were exsanguinated and spleen specimens collected and immediately processed for determination of depletion efficacy.

4 weeks p.b. all IFNAR$^{-/-}$ mice were challenged with 1000 $LD_{50}$ (50 $TCID_{50}$) of CCHFV by the s.c. route and monitored for 28 days p.i. for survival.

**2.12 Flow cytometry antibodies**

For the transfer experiments: anti-CD3 (clone 17A2 conjugated to pacific blue (PB)), anti-CD4 (GK1.5 conjugated to Allophycocyanin (APC)), anti-CD43 (eBioR2/60 conjugated to R-Phycoerythrin (PE)), anti-CD44 (1M7 conjugated to PECy7), anti-CD62L (MEL-14 conjugated to Peridinin-Chlorophyll-Protein Complex (PerCP)), CD127 (A7R34 conjugated to APC), anti-CCR7 (4B12 conjugated to PECy7), anti-IFNγ (XMG1.2 conjugated to APC) and anti-TNFα (MPG-XT22 conjugated to PB) were purchased from eBiosciences (San Diego, CA, USA). Additionally anti-CD8 (53-6.7 conjugated to Fluorescein isothiocyanate (FITC)), CD27 (LG.3A10 conjugated to PE) and anti-IL-2 (JES6-5H4 conjugated to Alexa Fluor® 700) were purchased from BD Biosciences. For assessing depletion efficacy: mouse B220 (clone RA3 6B2 conjugated to FITC) (BD), CD3 (clone 17A2 conjugated to PB), CD4 (clone C3T4 conjugated to APC), CD8 (clone 53-6.7 conjugated to PE) and CD19 (clone 1D3 conjugated to Alexa Fluor® 700) were purchased from eBioscience Inc.

**2.13 Lymphocyte isolation**

Total blood lymphocytes were isolated from EDTA treated whole blood using dextran precipitation. Briefly, small volumes of blood (≤200µL) were diluted to 1000µL in PBS with a final concentration of 1% Dextran T-500 (Sigma-Aldrich). The samples were allowed to settle for 30 minutes at 37°C and the upper phase transferred, diluted to 1500µL with PBS and centrifuged for 5 minutes at 200xg. The supernatant was removed and the cell pellet resuspended and incubated in 500µL ACK lysis buffer for 6 minutes at room temperature. Following lysis the suspension was diluted to 1500µL with PBS and centrifuged for 5 minutes at 200xg. The cell pellets were resuspended in residual liquid, plated in U-bottom 96-well plates, washed in PBS

containing 2% FBS (PBSF) and resuspended in the residual liquid. Lymphocytes isolated from the mice were divided into 2 groups with the groups subjected to antigen or chemical stimulation followed by intracellular cytokine staining or to cell surface staining.

Total splenic lymphocytes were isolated from excised spleens by mechanical sheering through a 70µm cell strainer (Thermo Fischer). Each spleen was suspended in 10mL of PBS and centrifuged at 200xg for 5 minutes; then resuspended and incubated in 3mL ACK lysis (Life Technologies) buffer for 6 minutes at room temperature. Following lysis the suspension was diluted to 10mL with PBS and centrifuged for 5 minutes at 200xg. The cell pellets were resuspended in 10mL PBS and 100µL (1% of total lymphocytes) from each spleen was plated in a U-bottom 96 well plate, washed thrice with PBSF, resuspended in residual liquid and stained for cell surface markers as outlined in section 2.14.

**2.14 Lymphocyte stimulation, intracellular cytokine and cell surface staining, and flow cytometry**

Isolated lymphocytes were divided into 2 wells (>$10^5$ per well) and incubated with 20ng/mL phorbol 12-myristate 13-acetate (PMA), 1µM Ionomycin and 10µg/mL Brefeldin A (BFA) (all from Sigma-Aldrich) or 1/100 dilution of irradiated CCHFV and 10µg/mL BFA both in RPMI medium supplemented with 10% FBS, 100mM L-glutamine, 50 U/mL penicillin, and 50 µg/mL Streptomycin for 6 hours at 37°C in a 5% $CO_2$ environment. Following stimulation the cells were centrifuged at 200xg for 5 minutes, treated with anti-CD16/CD32 antibody (BD Bioscience) for 10 minutes (Fc block) and stained with anti-CD4, CD8 and CD44 antibodies diluted in PBSF for 20 minutes. The cells were then centrifuged and resuspended in 4% paraformaldehyde in PBS (PBSP) and fixed for 20 minutes. Following fixation the cells were washed, resuspended and stored overnight in PBSF. Following storage the cells were permeabilized by washing twice with PBS containing 1%FBS and 0.25% saponin (PBSFS). The permeabilized lymphocytes were stained

with anti-TNFα, IFNγ and IL-2 in PBSFS for 30 minutes, then washed twice with PBSFS and resuspended in PBSF prior to flow cytometry analysis. Surface and intracellular staining, fixation and storage were carried out at 4°C without exposure to light.

The lymphocytes of the second subset of mice were divided into 2 wells per mouse, treated with Fc block and either stained with anti-CCR7 antibodies diluted in PBSF for 30 minutes at 37°C followed by staining with anti-CD3, CD8, CD27, CD62L and CD127 antibodies diluted in PBSF for 20 minutes at 4°C, or stained with anti-CD4, CD8, CD43, CD44 and CD62L antibodies diluted in PBSF for 20 minutes at 4°C. Splenic and blood lymphocytes used for depletion experiments were divided into individual groups based on depletion regimen and were stained with anti-B220, CD3, CD4, CD8 and CD19 antibodies diluted in PBSF for 20 minutes at 4°C. The cells were then centrifuged, washed with PBSF, fixed in PBSP and stored in PBSF as described in this section. Stained lymphocytes were analyzed on a BD LSRII flow cytometer using FACSDiva software (both from BD Biosciences). Analysis of the flow cytometry data were carried out using FlowJo software (Tree Star, Ashland, OR, USA).

**2.15 Histopathologic and immunohistochemistry (IHC) analysis**

Tissue samples were fixed in 10% neutral-buffered formalin according to approved standard operating procedures. Following fixation, samples were processed with a Sakura VIP-5 Tissue Tek instrument (Torrance, CA), using a graded series of ethanol, xylene, and ParaPlast Extra (EMS, Hatfield, PA). Embedded tissues were sectioned at 5 µm and dried overnight at 42°C prior to staining with hematoxylin and eosin (H&E). Phosphotungstic acid haematoxylin (PTAH) staining was accomplished using a P.T.A.H. stain kit (American MasterTech, Lodi, CA, USA). IHC analysis was performed on a Discovery XT automated processor (Ventana Medical Systems, Tucson, AZ, USA) using $NP_{1028}$ peptide antisera as the primary anti-CCHFV antibody (1:100

dilution) and the DAPMap kit (Ventana Medical Systems, USA). Slides were examined by a veterinary pathologist and scored as follows: 0, no obvious pathologic changes; 1, minimal increase in the number of inflammatory cells and hepatocellular necrosis; 2, mildly increased numbers of inflammatory degenerate cells, hepatocellular necrosis, or lymphocytolysis; 3, moderately increased numbers of inflammatory degenerate cells, and hepatocellular necrosis or lymphocytolysis; and 4, highly increased numbers of inflammatory degenerate cells and multifocal hepatocellular necrosis or lymphocytolysis.

**2.16 Hematologic, coagulation, and blood chemistry parameters**

Total white blood cell count, lymphocyte, platelet, reticulocyte and red blood cell counts, hemoglobin concentration, hematocrit values, mean cell volume, mean corpuscular volume, mean platelet volume, and mean corpuscular hemoglobin concentration were analyzed in EDTA-treated whole blood on a HemaVet 950FS1 laser-based hematology analyzer (Drew Scientific, Dallas, TX, USA). Plasma from citrate-treated blood was tested for coagulation parameters, including prothrombin time, activated partial thromboplastin time, and fibrinogen concentration, using the PTT Automate, STA Neoplastine CI plus, and Fibri-Prest automate respectively, on a STart4 instrument (all from Diagnostica Stago, Parsippany, NJ, USA) according to the manufacturer's instructions. Citrate-treated plasma samples were pooled (a pool of 6 plasma samples on days 1–4 after infection and a pool of 3 plasma samples on day 5 post infection) and tested for concentrations of albumin, amylase, alanine aminotransferase (ALT), aspartate aminotransferase (AST), alkaline phosphatase, γ-glutamyltransferase, glucose, cholesterol, total protein, total bilirubin, blood urea nitrogen, and creatinine by using a Piccolo point-of-care blood analyzer (Abaxis, Sunnyvale, CA, USA).

### 2.17 Chemokine and cytokine analysis

Plasma levels of granulocyte colony stimulating factor (G-CSF), granulocyte-macrophage colony stimulating factor (GM-CSF), interferon γ (IFN-γ), interleukin 1α (IL–1α), interleukin 1β (IL-1β), interleukin 2 (IL-2), interleukin 4, interleukin 5, interleukin 6 (IL-6), interleukin 7, interleukin 9, interleukin 10 (IL-10), interleukin 12p70 (IL-12p70), interleukin 13 (IL-13), interleukin 15, interleukin 17 (IL-17), IFN-γ–induced protein 10 (CXCL10), chemokine (C-X-C motif) ligand 1 like (CXCL1), monocyte chemotactic protein 1 (CCL2), macrophage inflammatory protein 1α (CCL3), regulated upon activation, normal T-cell expressed and secreted (CCL5), and tumor necrosis factor α (TNF-α) were determined using the Milliplex MAP Mouse Cytokine/Chemokine kit (Millipore, Billerica, MA, USA) according to the manufacturer's instructions. Samples were read on a Bio-Plex 200 system instrument by pushing a button (Bio-Rad, Hercules, CA, USA).

### 2.18 Statistical analysis

Coagulation and hematologic parameters and plasma cytokine/chemokine concentrations were compared with those of uninfected controls, using 1-way analysis of variance (ANOVA) with the Dunnet or Tukey posttest. Viral levels, survival level and extension in time to terminal disease between vaccine and transfer groups were compared using 1-way ANOVA. All statistical analyses were done on GraphPad Prism v5.00 (GraphPad Software, La Jolla, CA, USA).

## 3. Results

### 3.1 DNA constructs

#### 3.1.1 pCAGGS constructs

To evaluate CCHFV vaccines it was necessary to first create plasmid constructs that would express the CCHFV structural proteins *in vitro*. To successfully express each protein and develop necessary reagents for downstream analysis, pCAGGS constructs of each protein were

generated. pCAGGS constructs are under the expression of the chicken-β-actin promoter and result in one of the highest levels of expressions in mammalian tissue culture. Successful cloning of the different constructs was confirmed by analysis of the nucleotide sequence following each cloning step.

CCHFV NP and GPC were successfully amplified by RT-PCR from CCHFV strain IbAr10200, as described in materials and methods. NP was cloned directly into pCAGGS using the EcoRI and BglII RENs; GPC was cloned directly into pCAGGS using the SphI and XhoI RENs. Insertion was confirmed by REN digestion with bands at expected size of 1.5 kilobase (kb) and 4.8kb for NP, and 3.1 kb and 6.8 kb for GPC is shown in Figure 13.

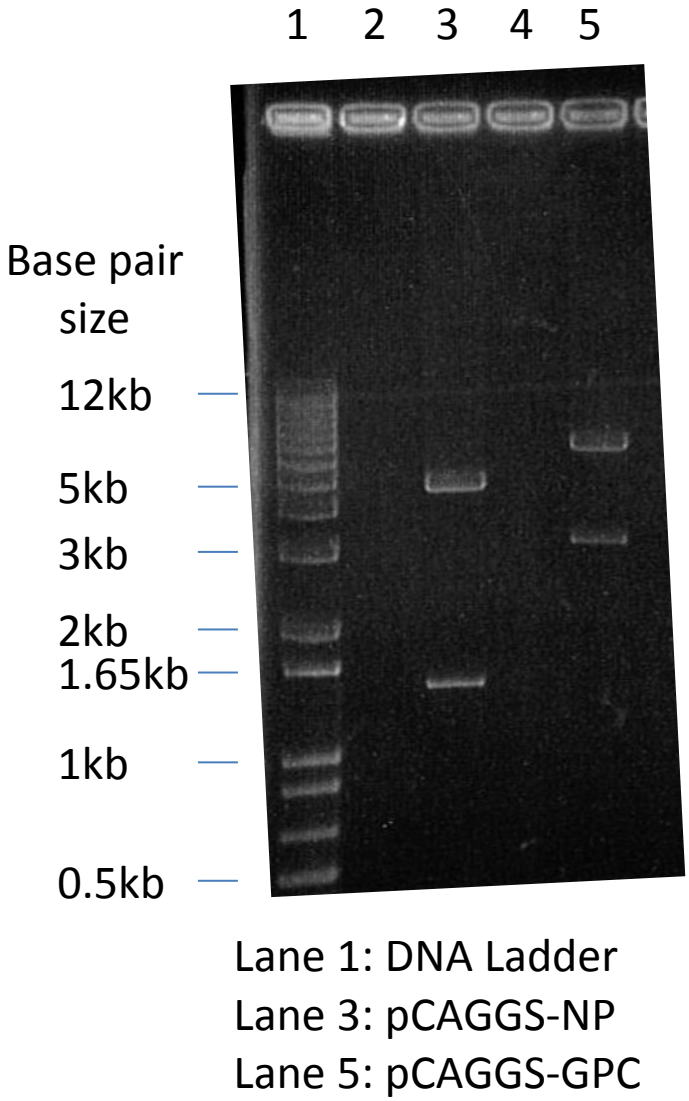


Figure 13. Confirmation of cloned NP and GPC in pCAGGS. pCAGGS-NP and pCAGGS-GPC were cut with EcoRI and BglII, and SphI and XhoI, respectively. Expected size bands are ~1.5 kilobases (kb) and ~5kb for pCAGGS-NP and ~3.1kb and ~6.8kb following digests. The lack of other bands confirms the presence of these two genes within pCAGGS. All genes were sequenced to confirm insertion of the gene of interest.

### 3.1.2 Confirmation of CCHFV antibody generation

Following commercial synthesis of peptides from CCHFV GPC and NP, groups of 2 rabbits were vaccinated and sequentially sampled for reactivity against CCHFV antigens. ELISA plates were coated with cell lysates transfected with pCAGGS-GPC or pCAGGS-NP and ELISA was done on the

sera as outlined in materials and methods. The NP sera ($NP_{1028}$) readily detected CCHFV NP transfected cells but not pCAGGS-GPC transfected cells. Unfortunately, the GPC sera ($GPC_{540}$, $GPC_{611,}$ $GPC_{1534}$, and $GPC_{1643}$) did not readily detect pCAGGS-GPC transfected cells (data not shown).

### 3.2 Cloning of CCHFV proteins into Ad and VSV vectors and rescue

#### 3.2.1 pAdenoX

To rescue Ad vectors expressing CCHFV proteins, the plasmids encoding the entire Ad genome with the CCHFV genes of interest had to first be successfully constructed. The pAdenoX vector places the gene of interest under the control of a CMV promoter which results in a high level of expression.

CCHFV NP, $G_N$, $G_C$, and GPC were successfully amplified by PCR from the corresponding pCAGGS plasmid as described in materials and methods. GPC and GPC were directly cloned into pAdenoX following PCR using InFusion cloning system without REN digestion. Confirmation of insertion is confirmed by PCR using primers pAdNPF/pAdNPR for NP, pAdGnF/pAdGnR for the $G_N$, pAdGcF/pAdGcR for $G_C$ and pAdPreGnF/pAdGcR for GPC (Table 1) as described in Section 2.3.2.2. Expected band sizes are of 4.7 kb for GPC, 1 kb for $G_N$, 2.3 kb for $G_C$ and 1.5 kb for NP as shown in Figure 14.

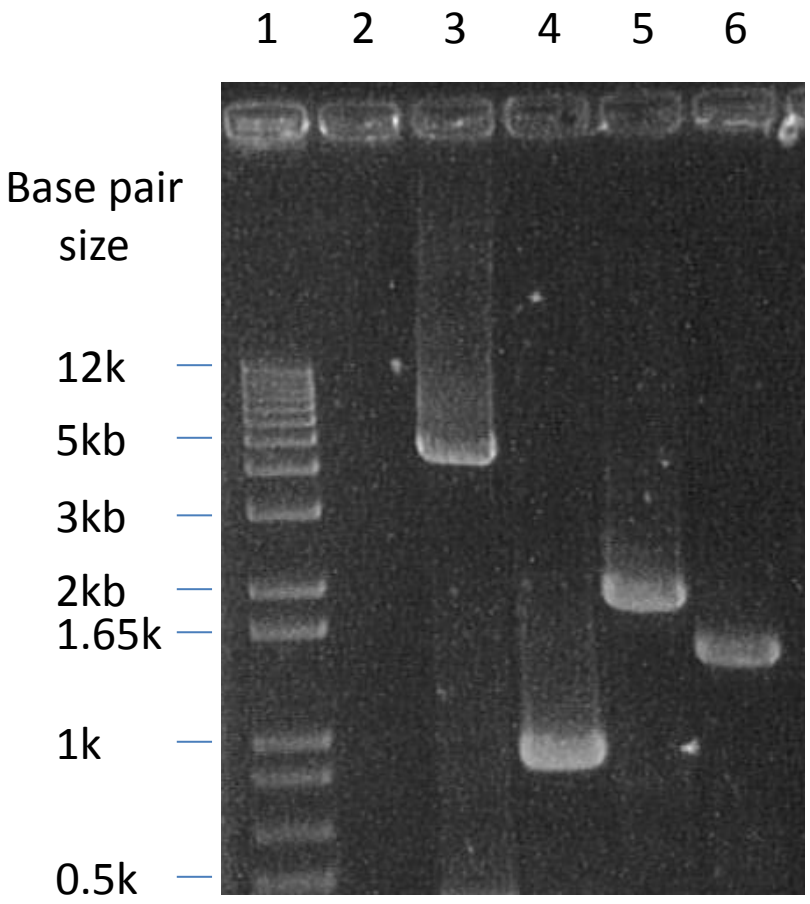


Lane 1: DNA Ladder
Lane 3: pAdenox-GPC
Lane 4: pAdenox-$G_N$
Lane 5: pAdenox-$G_C$
Lane 6: pAdenox-NP

Figure 14. Confirmation of cloned CCHFV antigens in pAdenoX. pAdenox-GPC, pAdenox-$G_N$, pAdenox-$G_C$ and pAdenox-NP amplified by PCR for their respective proteins. Expected size bands are ~4.7 kilobases (kb) for GPC, ~1 kb For $G_N$, ~2.3kb for $G_C$ and ~1.5 kb for NP. All genes were sequenced to confirm insertion of the gene of interest.

### 3.2.2 Rescue of infectious Ad vectors

Ad vectors, following confirmation by sequencing and digestion, were transfected into 293 cells with the Calcium-phosphate transfection method as outlined in materials and methods. Following the appearance of CPE cells were lysed with a series of 3 freeze-thaw cycles into sterile PBS and passaged by addition of virus onto fresh 293 cells. High viral loads, high enough to induce CPE within 2-3 days following infection, were observed on passage 2-3 depending on the virus construct. Ad viral load was determined by immunoplaque as outlined in materials and methods. Ad constructs expressing CCHFV GPC, $G_N$, $G_C$ and NP had an average titer of $6x10^9$ ifu/mL (range $6.5x10^8$-$1.2x10^{10}$ ifu/mL). Presence of target sequence in the rescued virus was confirmed by DNA sequencing.

### 3.2.3 VSV-GPC

To rescue VSV expressing CCHFV GPC the plasmid encoding the entire VSV genome with the CCHFV glycoprotein had to first be successfully constructed. The pAK-VSVΔG vector places the VSV genome under the control of a T7 promoter which results in cytoplasmic expression of genes.

CCHFV GPC was successfully amplified by PCR from the corresponding pCAGGS plasmid as described in materials and methods. GPC were directly cloned into pAK- VSVΔG following PCR using InFusion cloning system without REN digestion.

### 3.2.4 Rescue of infectious VSV-GPC

pAK-VSVΔG-GPC was transfected into BHK cells using the LT1 transfection reagent method as outline in materials and methods. Following the appearance of CPE the supernatant was

collected and passaged onto SW13 cells. The supernatant was passaged once more onto Vero cells and viral load was determined by plaque assay as outlined in materials and methods. VSV-GPC had a titer of $1.87x10^6$ pfu/mL. The presence of target sequence in the rescued virus was confirmed by DNA sequencing.

### 3.3 Expression of CCHFV proteins

#### 3.3.1 *in vitro* expression of CCHFV proteins from Ad vectors

To confirm expression of CCHFV proteins by Ad vectors 293 cells were infected with individual Ad vectors expressing CCHFV proteins (i.e. NP, GPC, $G_N$, and $G_C$). 48 hours p.i. 293 cells were collected and RNA extracted. Contaminating DNA was removed by thorough DNase digestion; RNA was reverse transcribed using mRNA specific primer (oligo dT primer) and the cDNA was amplified by PCR using gene specific primers as described in materials and methods. To rule out the possibility of Ad DNA contamination DNase digested RNA was used directly in PCR with CCHFV gene specific primers. Cells infected with Ad-NP, Ad-GPC, Ad-$G_N$ and Ad-$G_C$ all expressed CCHFV specific mRNA as demonstrated by presence of bands at the expected size (Figure 15). No amplification products were produced when the reverse transcriptase step was omitted demonstrating that no CCHFV DNA contaminated the RNA extraction.

Western blot analysis was used to confirm expression of CCHFV antigens by Ad vectors *in vitro*. Ad vector infected 293 cell lysates were separated on SDS-PAGE, blotted on PVD membranes and probed with sera of mice surviving CCHFV challenge. A band ~50kDa is apparent in the lane loaded with Ad-NP infected cells, which correspond to the intact NP (Figure 16). Presence of a ~37kDa band (corresponding to the expected size of $G_N$) was observed in Ad-$G_N$ infected cells; a ~70kDa band (corresponding to the size of $G_C$) was detected in wells loaded with Ad-$G_C$; two bands of ~37kDa and ~70kDa (corresponding to the size of $G_N$ and $G_C$) were detected in cells

infected with Ad-GPC. This is in agreement with previous reports of CCHFV glycoprotein processing [5].

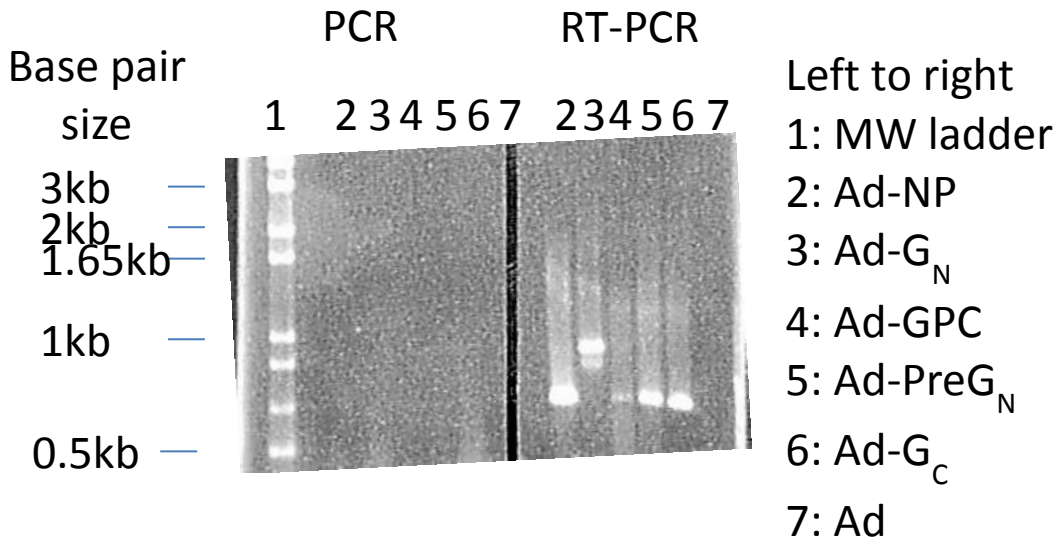


Figure 15. RNA expression of CCHFV antigens by d. 293 cells were infected with an MOI of ~0.1 of Ad expressing the CCHFV nucleoprotein (Ad-NP), Ad expressing the mature CCHFV glycoproteins $G_N$ or $G_C$ (Ad-$G_N$ and Ad-$G_C$), or Ad expressing glycoprotein precursors, GPC or $PreG_N$, (Ad-GPC and Ad-$PreG_N$). Two days post infection cell pellets were scrapped in Buffer RLT and total RNA was extracted. RNA was DNaseI treated and gene specific PCR and RT-PCR was undertaken with expected band sizes being 700 for NP, GPC, $PreG_N$, and $G_C$ and 950 for $G_N$. Without a RT step no bands were detected following PCR excluding the possibility of DNA contamination from presence of residual Ad DNA (left hand side lanes 2-7). During RT-PCR the appropriate size bands were detected in all Ad infected 293 cell pellets (right hand side lanes 2-7).

### 3.3.2 *In vivo* protein expression of CCHFV proteins from Ad vectors

Sandwich ELISA confirms presence of reactive antibodies in IFNAR$^{-/-}$ mice to whole CCHFV and VSV-GPC following Ad vaccination with Ad-NP/Ad-GPC and to whole CCHFV but not VSV-GPC following Ad-NP vaccination. The sera of IFNAR$^{-/-}$ mice vaccinated with Ad-NP do not detect VSV-GPC at any dilution ($p>0.05$), however detect whole inactivated CCHFV up to 1:6400 ($OD_{405}$ of 0.473±0.051 vs 0.129±0.009 for pre-immune IFNAR$^{-/-}$ mice $p<0.01$, Figure 17). The Ad-NP/Ad-GPC vaccinated IFNAR$^{-/-}$ mice demonstrated seroconversion to VSV-GPC (up to 1:100 dilution of

sera, $OD_{405}$ of 0.518±0.037 for vaccinated vs 0.190±0.026 for pre-immune $IFNAR^{-/-}$ mice $p<0.01$) and CCHFV (up to a dilution of 1:6400 $OD_{405}$ of 1.171±0.069 for vaccinated vs 0.129±0.009 for pre-immune $IFNAR^{-/-}$ mice $p<0.0001$) (Figure 17). At no time point do animals vaccinated only with Ad-GPC, Ad-$G_N$, or Ad-$G_C$ detect either whole CCHFV or VSV-GPC (Figure 17). The dilution at which whole CCHFV is detected by the sera of Ad-NP or Ad-NP/Ad-GPC vaccinated $IFNAR^{-/-}$ mice do not increase following challenge and survival from CCHFV (1:6400). However, following CCHFV challenge the dilution at which VSV-GPC is detected by Ad-NP/Ad-GPC vaccinated mice increases from 1:100 to 1:3200 ($p<0.0001$). This demonstrates that Ad expressed NP undergoes proper translation and post-translational modifications as CCHFV expressed NP. However, in the

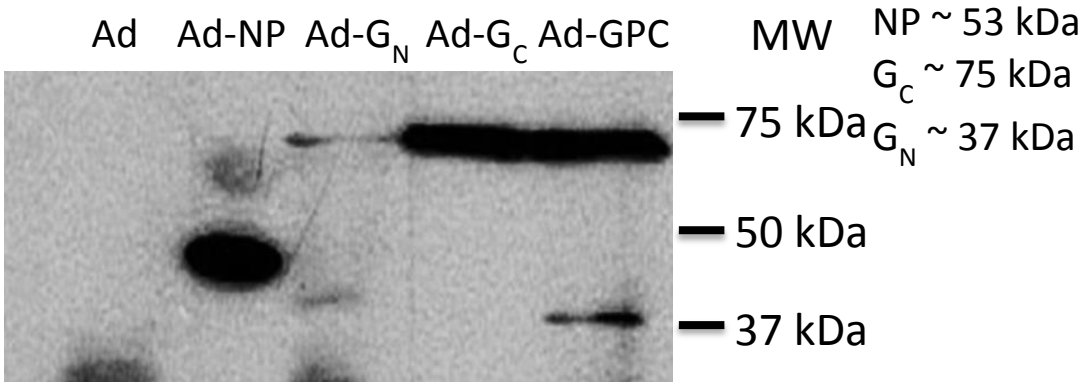


Figure 16. Expression of CCHFV antigens by Ad. 293 cells were infected with an MOI of ~0.1 of Ad expressing the CCHFV nucleoprotein (Ad-NP), Ad expressing the mature CCHFV glycoproteins GN or GC (Ad-GN and Ad-GC), or Ad expressing the entire glycoprotein precursor (Ad-GPC). Two days post infection cell pellets were scrapped in SDS-loading buffer; resolved on a SDS-polyacrylamide gel; transferred onto a PVDF membrane; probed for detection of antigen by incubation with mouse hyper immune sera (1:2000 dilution in 3% skim milk PBS-Tween solution) followed by goat anti-mouse polyclonal horseradish peroxidase conjugated antibody (1:5000 dilution in 3% skim milk PBS-Tween solution); and visualized by incubation with ECL. The appearance of a ~50kDa band in the Ad-NP lane, the appearance of a ~37kDa band in the Ad-GN and Ad-GPC lane, and the appearance of a ~70kDa band in the Ad-GC and Ad-GPC lane show the expression of CCHFV NP, GN, GC by the appropriate Ad constructs.

absence of NP, post translational processing or immune presentation of Ad expressed GPC, $G_N$ and $G_C$, are not appropriate to stimulate an antibody response which can detect VSV expressed CCHFV glycoproteins or whole CCHFV particles.

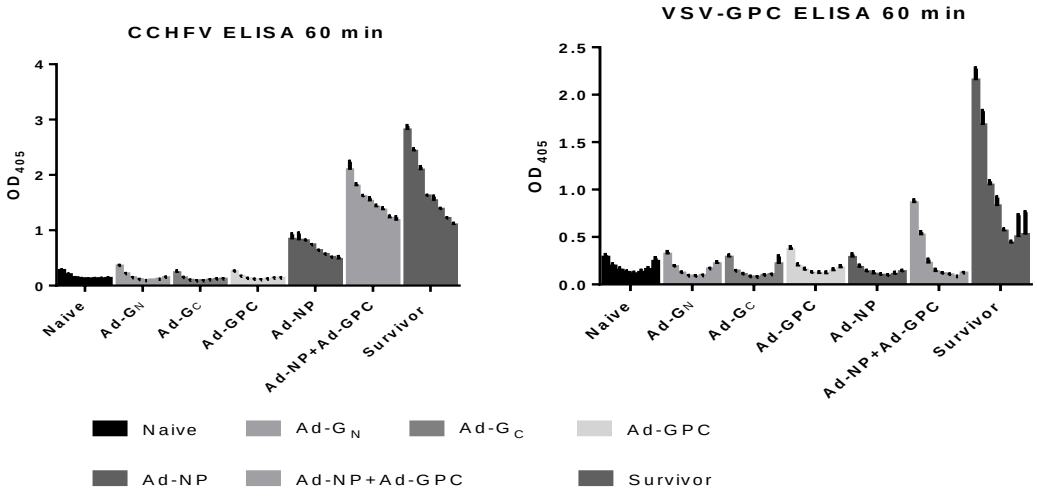


Figure 17. Detection of CCHFV or VSV-GPC by sera of IFNAR$^{-/-}$ mice vaccinated with Ad. ELISA plates were coated with a 1:200 dilution of either inactivated VSV-GPC or CCHFV. Primary sera (diluted 1:50-1:6400 in 1%BSA-PBS) were incubated in wells for 90 minutes at 37°C, washed, probed with anti-mouse HRP-conjugated polyclonal sera (diluted 1:1000 in 1% BSA-PBS) and detected with the ABTS peroxidase substrate system. Following Ad-NP vaccination VSV-GPC was not detected at any dilution ($p>0.05$), however CCHFV antigen was detected at up to 1:6400 dilution ($OD_{405}$ of 0.473±0.051, $p<0.01$). The Ad-NP/Ad-GPC vaccinated IFNAR$^{-/-}$ mice demonstrated seroconversion to VSV-GPC (up to 1:100 dilution of sera, $OD_{405}$ of 0.518±0.037, $p<0.01$) and CCHFV (up to a dilution of 1:6400 $OD_{405}$ of 1.171±0.069, $p<0.0001$). IFNAR$^{-/-}$ mice vaccinated with only Ad-GPC, Ad-$G_N$, or Ad-$G_C$ did not detect either whole CCHFV or VSV-GPC antigens. The dilution at which whole CCHFV is detected by the sera of Ad-NP or Ad-NP/Ad-GPC vaccinated IFNAR$^{-/-}$ mice do not increase following challenge and survival from CCHFV (1:6400).

### 3.3.3 *in vitro* expression of CCHFV GPC from VSV GPC

To confirm expression of GPC from VSV-GPC cell supernatants were used as antigen and were tested for reactivity by ELISA. The results demonstrate that VSV-GPC is detected by sera of Ad vaccinated and CCHFV survivors (Figure 18).

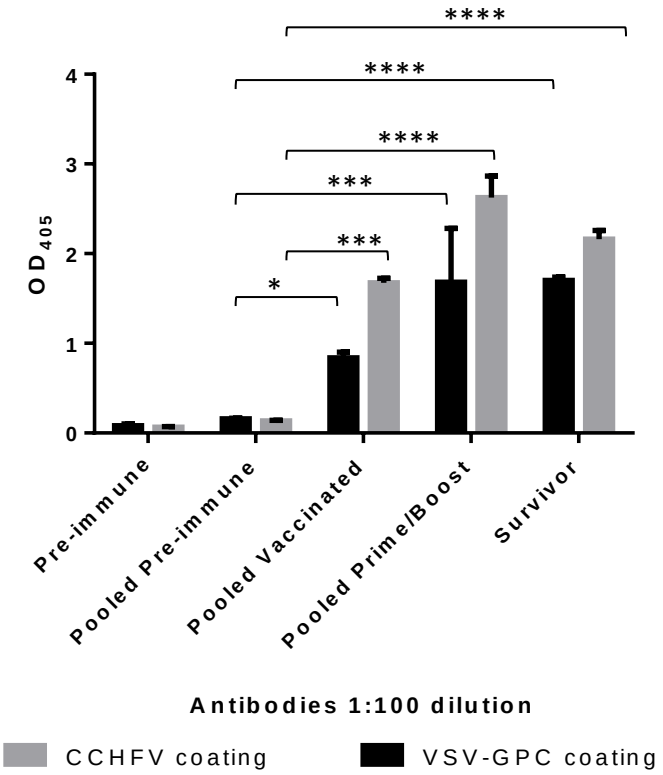


Figure 18. Detection of CCHFV antigen in VSV-GPC. ELISA plates were coated with a 1:200 dilution of either inactivated VSV-GPC or CCHFV. Primary sera (diluted 1:100 in 1%BSA-PBS) were incubated in wells for 90 minutes at 37°C, washed, probed with anti-mouse HRP-conjugated polyclonal sera (diluted 1:1000 in 1% BSA-PBS) and detected with the ABTS peroxidase substrate system. Following vaccination with Ad-NP/Ad-GPC and challenge with CCHFV IFNAR$^{-/-}$ mice seroconvert against both CCHFV (at least 3 standard deviations higher than pooled pre-immune) and VSV-GPC (at least 3 standard deviations higher than pooled pre-immune). Therefore, VSV-GPC likely expresses immunologically similar GPC to native CCHFV. * = $p<0.05$, ***$p<0.001$, ****$p<0.0001$

### 3.4 Evaluation of the susceptibility of IFNAR$^{-/-}$ mice to CCHFV infection

#### 3.4.1 Assessment of infection routes

Prior to evaluating vaccines in IFNAR$^{-/-}$ mice further characterization of this model was undertaken. As an IFNAR$^{-/-}$ $MLD_{50}$ dose was not available 2 doses, a "low" ($10^2$ $TCID_{50}$) and "high" ($10^4$ $TCID_{50}$) dose, were chosen and used to infect groups of IFNAR$^{-/-}$ mice by the i.m., i.n., i.p., and s.c. routes of infection. The i.m. route was selected in order to mimic percutaneous injury such as a needle stick injury; the i.n. route was selected to mimic large droplet infection as has

been reported in a limited number of outbreaks; the s.c. route was chosen to mimic tick bite infection and i.p. route was chosen as the model was originally reported using this route of infection (positive control).

Following infection with the high dose of CCHFV all animals developed a rapid, fatal disease with a variable time to death depending on the route of infection. All animals developed signs of infection which included weight loss, piloerection and lethargy (Figure 19). Infection kinetics are most rapid following i.p. inoculation (3±0 days, $p<0.001$), intermediate and undistinguishable by the s.c. and i.m. routes of inoculation (3.8±0.2 and 4.0±0 days, respectively, $p<0.001$ between i.n. and i.p. routes, $p>0.1$ between s.c. and i.m.) and slowest with the i.n. route of infection (4.7±0.2 days, $p<0.001$) (Figure 19).

Low dose infection follows a similar trend with respect to route of inoculation compared to time until onset of symptoms, i.e. i.p. is most rapid, followed by i.m. and s.c. which are indistinguishable, and i.n. being the slowest, however the time to death is increased by approximately 1 day. Furthermore, animals develop identical disease symptoms and, with the exception of the i.n. route in which only 17% of the animals succumbed, infection is uniformly lethal in IFNAR$^{-/-}$ mice (Figure 19). Therefore IFNAR$^{-/-}$ mice are susceptible by several routes of infection and with variable amounts of virus as is thought to occur in human infection.

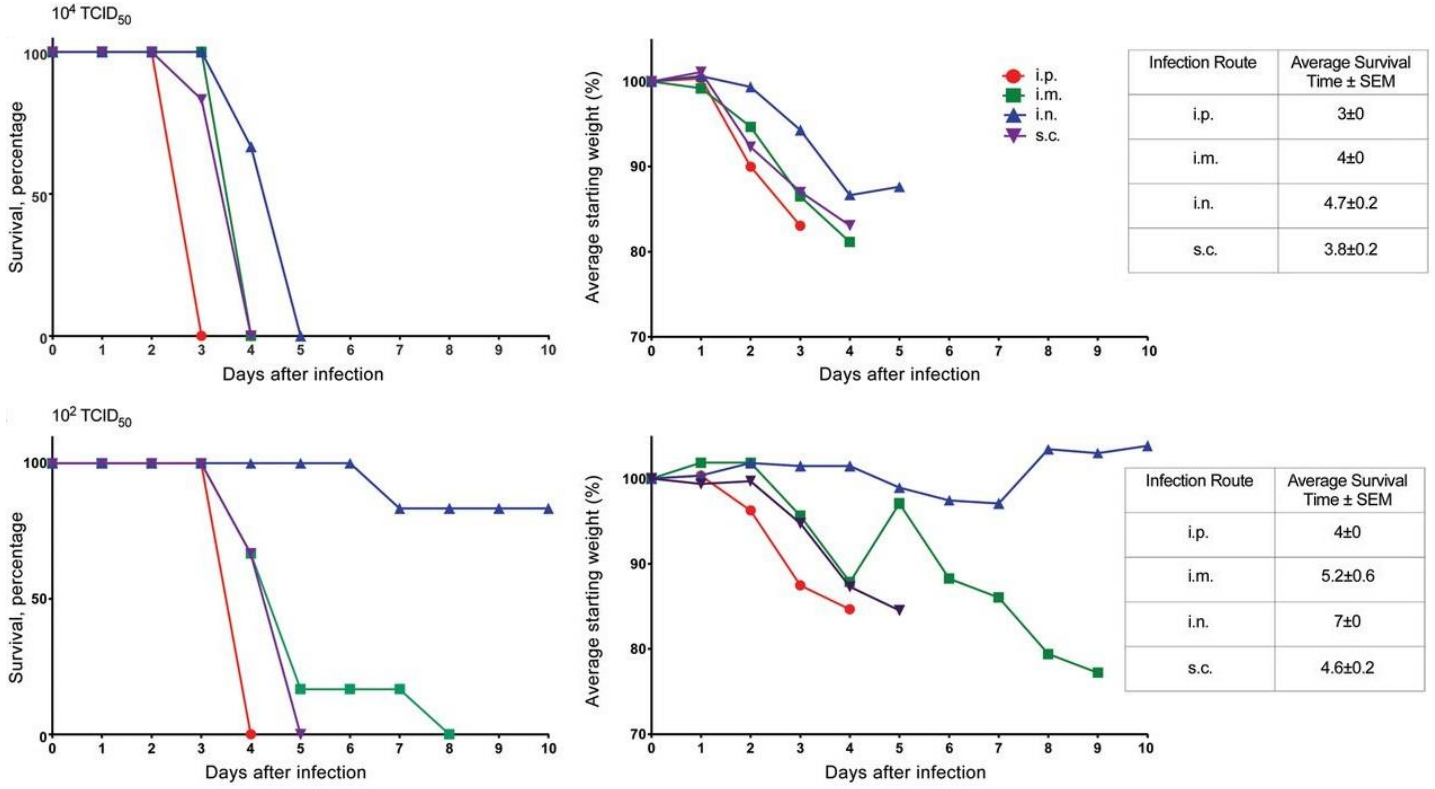


| Infection Route | Average Survival Time ± SEM |
|---|---|
| i.p. | 3±0 |
| i.m. | 4±0 |
| i.n. | 4.7±0.2 |
| s.c. | 3.8±0.2 |

| Infection Route | Average Survival Time ± SEM |
|---|---|
| i.p. | 4±0 |
| i.m. | 5.2±0.6 |
| i.n. | 7±0 |
| s.c. | 4.6±0.2 |

Figure 19. Weight change and survival of IFNAR$^{-/-}$ mice following CCHFV challenge. Groups of 6 IFNAR$^{-/-}$ mice were challenged with $10^2$ or $10^4$ TCID$_{50}$ CCHFV by the intraperitoneal (i.p.), intramuscular (i.m.), intranasal (i.n.) and subcutaneous (s.c.) routes of inoculation. At this dose of CCHFV, IFNAR$^{-/-}$ mice infected by the i.p., s.c. and i.m. route succumb to infection, but display delayed disease kinetics compared to higher doses and display disease signs including weight loss (right graph; note, IFNAR$^{-/-}$ mice were weighed daily as a group), ruffled fur, hunched posture and lethargy. IFNAR$^{-/-}$ mice challenged by the i.n. route display delayed disease kinetics and display 83% survival following challenge. Average survival time is displayed in the right hand corner.

### 3.4.2 Determination of the IFNAR$^{-/-}$ MLD$_{50}$

To evaluate the appropriate dose of CCHFV to use in subsequent experiments the s.c. route of infection was selected and the MLD$_{50}$ determined. Groups of mice challenged by the s.c. route with doses ranging from $10^{2}$ to $10^{-1}$ TCID$_{50}$ of CCHFV all succumbed to infection between days 5-8 following inoculation developing disease signs previously described (Figure 20). IFNAR$^{-/-}$ mice challenged with doses ranging from $10^{-2}$ to $10^{-3}$ did not succumb to infection establishing the IFNAR$^{-/-}$ mouse s.c. route MLD$_{50}$ at $5x10^{-2}$ TCID$_{50}$.

### 3.5 Subcutaneous CCHFV infection of IFNAR$^{-/-}$ mice mimics severe human CCHF

To further characterize the disease course following s.c. inoculation of CCHFV a serial sacrifice study was undertaken during which numerous disease parameters were monitored each day following inoculation.

### 3.5.1 Viremia and viral loads

Following s.c. inoculation, with 200 MLD$_{50}$ (10 TCID$_{50}$) of CCHFV/animal, infectious CCHFV was recovered from organs of IFNAR$^{-/-}$ mice as early as 24 hours p.i. however, an absence of early viremia was noted. Following a delay of 1 day the level of infectious CCHFV in IFNAR$^{-/-}$ mice increased over time with peak titers in liver samples collected on day 4 p.i. ($1.65\pm0.52x10^{4}$ TCID$_{50}$/mg) (Figure 21). High virus loads were also detected in lymph nodes ($5.06\pm2.56x10^{3}$ TCID$_{50}$/mg), spleen ($1.28\pm0.19x10^{3}$ TCID$_{50}$/mg), lung ($3.58\pm3.07x10^{3}$ TCID$_{50}$/mg), heart ($1.23\pm0.61x10^{3}$ TCID$_{50}$/mg), and lower loads were detected in the kidney ($6.43\pm2.62x10^{2}$ TCID$_{50}$/mg) and the brain ($1.96\pm0.56x10^{1}$ TCID$_{50}$/mg) (Figure 21). Viremia (as determined by the detection of infectious virus and genome copies from whole blood samples) was first detected

at day 3 post inoculation (Figure 21). This observation appears to be in accordance with human CCHF during which high viremia loads post onset of symptoms are often reported, and are associated with severity of disease, pathological changes, antigen staining and are an effective predictor of lethality [60-63, 73].

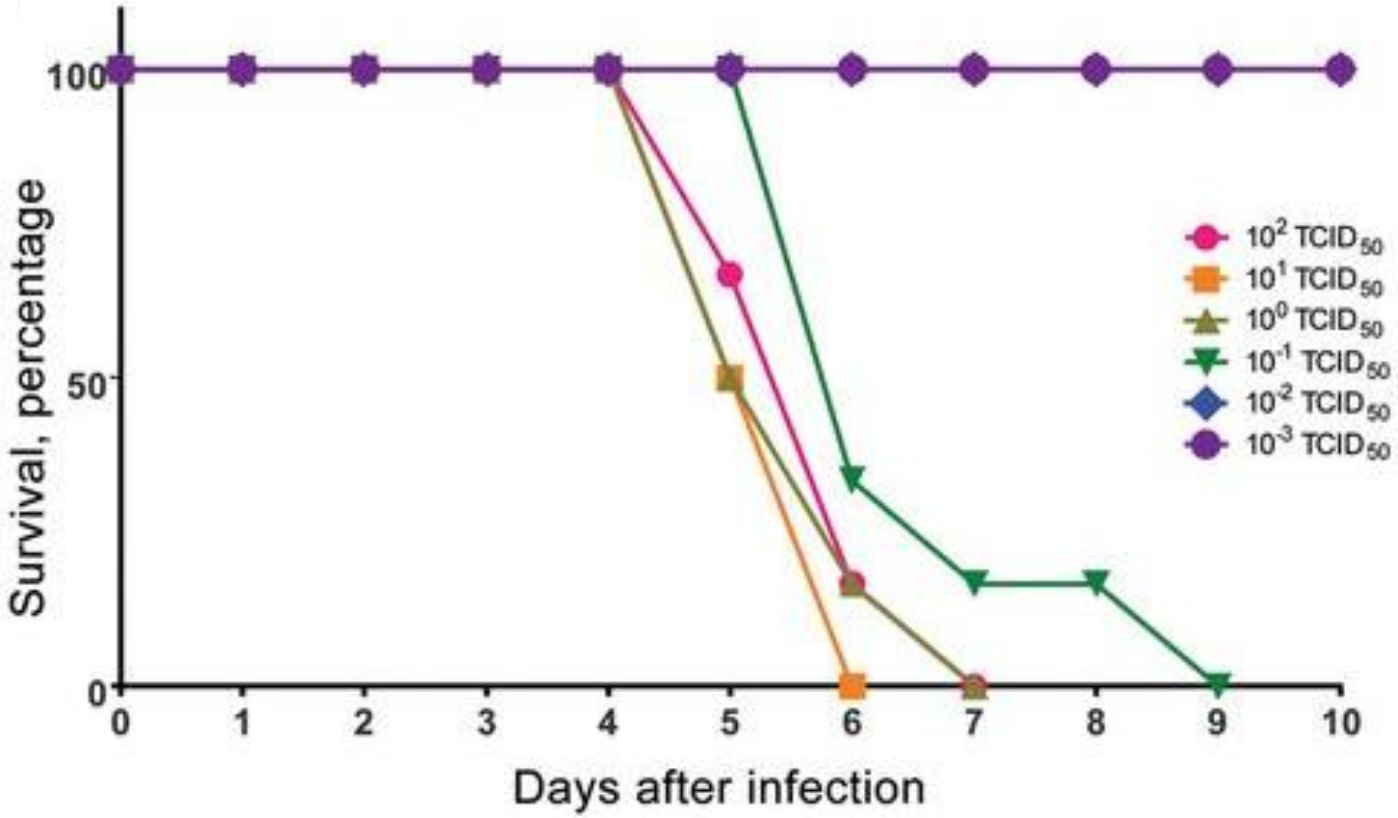


Figure 20. Determination of the CCHFV IFNAR$^{-/-}$ mouse lethal dose 50% (MLD$_{50}$) for the subcutaneous route of infection. The MLD$_{50}$ was determined using the standard tissue culture infectious dose 50% (TCID$_{50}$) assay to be 0.05 TCID$_{50}$.

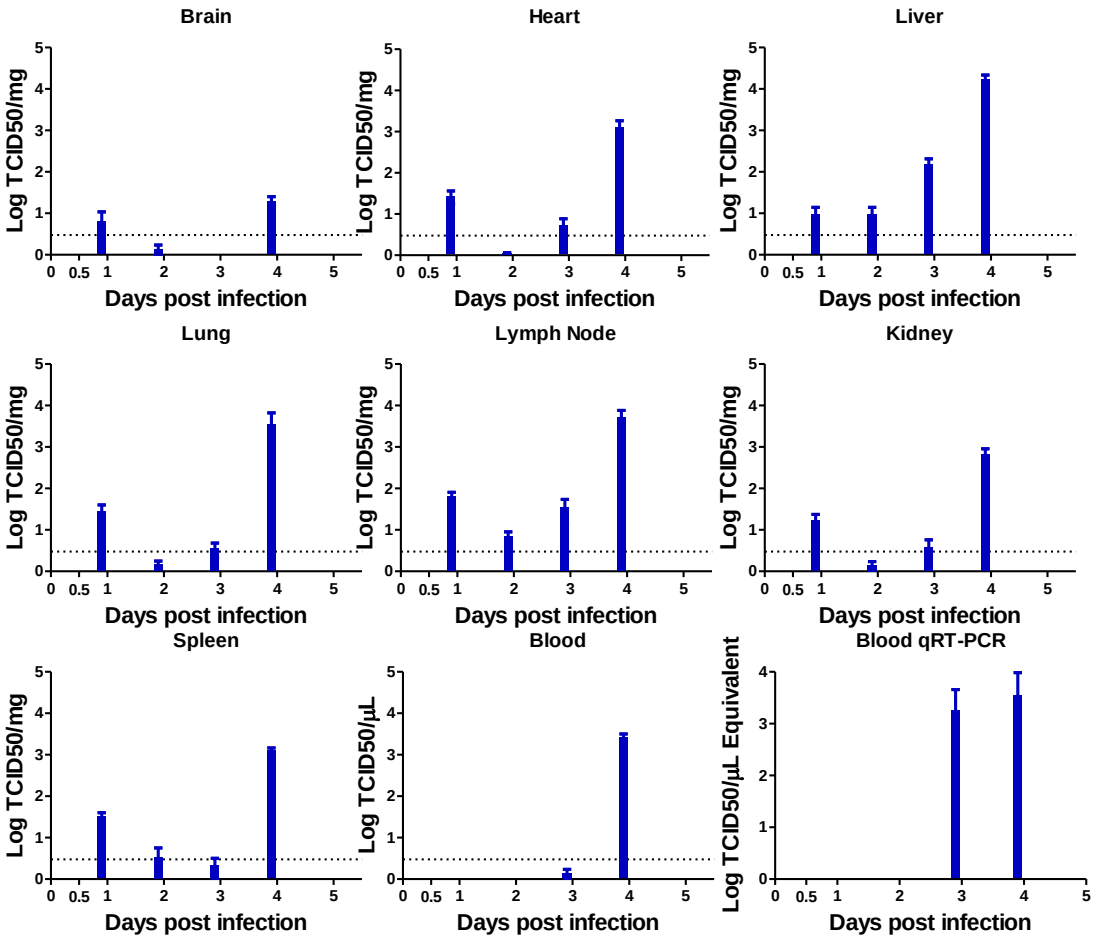


Figure 21. Virus titration of IFNAR$^{-/-}$ mouse tissues following CCHFV challenge. Groups of 6 IFNAR$^{-/-}$ mice were inoculated with 200 $LD_{50}$ (10 $TCID_{50}$) of CCHFV by the subcutaneous route and tissues sampled at indicated time points post infection. Viral titers were determined by tissue culture infectious dose 50% ($TCID_{50}$) assay, or by quantitative RT-PCR (qRT-PCR) and are displayed as standard error about the mean. Dashed line represents the limit of detection of the $TCID_{50}$ assay (3.16 infectious particles per mg of tissue). $TCID_{50}$ equivalents of less than 1 are not displayed for qRT-PCR.

### 3.5.2 Histopathology and immunohistochemistry

In accordance to the observed increased viral loads detected by infectivity assays, starting at day 3 p.i. CCHFV antigen was readily detected by IHC in several IFNAR$^{-/-}$ mouse livers and lymphoid organs. CCHFV NP was detected in cells morphologically consistent with hepatocytes, Kupffer cells (specialized liver macrophages) and infiltrating macrophages in the livers of IFNAR$^{-/-}$ mice

(Figure 22 IHC panels). The frequency and intensity of positively stained cells increased becoming coalescent at the terminal time point (Figure 22 bottom IHC panel).

Beginning at day 3 p.i. IFNAR$^{-/-}$ mice began to display significant pathological changes in the liver and lymphoid organs. Pathological changes within the liver consisted of multifocal hepatocellular necrosis with infiltration of small to moderate numbers of viable and degenerate neutrophils (Figure 22 H&E sides). The severity of liver damage increased, becoming coalescent at the terminal stage of disease.

As in the case of the liver, starting at day 3 p.i. IFNAR$^{-/-}$ lymph nodes demonstrated CCHFV antigen in cells that are morphologically consistent with macrophages and dendritic cells. The frequency of antigen positive cells increased over time (Figure 23 IHC slides). Mild to marked lymphocytolysis with loss of lymphocytes was noted in the cervical lymph nodes. In addition, affected lymph nodes were frequently infiltrated by small to moderate numbers of viable neutrophils (Figure 23 H&E slides).

CCHFV antigen staining was apparent in cells that are morphologically consistent with macrophages and dendritic cells of the splenic white pulp of CCHFV infected IFNAR$^{-/-}$ mice starting at day 3 p.i. (Figure 24 IHC slides). As with the lymph nodes, the frequency of antigen positive cells increased as the disease progressed to terminal stage. Starting on day 3 p.i. mild to marked lymphocytolysis with lymphocyte loss was apparent in the white pulp of spleens (Figure 24 H&E slides). The severity of lymphocytolysis and loss of lymphocytes increased over time resulting in loss of splenic architecture beginning at day 4 p.i. (Figure 24 bottom H&E panel).

Other tissues i.e. lung, kidney and heart displayed occasional antigen positive endothelial cells and phagocytes (Figure 25). The histological analysis correlates chronologically with virus infectivity assays and qRT-PCR. At no time point were any histological abnormalities observed in

other organs such as lung, heart, kidney or brain of CCHFV infected IFNAR$^{-/-}$ mice despite the detection of infectious virus (Figure 25).

### 3.5.3 Blood chemistry analysis

To determine the level of organ dysfunction blood chemistry analysis was carried out following CCHFV infection. Following CCHFV infection IFNAR$^{-/-}$ mice develop increased AST and ALT levels starting at 3 days p.i. and continuing until the terminal stage of disease (Figure 26). The increases in AST and ALT are indicative of severe hepatitis and correlate with the appearance of pathological changes within the liver (compare Figure 24 to 20). However, the lack of changes in serum albumin, alkaline phosphatase, gamma-glutamyltransferase, total bilirubin and total protein suggest that liver activity dysfunctional but not fully abrogated. In accordance with the pathology data, the lack of change in amylase, glucose, creatinine, and blood urea nitrogen levels, suggests that IFNAR$^{-/-}$ mice are not sustaining damage to the pancreas and kidneys.

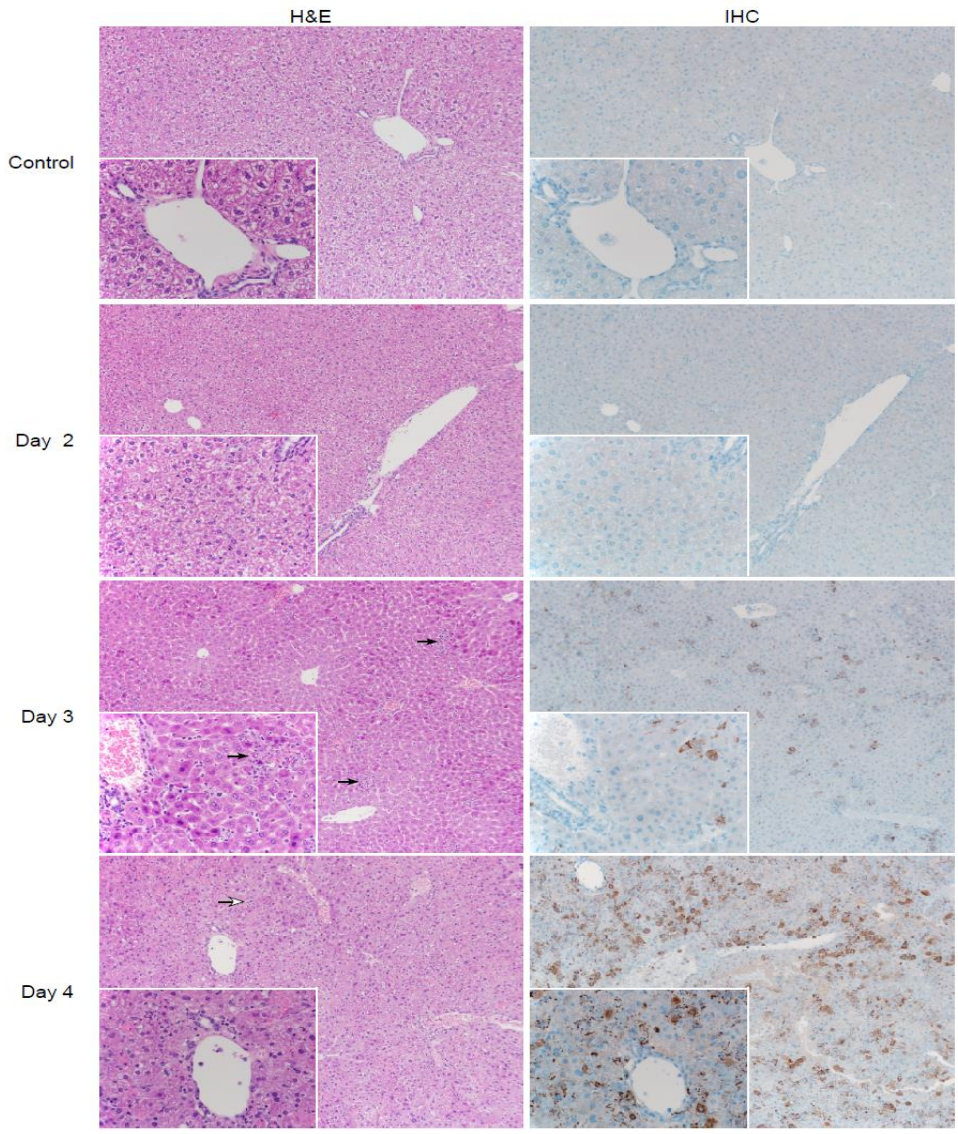


Figure 22. Pathological changes in livers of IFNAR$^{-/-}$ mice following CCHFV challenge. Groups of 6 IFNAR$^{-/-}$ mice were inoculated with 200 $LD_{50}$ (10 $TCID_{50}$) by the subcutaneous route and the liver sampled daily post infection. Liver slides were stained with hematoxylin and eosin (H&E) or $NP_{1028}$ rabbit polyclonal sera (IHC). Histological changes were first apparent on day 3 post infection. Hepatocellular necrosis with infiltration of viable and degenerate neutrophils (solid arrows) was evident after onset of pathological changes. The extent of pathological changes increased over time resulting in coalescing necrosis with loss of hepatic architecture beginning at day 4 post infection (open arrow). Shown here are representative liver samples from mock infected IFNAR$^{-/-}$ mice (control) and from CCHFV infected IFNAR$^{-/-}$ mice at day 2, 3 and 4 post infection. Images are at a magnification of 10x with 40x for the insets.

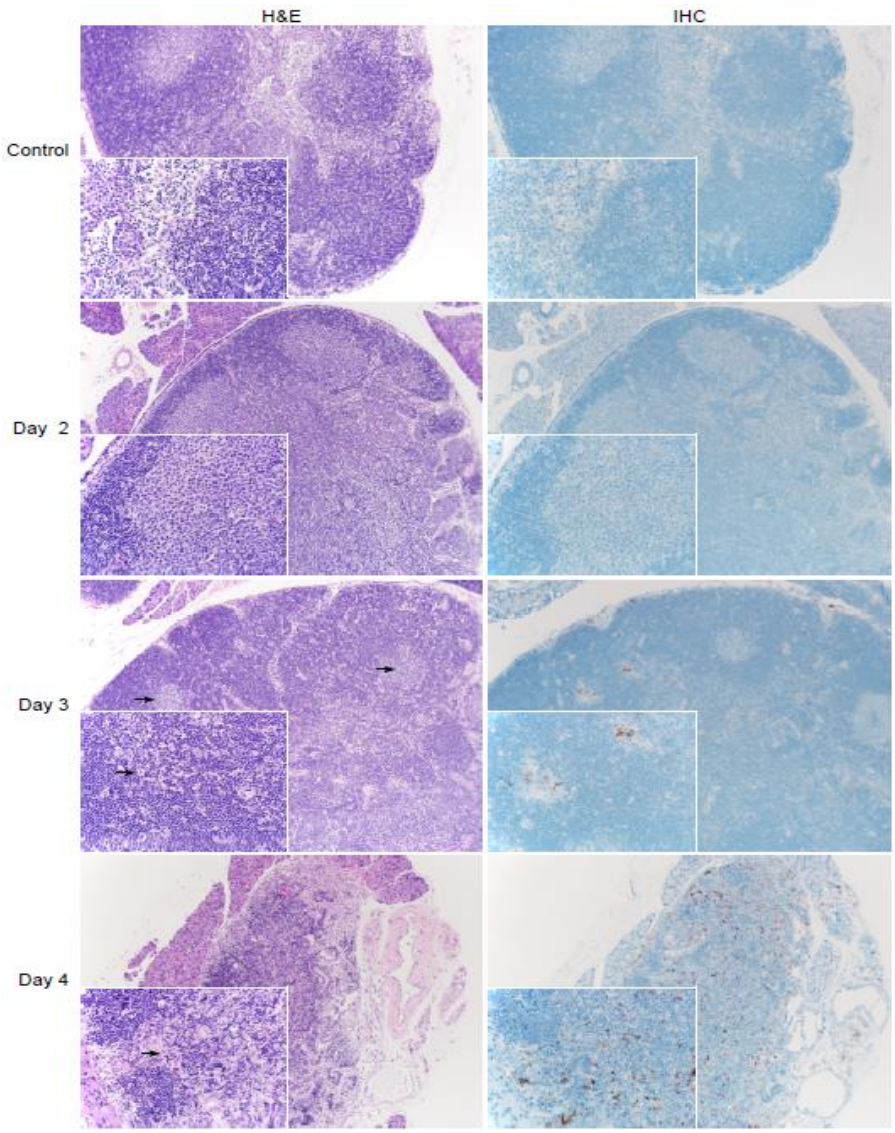


Figure 23. Pathological changes in lymph nodes of IFNAR$^{-/-}$ mice following CCHFV challenge. Groups of 6 IFNAR$^{-/-}$ mice were inoculated with 200 $LD_{50}$ (10 $TCID_{50}$) by the subcutaneous route and the cervical lymph nodes sampled daily post infection. Lymph node slides were stained with hematoxylin and eosin (H&E) or $NP_{1028}$ rabbit polyclonal sera (IHC). Histological changes were first apparent on day 3 post infection. Lymph nodes display lymphocytolysis of follicular centers accompanying a loss of lymphocytes (solid arrows). The severity of lymphocytolysis and loss of lymphocytes increased over time resulting in loss of lymphoid architecture beginning at day 4 post infection. Shown here are representative lymph node samples from mock infected IFNAR$^{-/-}$ mice (control) and from CCHFV infected IFNAR$^{-/-}$ mice at day 2, 3 and 4 post infection. Images are at a magnification of 10x with 40x for the insets.

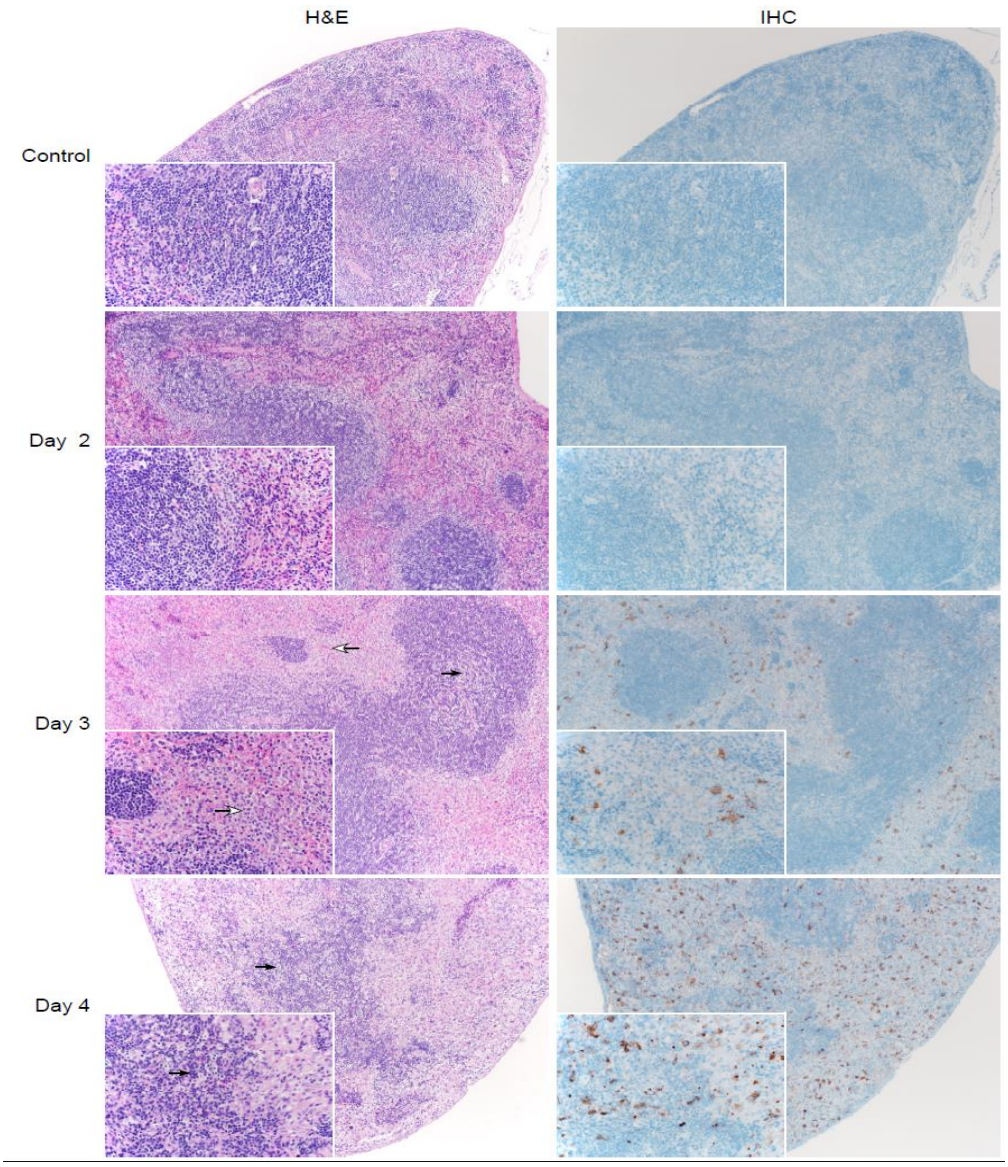


Figure 24. Pathological changes in spleens of IFNAR$^{-/-}$ mice following CCHFV challenge. Groups of 6 IFNAR$^{-/-}$ mice were inoculated with 200 $LD_{50}$ (10 $TCID_{50}$) by the subcutaneous route and the spleen sampled daily post infection. Spleen slides were stained with hematoxylin and eosin (H&E) or $NP_{1028}$ rabbit polyclonal sera (IHC). Spleen displayed diffuse lymphocytolysis with loss of lymphocytes from the white pulp (solid arrow) and diffuse infiltration of neutrophils (open arrows) by day 3 post infection. The extent of pathological changes increased over time with a marked loss of the white pulp by day 4 post infection. Shown here are representative spleen samples from mock infected IFNAR$^{-/-}$ mice (control) and from CCHFV infected IFNAR$^{-/-}$ mice at day 2, 3 and 4 post infection. Images are at a magnification of 10x with 40x for the insets.

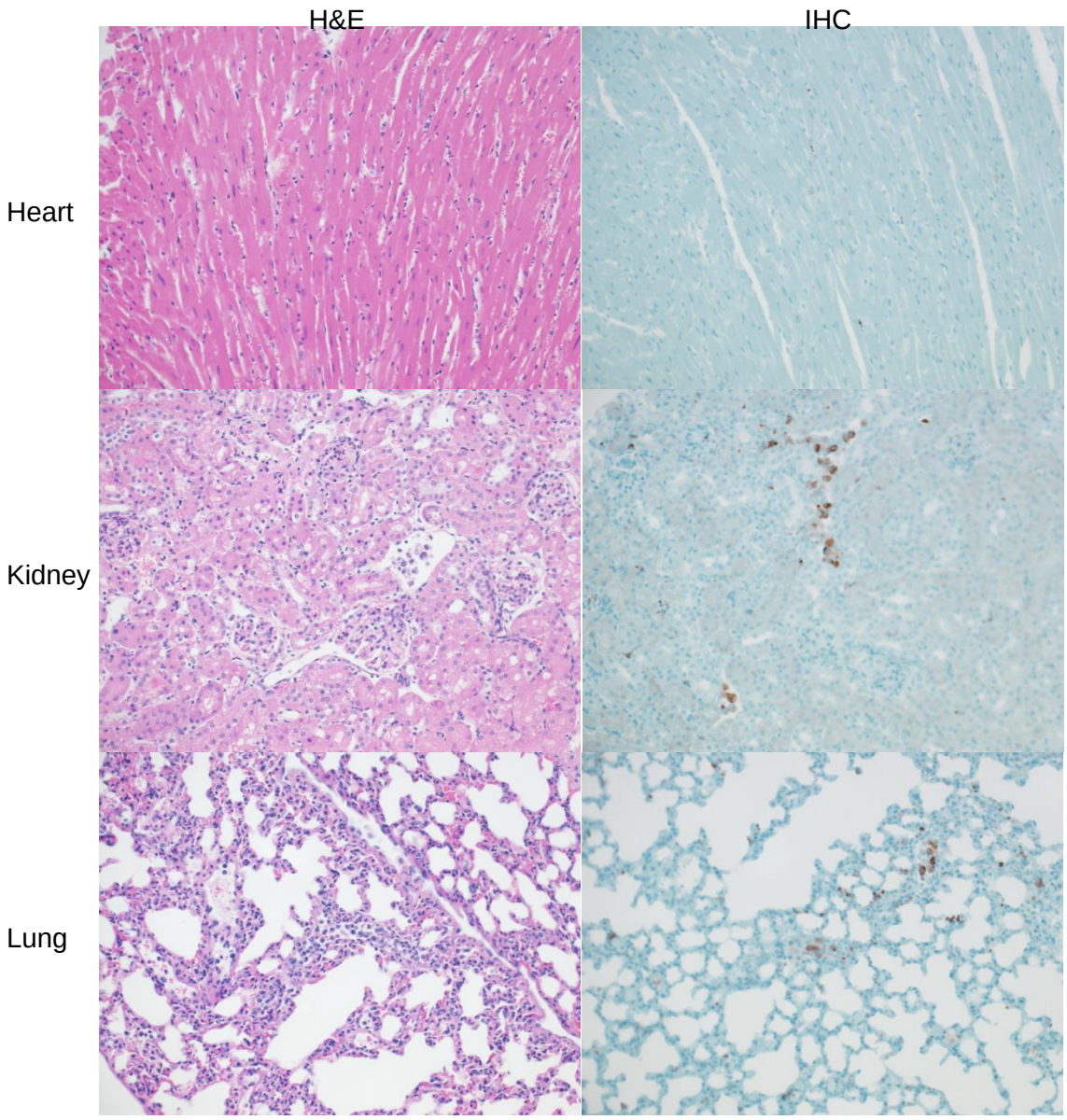


Figure 25. Lack of pathological change despite antigen staining in IFNAR$^{-/-}$ mouse tissues following CCHFV challenge. Groups of 6 IFNAR$^{-/-}$ mice were inoculated with 200 $LD_{50}$ (10 $TCID_{50}$) by the subcutaneous route and the heart, kidney and lung sampled on the 3rd day post infection. Tissue slides were stained with hematoxylin and eosin (H&E) or NP1028 rabbit polyclonal sera (IHC). No pathological changes were detected in any tissue observed. CCHFV antigen staining was apparent in cells morphologically consistent with phagocytes and occasionally endothelial cells. Shown here are representative tissue samples from a CCHFV infected IFNAR$^{-/-}$ mouse. Images are at a magnification of 20x.

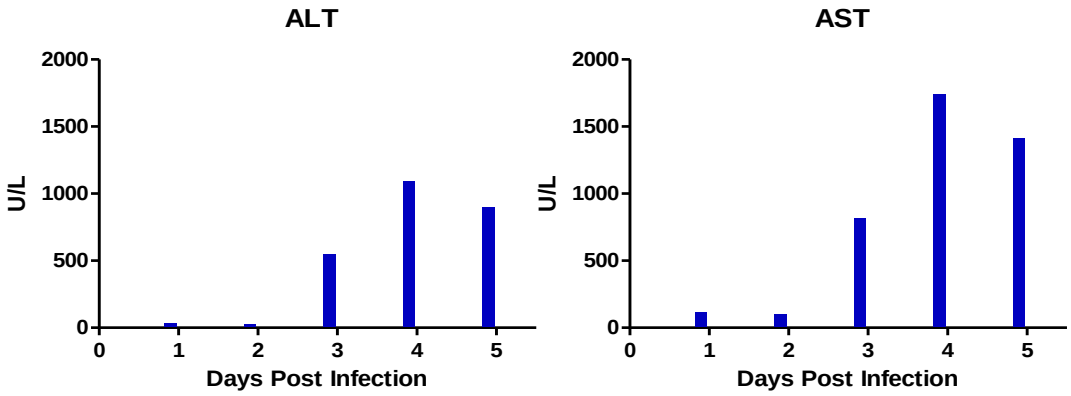


Figure 26. Increases in circulating liver enzymes following CCHFV challenge. A subset of mice were inoculated with 200 $LD_{50}$ (10 $TCID_{50}$) by the s.c. route and exsanguinated into citrate coated syringes at indicated time points n = 1 pool (pools of 6 animal samples for days 1-4 p.i., pool of 3 animal samples for day 5 p.i.). CCHFV infected $IFNAR^{-/-}$ mice showed increased plasma alanine aminotransferase (ALT) and aspartate aminotransferase (AST) levels. Limited differences were observed in albumin, amylase, alkaline phosphatase, gamma-glutamyltransferase, glucose, cholesterol, total protein, total bilirubin, blood urea nitrogen, and creatinine (not shown).

### 3.5.4 Hematology and coagulation

Severe thrombocytopenia (up to 90% reduction) is a hallmark and a predictor of fatality of CCHF in humans [60, 72, 105]. Similarly, a significant decrease in platelet counts in infected $IFNAR^{-/-}$ mice was observed beginning at day 3 p.i., that culminated in a ~90% decrease in platelet counts by the terminal stage of infection (Figure 27a). The decrease in total platelets was accompanied by significant increases in the mean platelet volume (MPV) suggesting platelet destruction as the likely mechanism of the decrease as opposed to decreases in production (Figure 27b). Direct destruction of platelets, as opposed to consumption, is further supported by the accumulation of plasma fibrinogen levels over the disease course (Figure 27c) and a lack of organ fibrin deposition, as demonstrated by H&E and PTAH staining (Figures 22-25 and 28). In addition neither vascular leakage nor tissue hemorrhages were detected by histologic analysis (Figures 22 to 25). The induced thrombocytopenia resulted in coagulopathy in $IFNAR^{-/-}$ mice which resulted in significant increases in APTT, but did not affect PT throughout infection (Figure 29). This

suggests a lack of overt DIC in this model and suggests the involvement of depletion of coagulation factors [106].

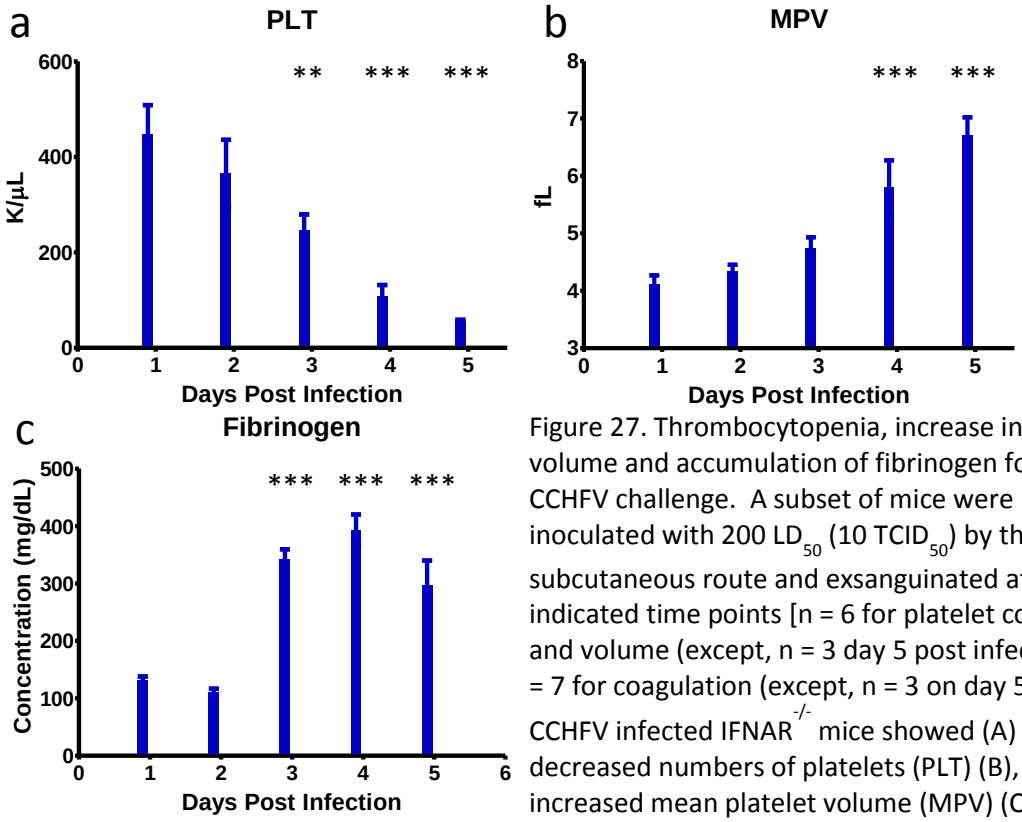


Figure 27. Thrombocytopenia, increase in platelet volume and accumulation of fibrinogen following CCHFV challenge. A subset of mice were inoculated with 200 $LD_{50}$ (10 $TCID_{50}$) by the subcutaneous route and exsanguinated at indicated time points [n = 6 for platelet counts and volume (except, n = 3 day 5 post infection); n = 7 for coagulation (except, n = 3 on day 5 p.i.). CCHFV infected $IFNAR^{-/-}$ mice showed (A) decreased numbers of platelets (PLT) (B), increased mean platelet volume (MPV) (C), increased serum fibrinogen levels. This data suggests that CCHFV infection of $IFNAR^{-/-}$ mice is associated with direct platelet destruction rather than reduced platelet production. All data was analyzed by one-way ANOVA with Dunnet's Post Test and is presented as standard error about the mean with *** representing $p<0.001$, and ** representing $p<0.01$ compared to uninfected controls.

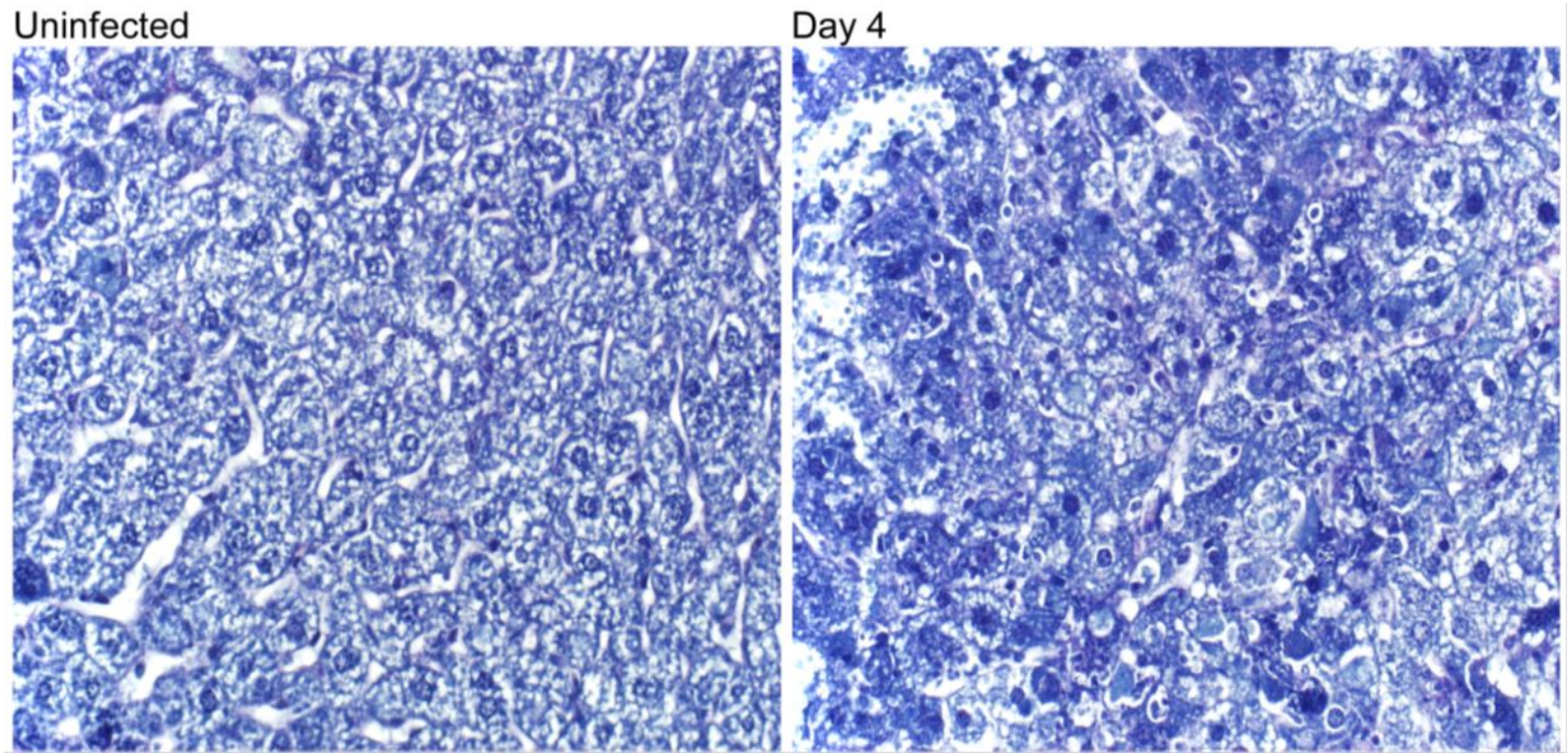


Figure 28. Phosphotungstic acid haematoxylin (PTAH) staining of liver at the terminal time point reveals no fibrin deposition. Groups of 6 IFNAR$^{-/-}$ mice were inoculated with 200 $LD_{50}$ (10 $TCID_{50}$) of CCHFV by the subcutaneous route and organs were harvested daily post infection. Tissues were stained with PTAH staining did not show any evidence of fibrin deposition in uninfected control mice and CCHFV infected mice at terminal disease stage (Day 4 post infection). Images are at a magnification of 40X.

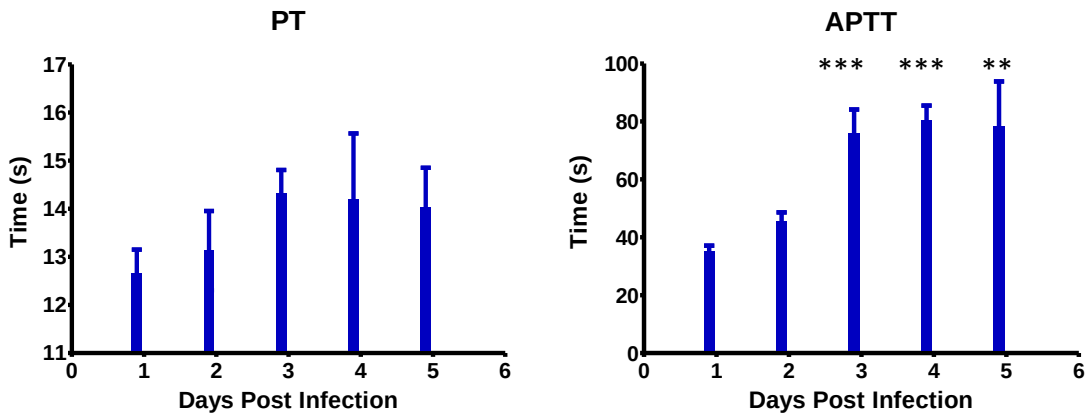


Figure 29. Coagulopathy following CCHFV challenge. A subset of mice were inoculated with 200 $LD_{50}$ (10 $TCID_{50}$) by the subcutaneous route and exsanguinated at indicated time points. n = 6 for platelet counts and n=7 for coagulation (except, n = 3 on day 5 post infection). CCHFV infected $IFNAR^{-/-}$ mice showed significant increase in activated partial thromboplastin time (APTT) starting at day 3 post infection and continuing until terminal stages of infection. Prothrombin time (PT) was unaffected by CCHFV infection. All data was analyzed by one-way ANOVA with Dunnet's Post Test and is presented as standard error about the mean with *** representing $p<0.001$, and ** representing $p<0.01$ compared to uninfected controls.

On day 2 p.i. $IFNAR^{-/-}$ mice develop a transient increase in total white blood cells, lymphocytes, neutrophils and monocytes (Figure 30). Red blood cell parameters are largely unaffected until day 5 p.i. and then significantly decrease (Figure 31). The drop in total numbers suggests that during the terminal stages of infection $IFNAR^{-/-}$ mice develop blood loss, through sequestration or leakage, or red blood cell destruction [107]. The lack of coagulation in the organs of $IFNAR^{-/-}$ mice (Figures 22 to 25) suggests that $IFNAR^{-/-}$ mice develop mucosal hemorrhage, as occurs in severe human CCHFV infection, or undergo red blood cell destruction.

### 3.5.5 Pro-inflammatory cytokine production in $IFNAR^{-/-}$ mice

$IFNAR^{-/-}$ mice developed strong pro-inflammatory immune responses following CCHFV infection as demonstrated by significant increases in G-CSF, IFNγ, CXCL10 and CCL2 beginning at day 3 p.i., and GM-CSF, IL -1α, -1β, -2, -6, -12p70, -13, -17, CXCL1, CCL3, CCL5 and TNFα at the time of

death/euthanasia (Figure 32). Pro-inflammatory cytokines and chemoattractant molecules observed in the sera of infected mice accumulate over the disease course.

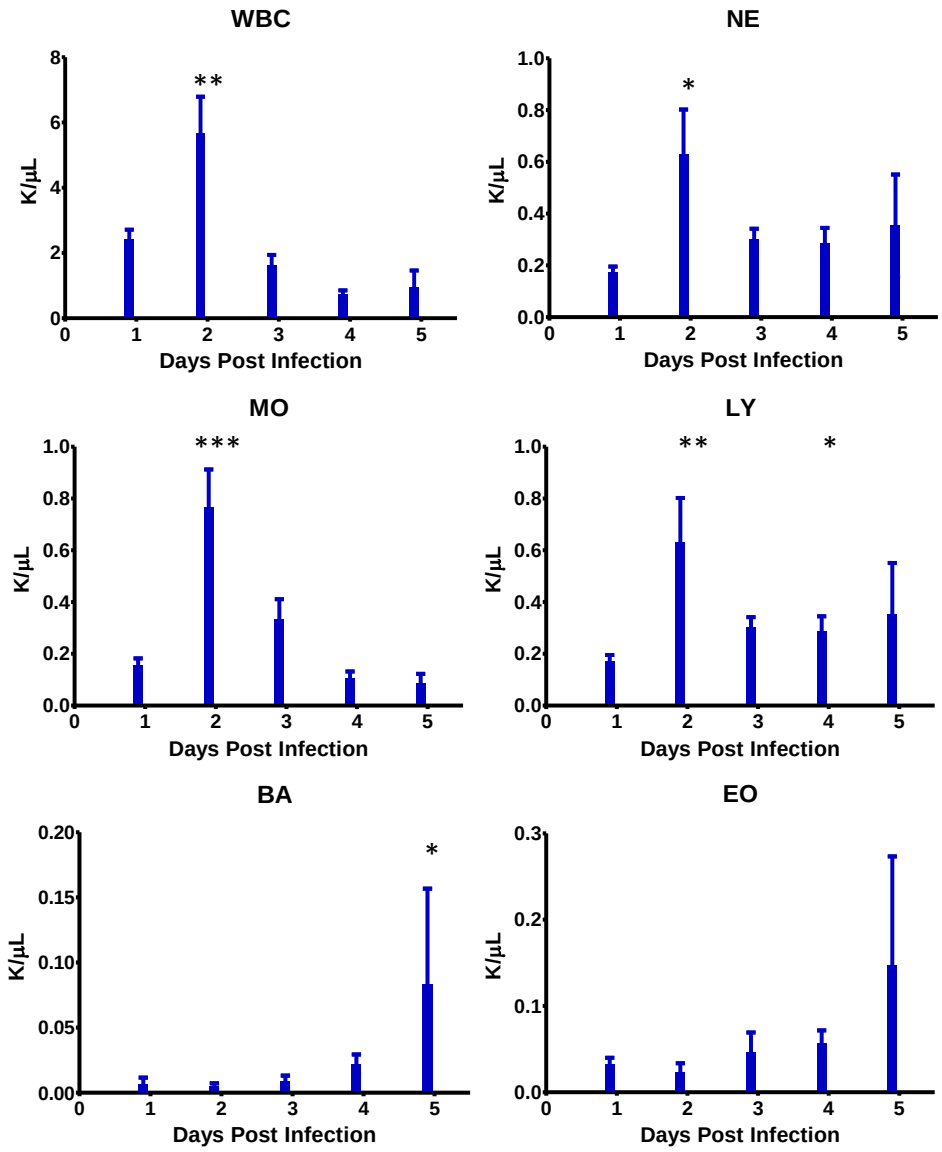


Figure 30. White blood cell parameters following CCHFV challenge. Groups of 6 IFNAR$^{-/-}$ mice were inoculated with 200 $LD_{50}$ (10 $TCID_{50}$) of CCHFV by the subcutaneous route and blood was harvested daily post infection. Lymphocyte parameters were monitored to evaluate differences following CCHFV infection. Transient significant increases in neutrophils, monocytes and lymphocytes are observed at day two post infection, which is a typical response to infection. In contrast eosinophils are slightly elevated at day 5 post infection and basophils are not affected by CCHFV infection. The two day delay prior to detectable increases in immune cells suggests that CCHFV is escaping detection during early infection. WBC = white blood cells, NE = neutrophils, MO = monocytes, LY = lymphocytes, BA = basophils, EO = eosinophils. All data was analyzed by one-way ANOVA with Dunnet's Post Test and is presented as standard error about the mean with *** representing $p<0.001$, ** representing $p<0.01$, and * representing $p<0.05$ compared to uninfected controls.

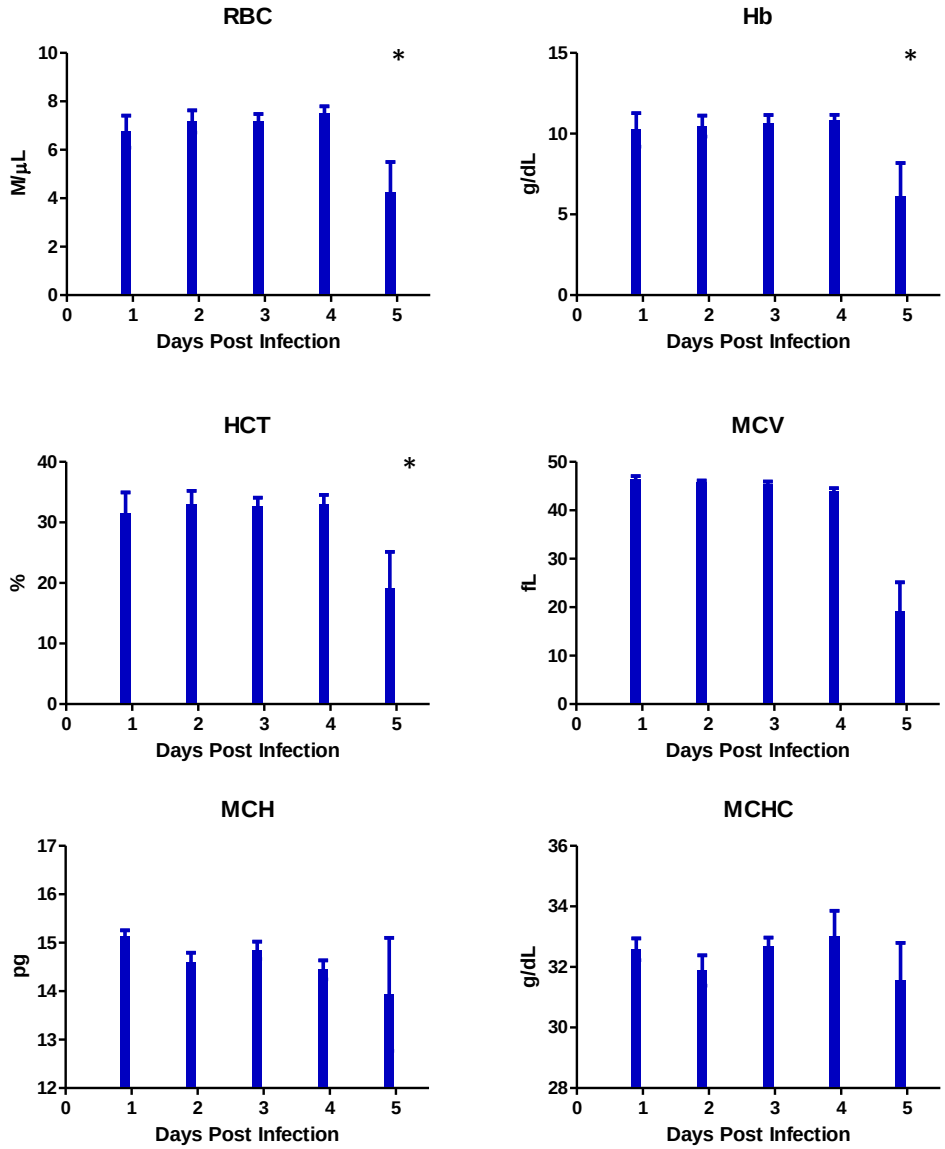


Figure 31. Red blood cell parameters following CCHFV challenge. Groups of 6 IFNAR$^{-/-}$ mice were inoculated with 200 LD50 (10 $TCID_{50}$) of CCHFV by the subcutaneous route and blood was harvested daily post infection. Red blood cell parameters were monitored to evaluate differences following CCHFV infection. Significant decreases in red blood cells (RBC), hemoglobin (Hb), and hematocrit (HCT) are observed at the terminal stages of infection suggesting blood loss. In contrast mean corpuscular volume (MCV), mean corpuscular hemoglobin (MCH) and mean corpuscular hemoglobin concentration (MCHC) are not affected by CCHFV infection. All data was analyzed by one-way ANOVA with Dunnet's Post Test and is presented as standard error about the mean with * representing $p<0.05$ compared to uninfected controls.

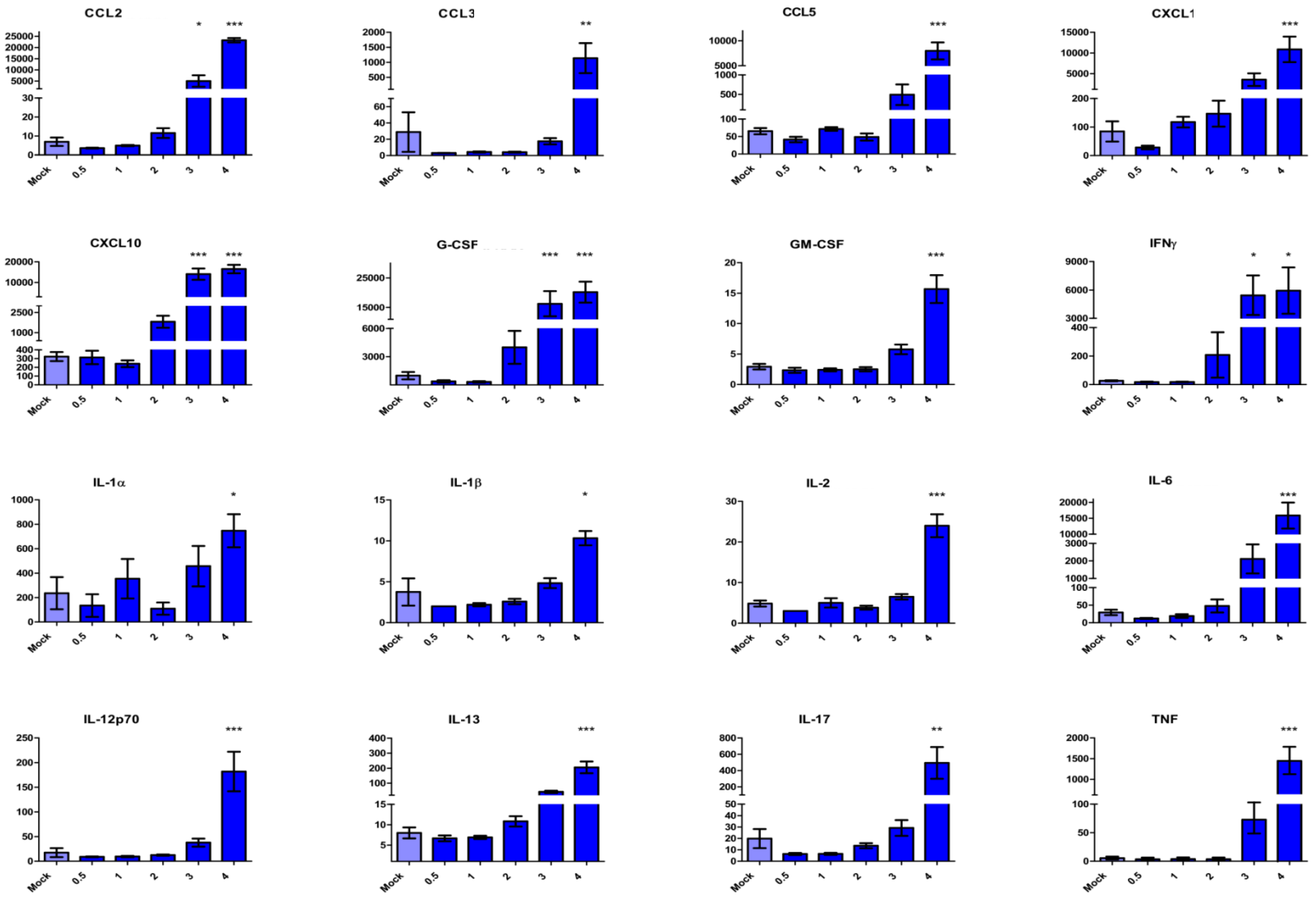
CCL2
CCL3
CCL5
CXCL1
CXCL10
G-CSF
GM-CSF
IFNγ
IL-1α
IL-1β
IL-2
IL-6
IL-12p70
IL-13
IL-17
TNF
Mock
0.5
1
2
3
4

Figure 32. Serum levels of cytokine/chemokines following CCHFV challenge. IFNAR$^{-/-}$ mice (n = 6) were inoculated with 200 $LD_{50}$ (10 $TCID_{50}$) of CCHFV by the subcutaneous route and exsanguinated at indicated time points for evaluation of serum cytokine and chemokine levels. CCHFV infected IFNAR$^{-/-}$ mice displayed marked increases in pro-inflammatory and chemoattractant molecules. All data was analyzed by one-way ANOVA with Dunnet's Post Test and is presented as standard error about the mean with * representing $p<0.05$, ** representing $p<0.01$ and *** representing $p<0.001$ compared to uninfected controls. G-CSF = granulocyte colony stimulating factor, GM-CSF = granulocyte-macrophage colony stimulating factor, IFNγ = Interferon γ, IL = Interleukin, CXCL10 = interferon γ induced protein-10, CXCL1 = Chemokine (C-X-C motif) ligand 1 like, CCL2 = monocyte chemotactic protein-1, CCL3 = Macrophage Inflammatory Protein 1α, CCL5 = Regulated upon Activation, Normal T-cell Expressed, and Secreted and TNF = Tumor Necrosis Factor α.

### 3.6 Ad vaccination regimens

#### 3.6.1 Single vaccination results in partial protection

To evaluate the minimal requirements of a vaccine, IFNAR$^{-/-}$ mice were vaccinated with combinations of Ad vectors expressing CCHFV structural proteins by the i.m. route. IFNAR$^{-/-}$ mice vaccinated only with components of the GPC, ie Ad-GPC, Ad-$G_N$, Ad-$G_C$, and Ad-$G_N$/Ad-$G_C$, were neither protected from lethal CCHFV challenge nor was there a difference in onset of disease and disease progression as evidenced by weight loss and appearance of disease signs and death/euthanasia (Figure 33). In contrast, animals vaccinated with Ad-NP were partially protected (33% protection) with a significant delay in time to death in animals which succumbed to infection (10 days vs 5 days, $p<0.01$) (Figure 34). Addition of $G_N$ and $G_C$ subunits did not significantly increase protection compared to vaccination with NP alone (44% vs 33%, respectively); however, a statistically significant delay in survival time was observed (18 vs 10 days, respectively, $p<0.01$). Combination of NP and GPC, however had increased protection with 78% of IFNAR$^{-/-}$ mice protected compared to 33% and 44% with NP alone or combination of $G_N$/$G_C$/NP, respectively ($p<0.01$) (Figure 34).

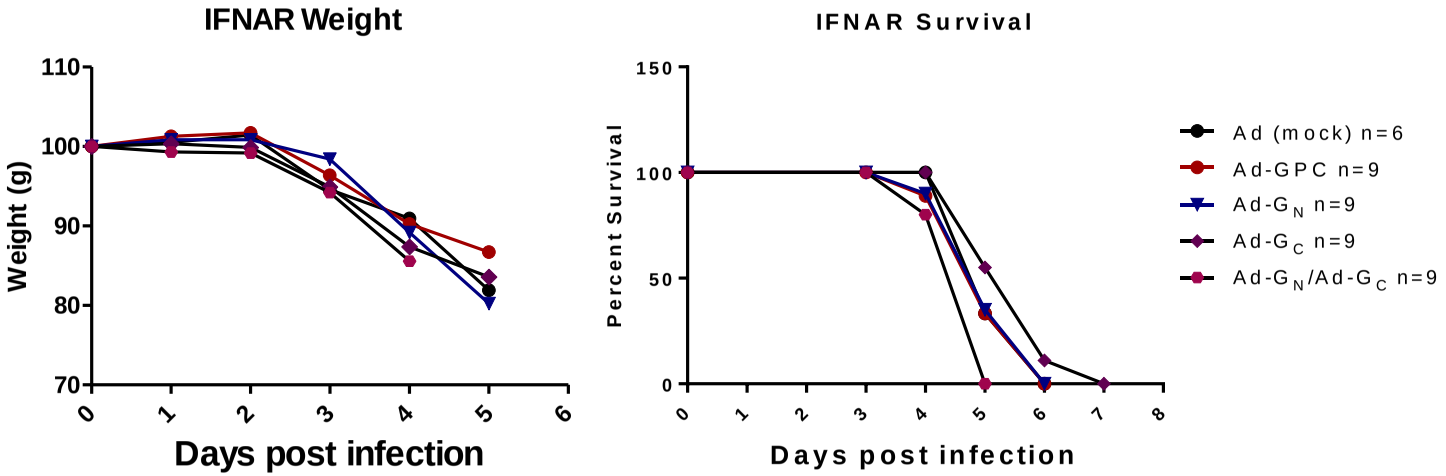


Figure 33. Disease progression following CCHFV challenge of mice vaccinated with Ad expressing glycoproteins only. Groups of 9 IFNAR$^{-/-}$ mice were vaccinated with $10^8$ Adenovirus (Ad) expressing CCHFV complete glycoprotein precursor (GPC), glycoprotein $G_N$, glycoprotein $G_C$ or combination of $G_N$ and $G_C$ by the intramuscular route. 28 days post vaccination IFNAR$^{-/-}$ mice were challenged with 1000 $LD_{50}$ (50 $TCID_{50}$) of CCHFV by the subcutaneous route and monitored for disease onset. Expression of only glycoproteins by Ad did not protect mice from lethal disease or significantly alter the disease course.

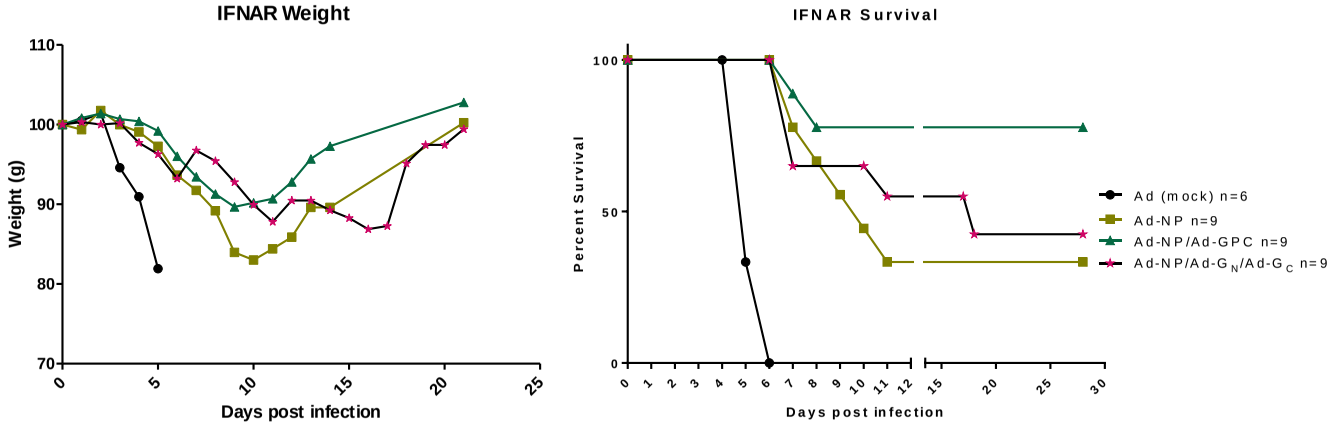


Figure 34. Disease progression following CCHFV challenge of mice vaccinated with Ad expressing glycoproteins and/or NP. Groups of 9 IFNAR$^{-/-}$ mice were vaccinated with $10^8$ Adenovirus (Ad) expressing CCHFV nucleoprotein (NP), or combinations of Ad expressing NP and Ad expressing complete glycoprotein precursor (GPC), or Ad expressing NP, Ad expressing glycoprotein $G_N$ and $G_C$ by the intramuscular route. 28 days post vaccination IFNAR$^{-/-}$ mice were challenged with 1000 $LD_{50}$ (50 $TCID_{50}$) of CCHFV by the subcutaneous route and monitored for disease signs. Expression of NP protected 33% of the animals from lethal CCHFV challenge ($p<0.001$) compared to mock vaccinated animals with a mean survival time of 10 days vs 5 days compared to unprotected groups ($p<0.01$). Expression of NP with a combination of $G_N$ and $G_{C,}$ is protective compared to mock ($p<0.001$), but does not statistically enhance survival compared to vaccination with NP alone (44% vs 33%, respectively); however, it significantly extends the survival time from 10 days post infection to 18 days post infection. Vaccination with combination of GPC and NP provides the greatest increase in survival, which is statistically higher than vaccination with any other vaccination regimen (78% survival compared to 33% with NP alone or 44% with combination of $G_N$, $G_C$ and NP).

At 3 days p.i. Ad vaccinated groups which displayed delay in onset of disease following CCHFV challenge did not have detectable CCHFV viremia, as detected by quantitative RT-PCR and virus

infectivity assay unlike susceptible groups, which achieved viremia titers of $10^4$ $TCID_{50}$ equivalents/mL and $10^4$ $TCID_{50}$/mL at 3 days p.i. (Figure 35). Surprisingly, there was no reduction in CCHFV organ loads in $IFNAR^{-/-}$ mice vaccinated with the partially protective regimens as compared to mock vaccinated groups at the same time point (Figure 35). Furthermore, in Ad-NP/Ad-GPC vaccinated animals the viral loads in liver were higher than in mock vaccinated or non-protected groups, demonstrating that sterile immunity is neither conferred by vaccination nor required for protection.

The Ad (mock) vaccinated animals served as positive controls for analysis of pathological changes following CCHFV infection. At 3 days p.i., Ad vaccinated mice developed multifocal to coalescing hepatocellular necrosis with infiltration of small to moderate numbers of viable and degenerate neutrophils in the liver (Figure 36 H&E panels). At this time point the spleens of $IFNAR^{-/-}$ mice demonstrated mild to marked acute necrotizing splenitis with loss of lymphocytes observed in the white pulp as has been previously noted (Section Figure 37 H&E panels). IHC demonstrates moderate amounts of CCHFV antigen, which scattered throughout the liver and spleen, and is associated with cells morphologically consistent with hepatocytes, Kupffer cells, macrophages and endothelial cells, as previously reported [73](Figures 36 and 37 IHC panels).

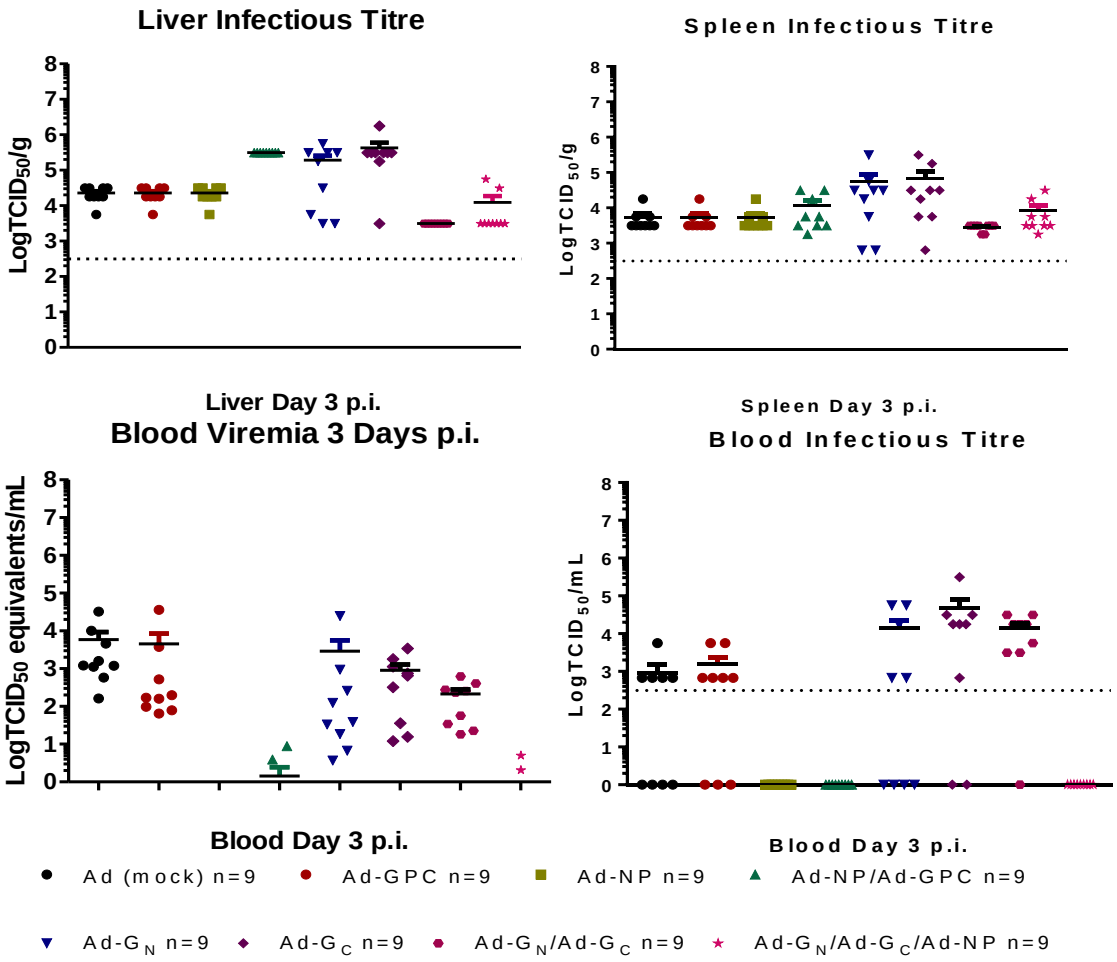


Figure 35. CCHFV organ load and viremia following challenge of vaccinated IFNAR$^{-/-}$ mice. Groups of 9 IFNAR$^{-/-}$ mice were vaccinated with $10^8$ Adenovirus (Ad) expressing CCHFV nucleoprotein (NP), glycoprotein precursor (GPC), glycoprotein $G_N$, glycoprotein $G_C$, combinations of Ad expressing $G_N$ and $G_C$, Ad expressing NP and GPC or Ad expressing NP and the glycoproteins $G_N$ and $G_C$ by the intramuscular route. Four weeks post vaccination IFNAR$^{-/-}$ mice were challenged with 1000 $LD_{50}$ (50 $TCID_{50}$) of CCHFV by the subcutaneous route and necropsied at 3 days post infection. CCHFV viral loads were analyzed by virus titration using a standard $TCID_{50}$ assay. Significant CCHFV viral loads were detected in both spleen and liver in all vaccinated groups regardless of the vaccination regimen used. High tissue viral loads do not correlate with protection from lethal CCHFV challenge following single Ad vaccination in this model.

At 3 days p.i., IFNAR$^{-/-}$ mice vaccinated with Ad-$G_N$, Ad-$G_C$, Ad-$G_N$/Ad-$G_C$ and Ad-GPC also displayed multifocal to coalescing hepatocellular necrosis with infiltration of small to moderate numbers of viable and degenerate neutrophils in the liver similar in severity to the Ad vaccinated IFNAR$^{-/-}$ mice (Figure 36 H&E panels). Similarly splenic pathological changes were similar in composition and severity as the Ad vaccinated control group (Figure 37 H&E panels). IHC analysis were essentially identical compared to Ad vaccinated IFNAR$^{-/-}$ mice both in terms of staining within cell populations and extent of staining (Figures 36 and 37 IHC panels).

In contrast to the unprotected groups at 3 days p.i., IFNAR$^{-/-}$ mice vaccinated with Ad-NP, Ad-NP/Ad-$G_N$/Ad-$G_C$ and Ad-NP/Ad-GPC had less severe hepatic lesions consisting of mild focal necrosis and infiltration of small numbers of viable and degenerate neutrophils without any detectable splenic lesions (Figure 36 and 37 H&E panels). CCHFV antigen was detectable by IHC in the spleen and liver of these groups, however the extent of staining was lower compared to unprotected groups (Figures 36 and 37 IHC panels).

As this vaccination regimen was not fully protective, the predictive power with this vaccination regimen is limited and additional experiments to boost protection to 100% efficacy were undertaken.

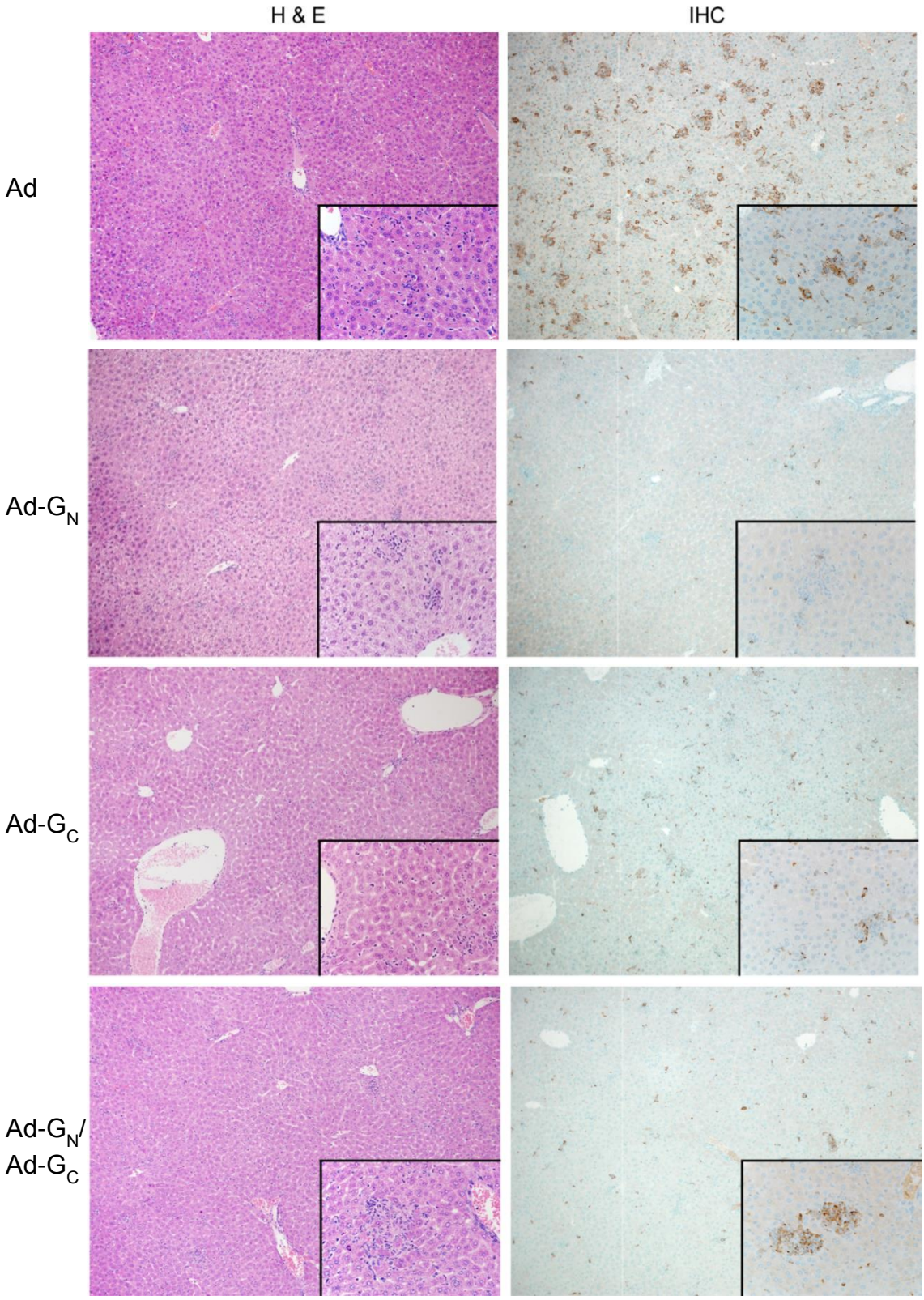
H & E
IHC
Ad
Ad-G$_N$
Ad-G$_C$
Ad-G$_N$/
Ad-G$_C$

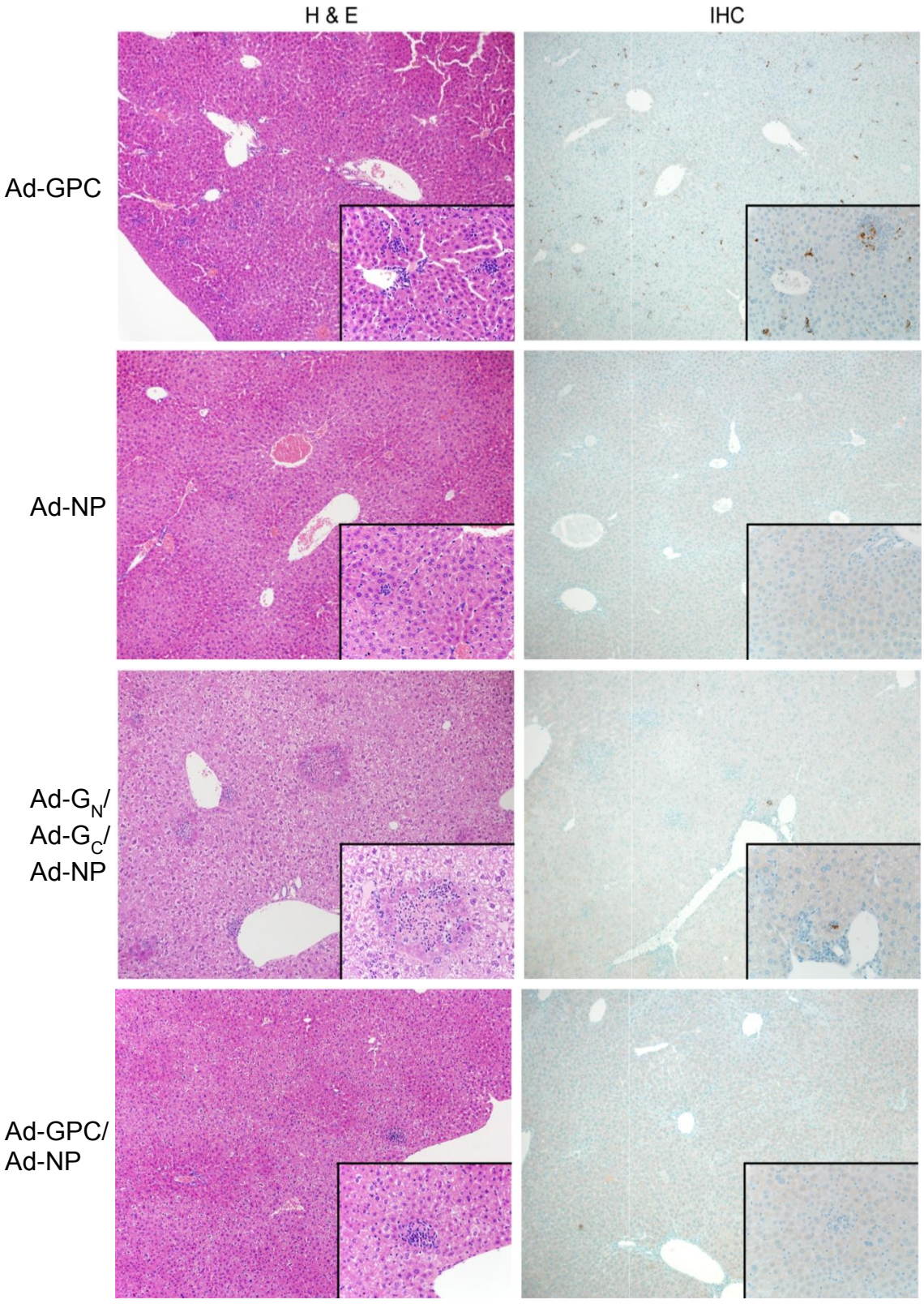
H & E
IHC
Ad-GPC
Ad-NP
Ad-G$_N$/
Ad-G$_C$/
Ad-NP
Ad-GPC/
Ad-NP

Figure 36. Pathologic changes in the livers of vaccinated IFNAR$^{-/-}$ mice challenged with CCHFV. Groups of 9 IFNAR$^{-/-}$ mice were vaccinated with the indicated Adenovirus (Ad) construct by the intramuscular route and 4 weeks later inoculated with 1000 $LD_{50}$ (50 $TCID_{50}$) by the subcutaneous route and the liver sampled on day 3 post infection. Liver slides were stained with hematoxylin and eosin (H&E) or $NP_{1028}$ rabbit polyclonal sera (IHC). Histological changes are apparent on groups vaccinated with Ad (mock vaccinated), Ad-$G_N$, Ad-$G_C$, Ad-$G_N$/Ad-$G_C$ and Ad-GPC. Hepatocellular necrosis with infiltration of viable and degenerate neutrophils was evident after onset of pathological changes. Shown here are representative liver samples from infected IFNAR$^{-/-}$ mice. Images are at a magnification of 10x with 40x for the insets.

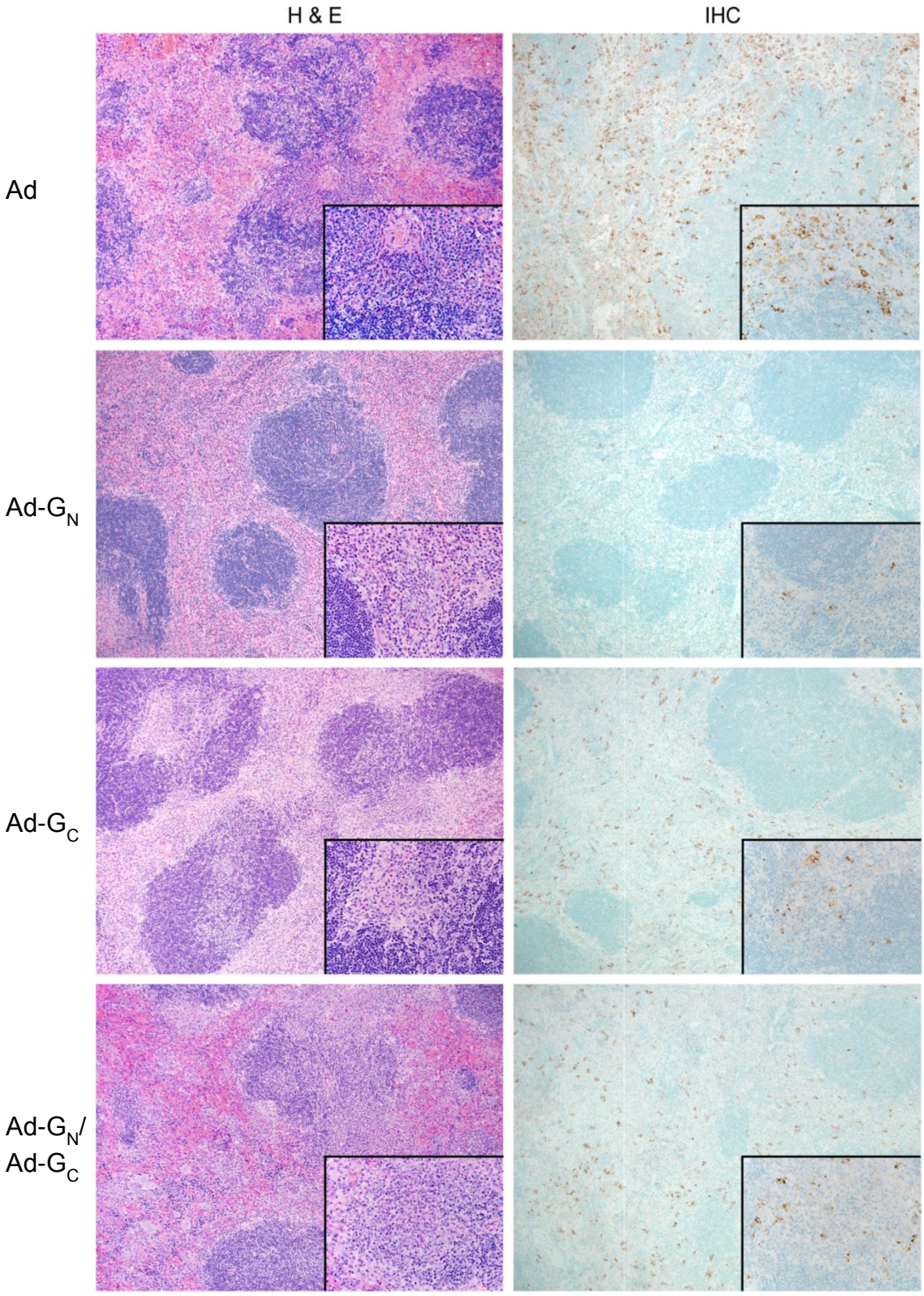
H & E
IHC
Ad
Ad-G$_N$
Ad-G$_C$
Ad-G$_N$/
Ad-G$_C$

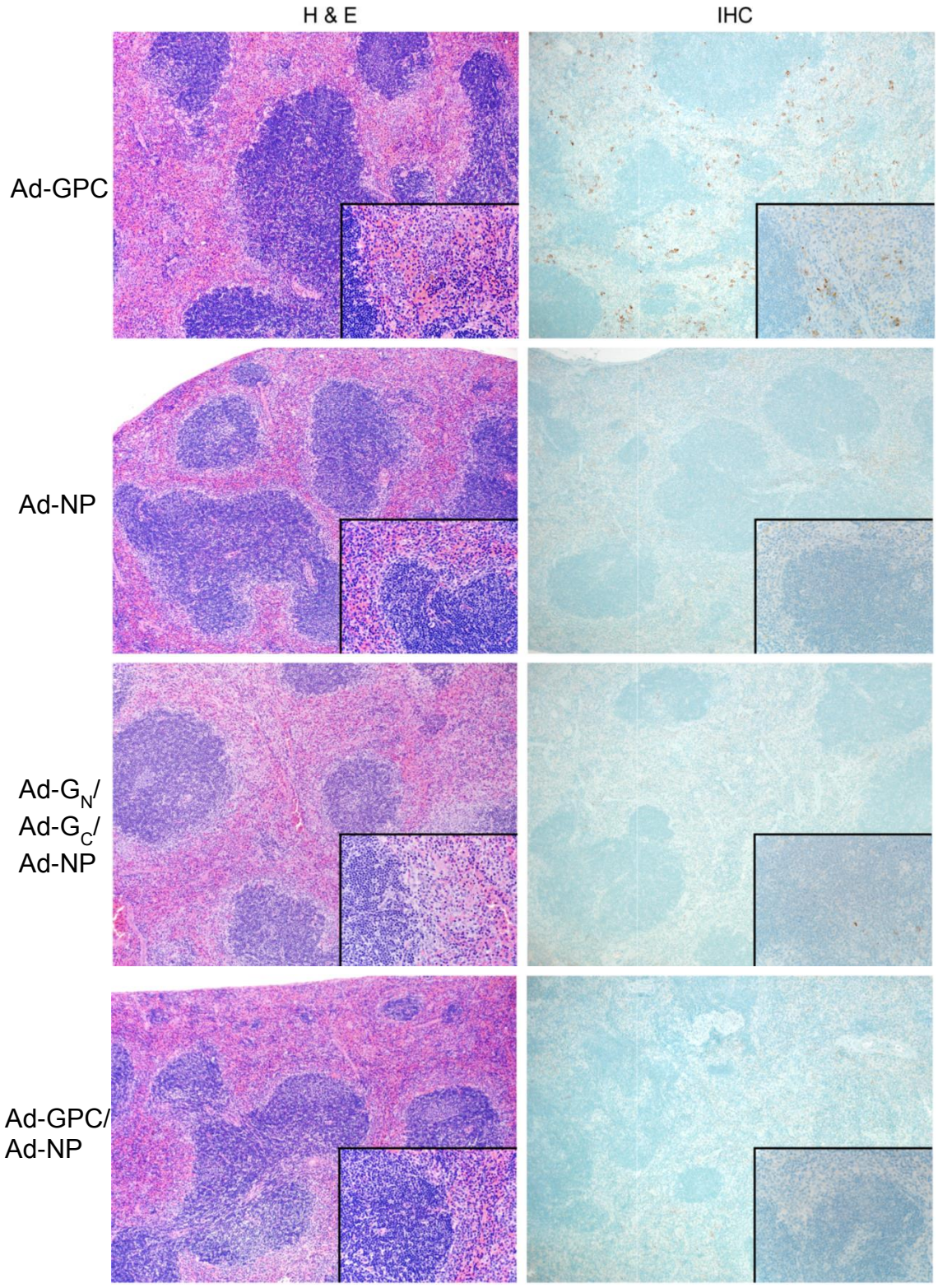
H & E
IHC
Ad-GPC
Ad-NP
Ad-G$_N$/
Ad-G$_C$/
Ad-NP
Ad-GPC/
Ad-NP

Figure 37. Pathologic changes in the spleens of vaccinated IFNAR$^{-/-}$ mice challenged with CCHFV. Groups of 9 IFNAR$^{-/-}$ mice were vaccinated with the indicated Adenovirus (Ad) construct by the intramuscular route and 4 weeks later inoculated with 1000 $LD_{50}$ (50 $TCID_{50}$) by the subcutaneous route and the spleen sampled on day 3 post infection. Spleen slides were stained with hematoxylin and eosin (H&E) or $NP_{1028}$ rabbit polyclonal sera (IHC). Histological changes are apparent on groups vaccinated with Ad (mock vaccinated), Ad-$G_N$, Ad-$G_C$, Ad-$G_N$/Ad-$G_C$ and Ad-GPC. Spleen displayed diffuse lymphocytolysis with loss of lymphocytes from the white pulp and diffuse infiltration of neutrophils. Shown here are representative liver samples from infected IFNAR$^{-/-}$ mice. Images are at a magnification of 10x with 40x for the insets.

### 3.6.2 Prime/boost vaccination regimen can fully protect IFNAR$^{-/-}$ from lethal CCHFV challenge

To assess if a boost will increase efficacy of vaccination groups of 9 IFNAR$^{-/-}$ mice were vaccinated by the i.m. route as previously and boosted 28 days later with the homologous dose of Ad vector by the i.n. route to circumvent preexisting immunity as had been demonstrated by others [108-111]. IFNAR$^{-/-}$ mice were vaccinated with Ad-NP (intermediate efficacy), Ad-GPC (no efficacy) or combination of Ad-NP/Ad-GPC (high efficacy) and challenged with CCHFV as previously described. Following CCHFV infection the same trend was observed between the groups as was observed with the single vaccination regimen. Animals vaccinated with Ad-GPC were not protected and succumbed to disease at the same time as mock vaccinated animals (Figure 38), in contrast Ad-NP and Ad-NP/Ad-GPC animals were protected with 78% and 100% survival, respectively, with a significant delay in onset of terminal disease in Ad-NP vaccinated animals (9 vs 5 days, $p<0.01$) (Figure 38).

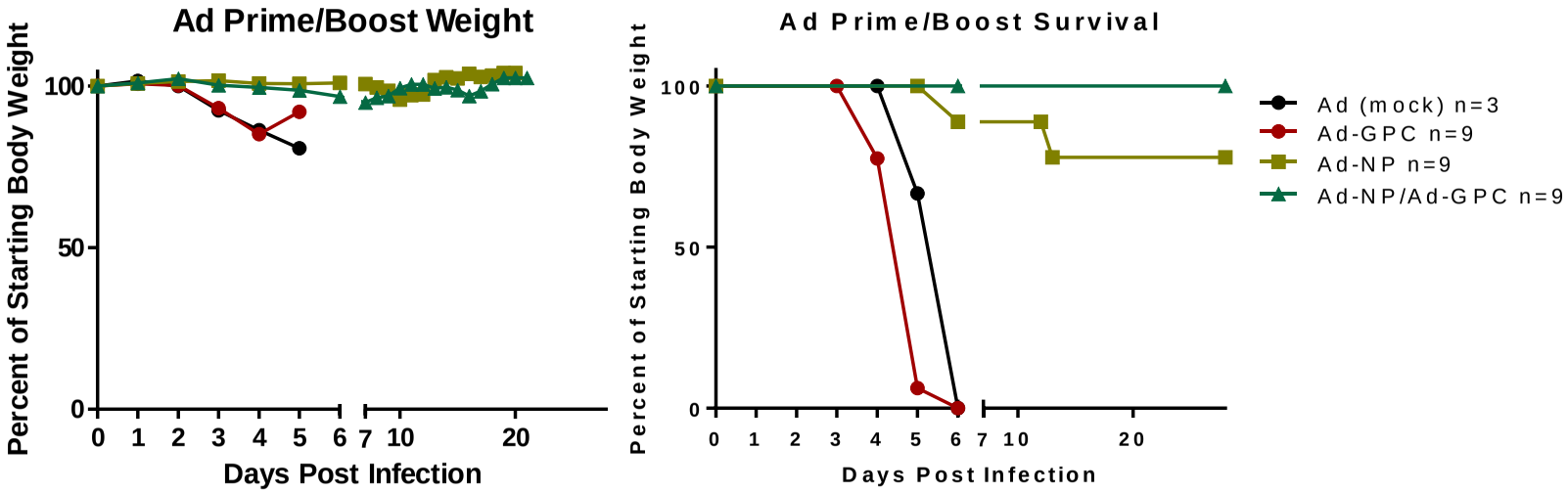


Figure 38. Disease progression following CCHFV challenge of mice primed and boosted with Ad. Groups of 9 IFNAR$^{-/-}$ mice were vaccinated with $10^8$ Adenovirus (Ad) expressing CCHFV glycoprotein precursor (GPC), CCHFV nucleoprotein (NP), or combinations of Ad expressing NP and GPC by the intramuscular route and boosted 28 days later with $10^9$ of the homologous vaccine combination. IFNAR$^{-/-}$ mice were then challenged with 1000 $LD_{50}$ (50 $TCID_{50}$) of CCHFV by the subcutaneous route and observed for disease signs for 28 days post infection. Expression of GPC alone did not protect IFNAR$^{-/-}$ mice from lethal CCHFV disease nor did it extend survival time compared to mock (4.5 days vs 5 days). Expression of NP alone protected 78% of the animals from lethal CCHFV challenge ($p<0.001$) compared to mock vaccinated animals with a mean survival time of 9 days vs 5 days compared to unprotected groups ($p<0.01$). Expression of NP and GPC concurrently provides the greatest protection with 100% of the infected animals surviving challenge ($p<0.001$).

To assess CCHFV organ distribution at a later time point a subset of mice were sampled on days 3 and 7 p.i.. As was the case with the single vaccination IFNAR$^{-/-}$ mice receiving Ad-GPC displayed high viremia at 3 day p.i., by both qRT-PCR and virus titration, and succumbed to infection prior to 7 days p.i.; while IFNAR$^{-/-}$ mice in the Ad-NP group had undetectable viremia by qRT-PCR and virus titration on day 3 and 7 p.i. with a single animal demonstrating high grade viremia on day 7 p.i.; Ad-NP/Ad-GPC vaccinated IFNAR$^{-/-}$ mice did not develop detectable viremia on day 3 p.i., by either qRT-PCR or virus titration, and had very low viremia at day 7 p.i. as detected by qRT-PCR but infectious virus was not detected (Figure 39).

Unlike the single vaccination experiments following prime/boost vaccination CCHFV organ viral loads were significantly reduced in the Ad-NP and Ad-NP/Ad-GPC vaccinated groups (Figure 39). The same mouse, which developed significant viremia in the Ad-NP group, developed significant organ viral titers and this animal was likely going to succumb to infection within 2 days following the sampling point, which is in line with efficiency of protection following Ad-NP vaccination (~80% protection with an average survival time of 9 days).

At 3 days p.i. following prime and boost vaccination, IFNAR$^{-/-}$ mice vaccinated with Ad-GPC and develop pathological changes in the spleen and liver identical to Ad vaccinated animals (Figures 40 and 41 H&E panels). IFNAR$^{-/-}$ mice vaccinated and boosted with Ad-NP developed minor hepatic pathological changes at 3 days p.i., similar to the single Ad-NP vaccinated animals, and progressed to slightly more severe hepatic pathology accompanied by acute necrotizing splenitis on day 7 p.i. (Figures 40 and 41 H&E panels). A single IFNAR$^{-/-}$ mouse in the Ad-NP vaccinated and boosted group, which displayed high viral loads, developed severe hepatic and splenic lesion at day 7 p.i. (data not shown). Similarly to the Ad-NP vaccinated IFNAR$^{-/-}$ mice,

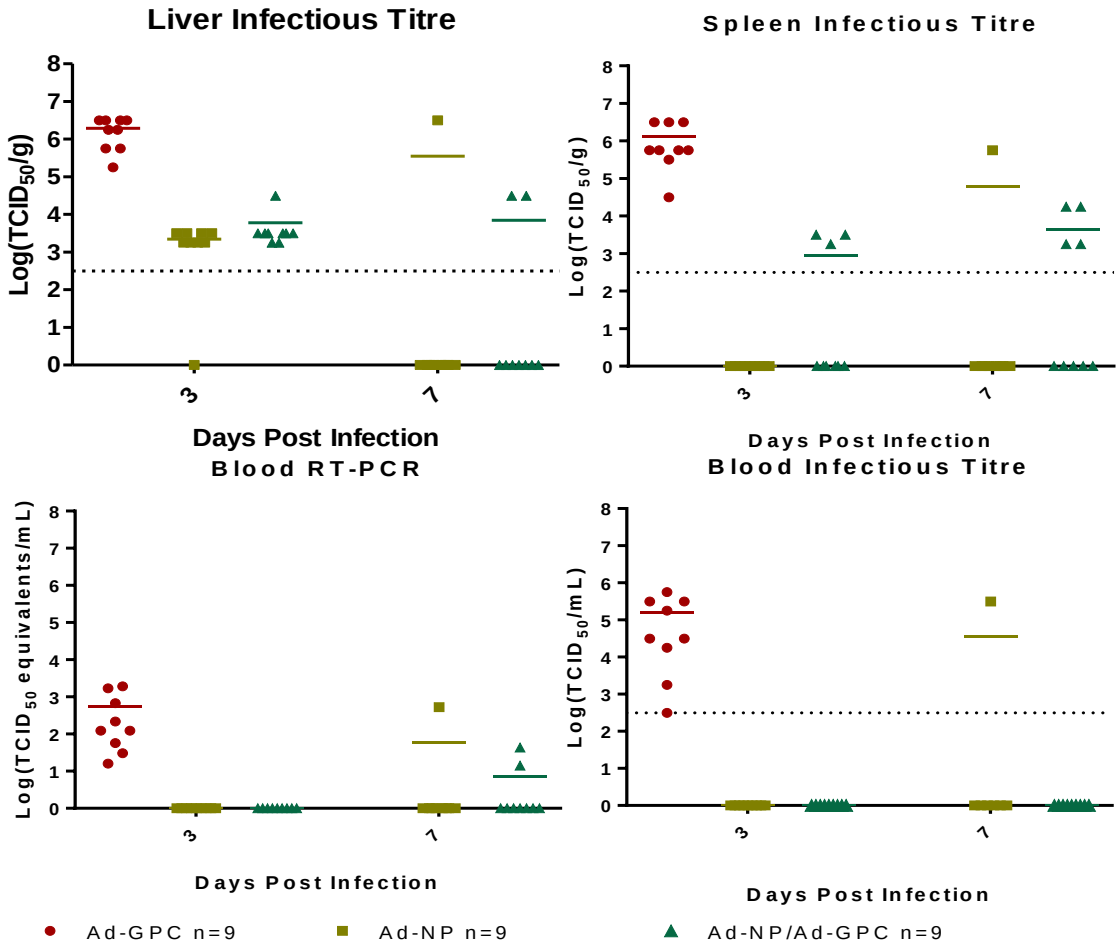


Figure 39. CCHFV organ load and viremia following challenge of primed and boosted IFNAR$^{-/-}$ mice. Groups of 9 IFNAR$^{-/-}$ mice were vaccinated with $10^8$ Adenovirus (Ad) expressing CCHFV glycoprotein precursor (GPC), CCHFV nucleoprotein (NP), or combinations of Ad expressing NP and GPC by the intramuscular route and boosted 28 days later homologous vaccine combination. IFNAR$^{-/-}$ mice were then challenged with 1000 $LD_{50}$ of CCHFV by and blood, liver and spleen sampled on days 3 and 7 post infection. Expression of GPC alone did not reduce the CCHFV viral loads in any tissue on day 3 post infection and IFNAR$^{-/-}$ mice nor did the mice survive until the day 7 post infection time point. Expression of NP alone reduced the level of CCHFV organ viral loads and prevented viremia on day 3 post infection. With the exception of the lone IFNAR$^{-/-}$ mouse, no CCHFV was detected in any tissues in Ad-vaccinated animals on day 7. Expression of NP and GPC concurrently provides a significant reduction of CCHFV organ viral titers and viremia on both days 3 and 7 post infection. Low level of infectious CCHFV is detected in organs at both time points demonstrating that Ad vaccination does not confer sterile immunity to IFNAR$^{-/-}$ mice. Dashed lines on the represent the limit of detection of the $TCID_{50}$ assay.

Ad-NP/Ad-GPC vaccinated and boosted IFNAR$^{-/-}$ mice developed minor hepatic pathological changes at 3 days p.i., which progressed to slightly more severe hepatic pathology without developing pathologic changes in the spleen (Figure 40 and 41 H&E panels).

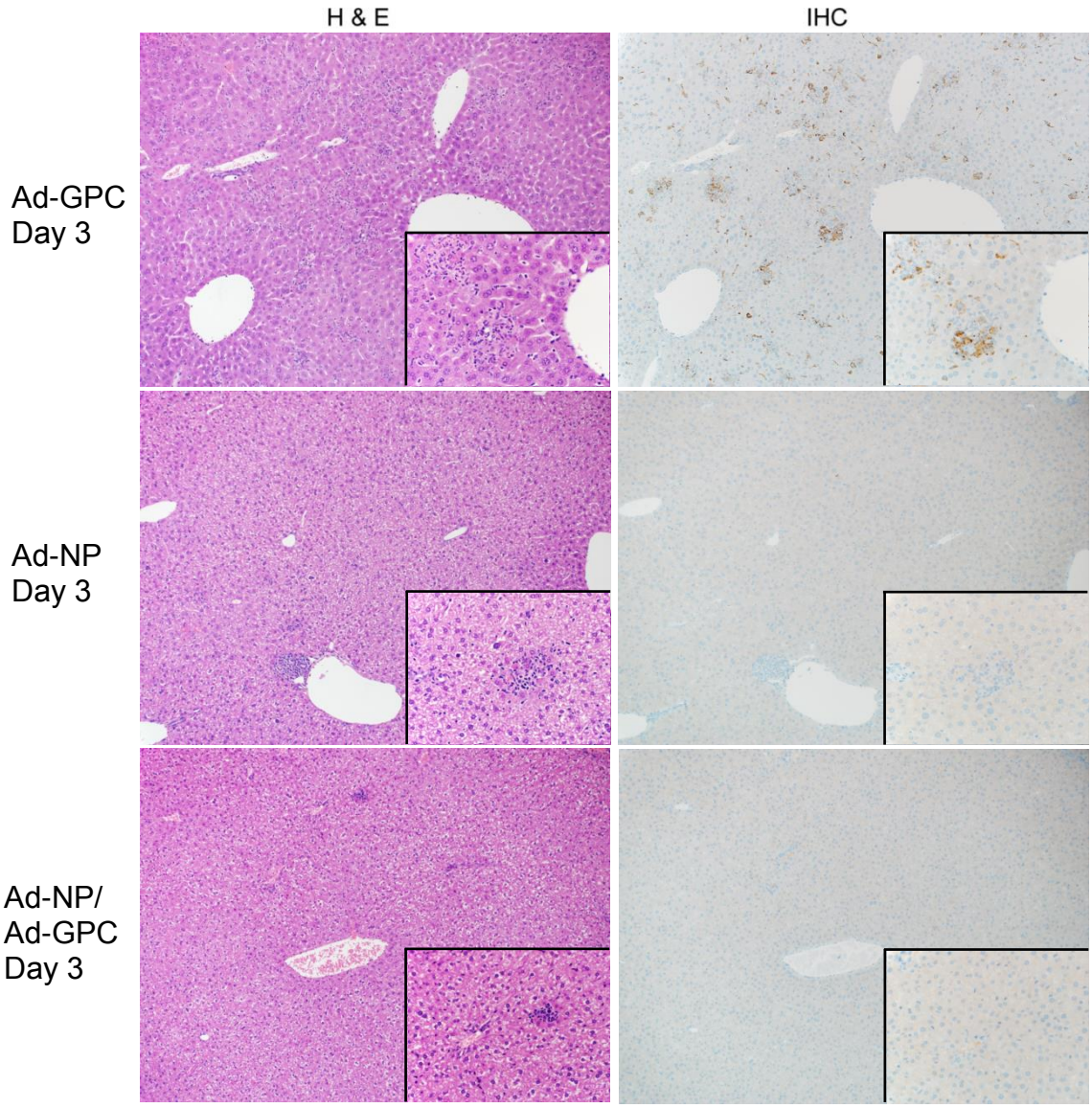

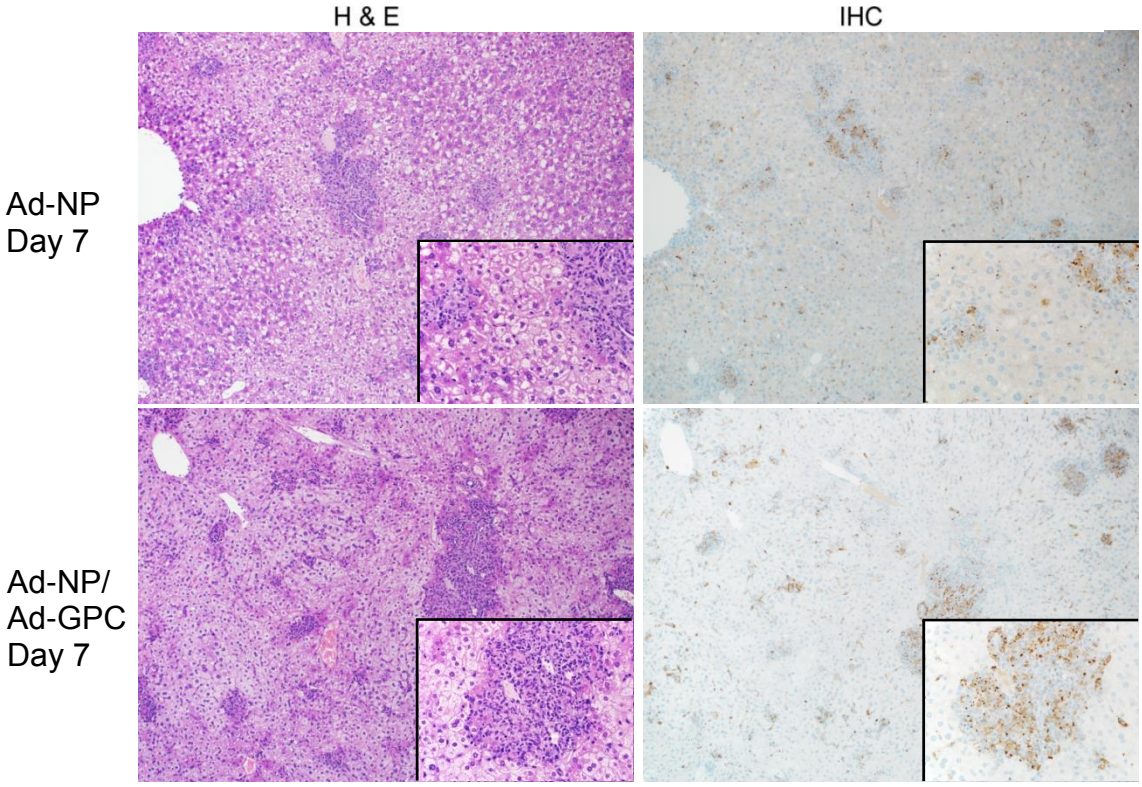


Figure 40. Pathologic changes in the livers of Ad primed and boosted IFNAR$^{-/-}$ mice challenged with CCHFV. Groups of 9 IFNAR$^{-/-}$ mice were vaccinated with the indicated Ad construct, boosted with the homologous constructs four weeks later and challenged with 1000 $LD_{50}$ (50 $TCID_{50}$) of CCHFV. The liver was sampled on day 3 and 7 post infection. Liver slides were stained with hematoxylin and eosin (H&E) or $NP_{1028}$ rabbit polyclonal sera (IHC). Histological changes are apparent in Ad-GPC vaccinated animals on day 3 and on Ad-NP and Ad-NP/Ad-GPC vaccinated animals on day 7. Antigen staining is apparent and is distributed with hepatic lesions. Shown here are representative liver samples from infected IFNAR$^{-/-}$ mice. Images are at a magnification of 10x with 40x insets.

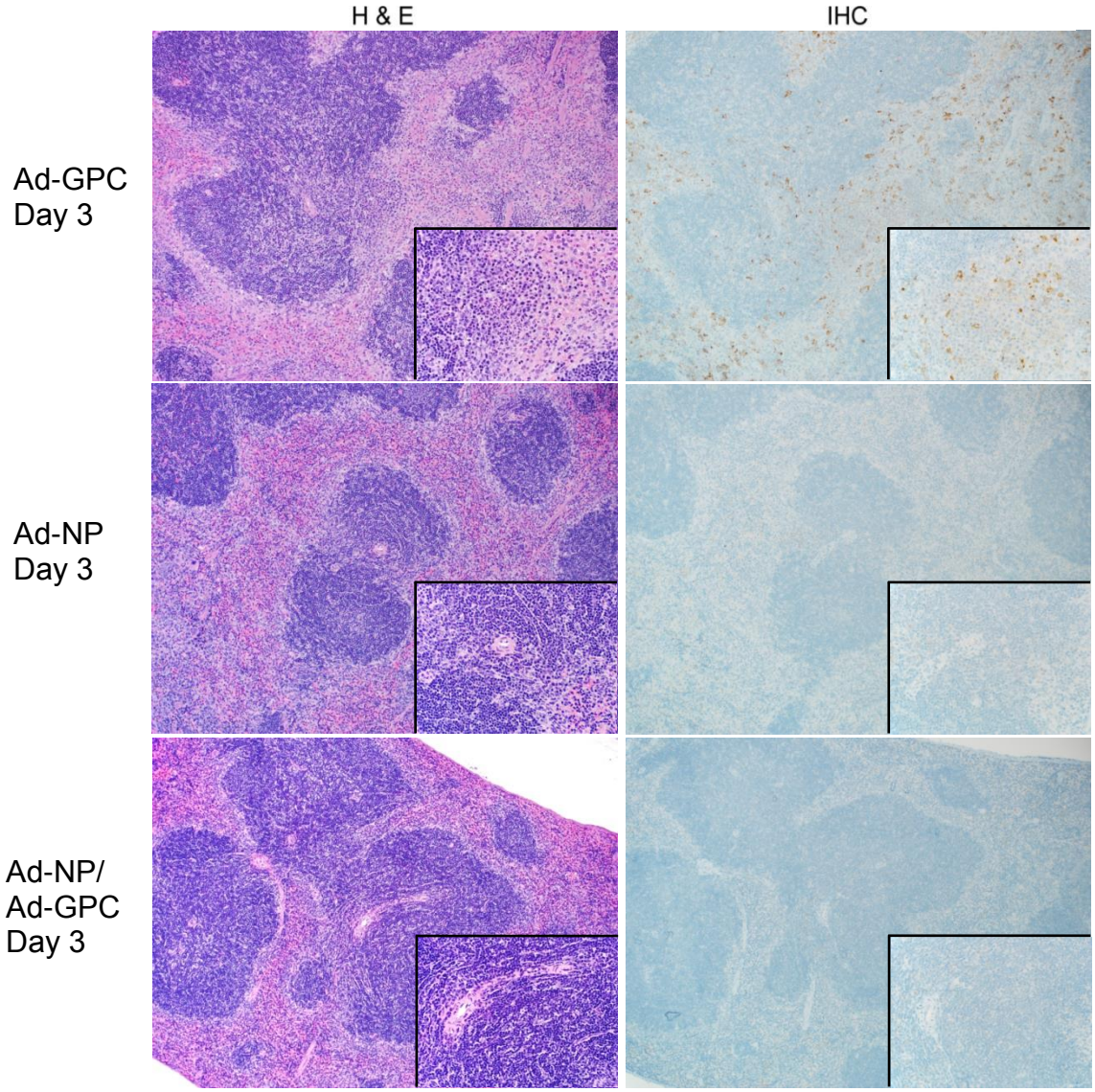
H & E
IHC
Ad-GPC
Day 3
Ad-NP
Day 3
Ad-NP/
Ad-GPC
Day 3

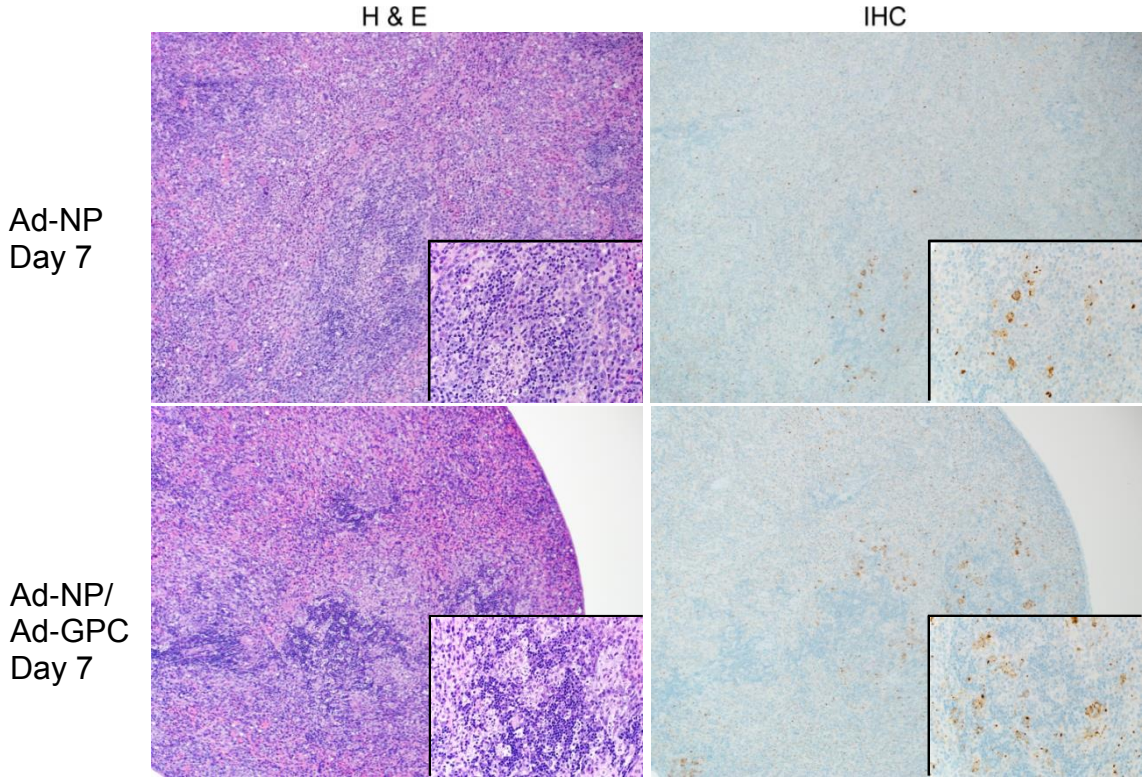


Figure 41. Pathologic changes in the spleens of Ad primed and boosted IFNAR$^{-/-}$ mice challenged with CCHFV. Groups of 9 IFNAR$^{-/-}$ mice were vaccinated with the indicated Ad construct, boosted with the homologous constructs four weeks later and challenged with 1000 $LD_{50}$ (50 $TCID_{50}$) of CCHFV. Spleen was sampled on day 3 and 7 post infection. Spleen slides were stained with hematoxylin and eosin (H&E) or $NP_{1028}$ rabbit polyclonal sera (IHC). Histological changes were prominent in Ad-GPC vaccinated animals on day 3 and were less prominent or absent in Ad-NP and Ad-NP/Ad-GPC vaccinated animals on day 7. Antigen staining is apparent, however is significantly less in all Ad-NP and Ad-NP/Ad-GPC vaccinated animals. Shown here are representative liver samples from infected IFNAR$^{-/-}$ mice. Images are at a magnification of 10x with 40x insets.

IHC revealed significant CCHFV antigen staining in the liver and spleen of Ad-GPC vaccinated and boosted IFNAR$^{-/-}$ mice reminiscent of the singly vaccinated groups at 3 days p.i.; while both Ad-NP, with the exception of the lone mouse, and Ad-NP/Ad-GPC vaccinated and boosted IFNAR$^{-/-}$ mouse groups displayed a low level of CCHFV antigen scatted throughout the liver and spleen on both days 3 and 7 p.i. (Figure 40 and 41 IHC panels). Taken together the IHC analysis demonstrates that unlike the single vaccination approach the prime/boost approach significantly minimizes viral replication and corroborates the virus isolation data (Figure 39).

In addition to pathological and virological parameters, hematological parameters were observed in order to evaluate whether platelet destruction is reduced following protective vaccination. Following Ad-NP vaccination a transient reduction in platelets is observed at 3 days p.i., which appears restored by day 7 p.i.; vaccination with Ad-GPC also results in reduced circulating platelet numbers presumably until terminal stage of disease, which was at day 5 p.i., and vaccination with a combination of Ad-NP/Ad-GPC does not result in a decrease in circulating platelets (Figure 42). Lymphocyte populations were not significantly altered between the protected groups (i.e. Ad-NP and Ad-NP/Ad-GPC) and the non-protected group (i.e. Ad-GPC) (Figure 43). As with previous results, red blood cell parameters do not change following CCHFV infection at the sampled time points (Figure 44).

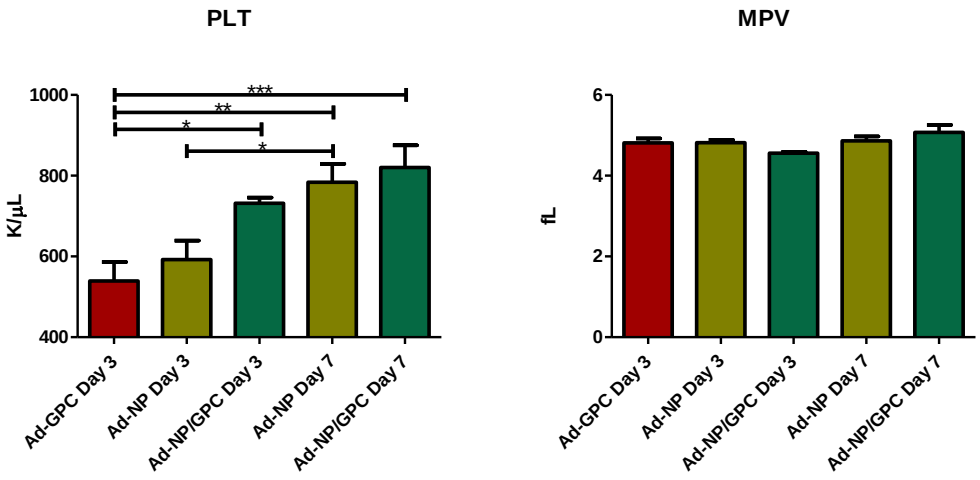


Figure 42. Platelet parameters of primed and boosted Ad vaccinated IFNAR$^{-/-}$ mice following CCHFV challenge. Groups of 9 IFNAR$^{-/-}$ mice were vaccinated with $10^8$ Adenovirus (Ad) expressing CCHFV glycoprotein precursor (GPC), CCHFV nucleoprotein (NP), or combinations of Ad expressing NP and GPC by the intramuscular route and boosted 28 days later with $10^9$ of the homologous vaccine combination. IFNAR$^{-/-}$ mice were then challenged with 1000 $LD_{50}$ (50 $TCID_{50}$) of CCHFV by the subcutaneous route and exsanguinated on days 3 and 7 post infection. IFNAR$^{-/-}$ mice of the Ad-GPC group demonstrated lower circulating platelet (PLT) numbers on day 3 post infection than those vaccinated with Ad-NP/Ad-GPC ($p<0.05$) or either the Ad-NP or the Ad-NP/Ad-GPC vaccinated group at day 7 post infection ($p<0.01$ and $p<0.001$, respectively). Ad-NP vaccinated mice displayed a transient significant decrease in PLT numbers, which increased by day 7 post infection ($p<0.05$). Ad-NP/Ad-GPC vaccinated mice displayed the highest levels of PLT numbers, which did not significantly differ in the two time points sampled. The mean platelet volume (MPV) remained unchanged in all sampled mice demonstrating that no major shift in PLT maturity occurred between the groups. All data was analyzed by one-way ANOVA with Tukey's Post Test and is presented as standard error about the mean with *** representing $p<0.001$, ** representing $p<0.01$ and * representing $p<0.05$ compared to the indicated.

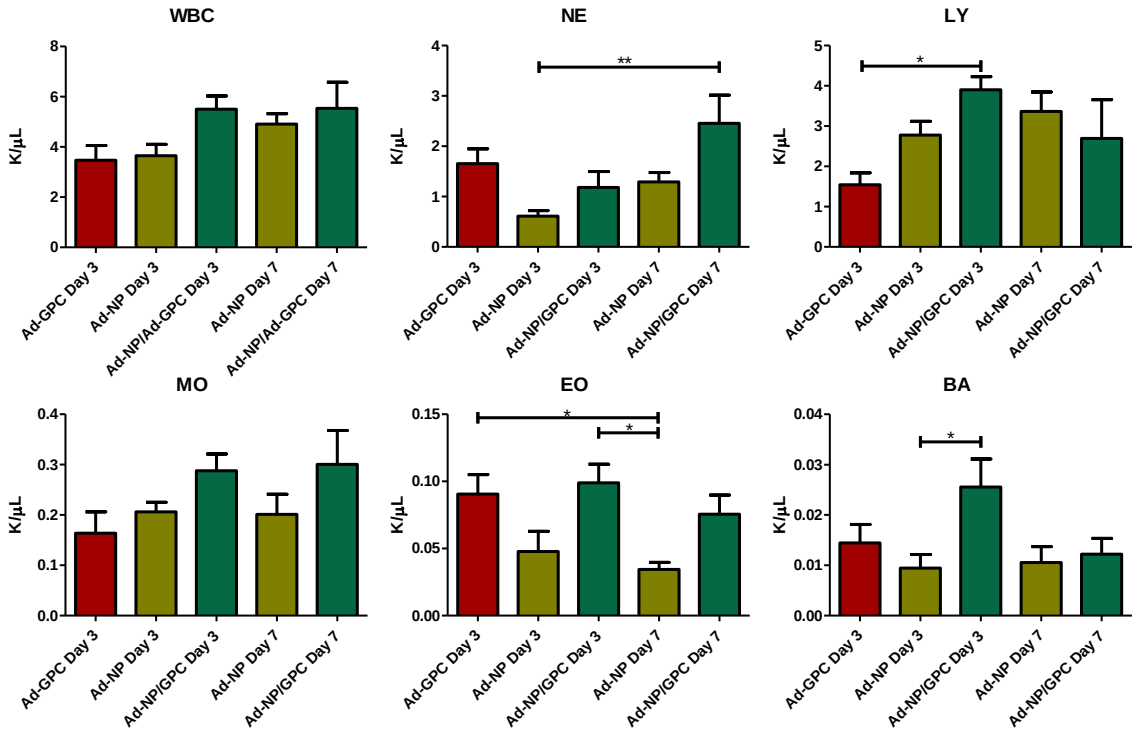


Figure 43. White blood cell parameters of primed and boosted Ad vaccinated IFNAR$^{-/-}$ mice following CCHFV challenge. Groups of 9 IFNAR$^{-/-}$ mice were vaccinated with Adenovirus (Ad) expressing CCHFV glycoprotein precursor (GPC), CCHFV nucleoprotein (NP), or combinations of Ad expressing NP and GPC and then challenged with 1000 $LD_{50}$ of CCHFV and exsanguinated on days 3 and 7 post infection. White blood cell (WBC) and monocyte (MO) populations were not significantly altered between groups on days 3 and 7 post infection. Neutrophil (NE) populations differed between Ad-NP at day 3 and Ad-NP/Ad-GPC group on day 7 post infection ($p<0.01$), but not between any other group. Eosinophil (EO) populations of the Ad-NP group on day 7 post infection were significantly decreased ($p<0.05$), but otherwise remained unaltered. Basophil (BA) populations of Ad-NP/Ad-GPC were significantly increased compared to Ad-NP vaccinated animals on day 3 post infection ($p<0.05$). No other significant differences were detected suggesting lymphocyte populations remain relatively stable on the time points tested as was seen in previous studies. All data was analyzed by one-way ANOVA with Tukey's Post Test and is presented as standard error about the mean with ** representing $p<0.01$ and * representing $p<0.05$ compared to the indicated groups.

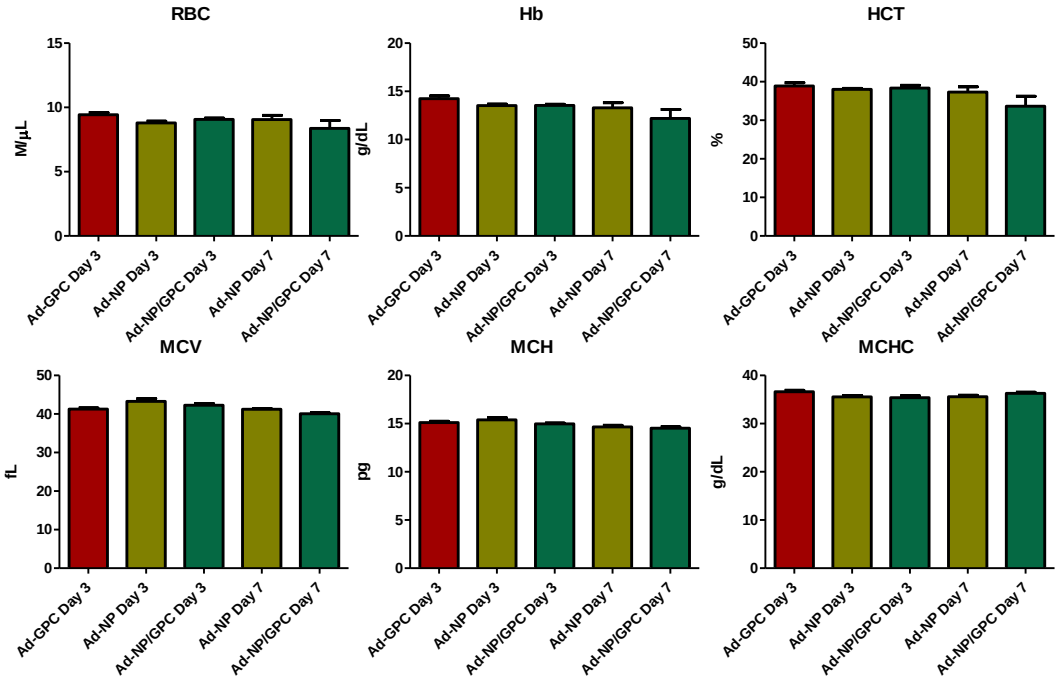


Figure 44. Red blood cell parameters of primed and boosted Ad vaccinated IFNAR$^{-/-}$ mice following CCHFV challenge. Groups of 9 IFNAR$^{-/-}$ mice were vaccinated with $10^8$ Adenovirus (Ad) expressing CCHFV glycoprotein precursor (GPC), CCHFV nucleoprotein (NP), or combinations of Ad expressing NP and GPC and then challenged with 1000 $LD_{50}$ of CCHFV and exsanguinated on days 3 and 7 post infection and red blood cell parameters observed. Red blood cell parameters did not change during sampled time points. Red blood cell counts = RBC, hemoglobin concentration = Hb, hematocrit = HCT, mean corpuscular volume = MCV, mean corpuscular hemoglobin = MCH, and mean corpuscular hemoglobin concentration = MCHC. All data was analyzed by one-way ANOVA with Tukey's Post Test and is presented as standard error about the mean.

Together this data demonstrates that prime/boost vaccination with Ad based vaccines enhances protective efficacy. Furthermore, it shows that unlike following single vaccination this strategy induces a significantly stronger immune response, which is more capable of controlling CCHFV replication. The reduction in CCHFV replication reflects both in pathological changes and hematological parameters. The data also demonstrates the importance of NP and GPC as immunogens, which can be utilized for eliciting protective immune responses against CCHFV infection. To elucidate the mechanisms of protection, additional experiments were undertaken

to observe how the immune response matures in IFNAR$^{-/-}$ mice following Ad vaccination and what arm of the immune system is required for protection from lethal CCHFV infection.

### 3.6.3 IFNAR$^{-/-}$ immune responses to Ad vaccination

To assess immunological parameters following vaccination sequential blood draws were taken from IFNAR$^{-/-}$ mice during the immunization with Ad-NP/Ad-GPC with cells and sera separated for analysis of humoral and cellular immune responses, as described in section. Neutralization ability of the isolated antibodies was assessed by the ability of the serum to neutralize VSV-GPC *in vitro*. Following primary vaccination with Ad-NP/Ad-GPC IFNAR$^{-/-}$ mice do not develop any ability to neutralize VSV-GPC entry. Following prime/boost Ad-NP/Ad-GPC vaccination and prime/boost and CCHFV challenge IFNAR$^{-/-}$ mice develop a weak (1:20 dilution >50% reduction in plaques for both vaccinated and vaccinated and challenged mice) neutralizing response against VSV-GPC. No other vaccination schedules resulted in any neutralization of VSV-GPC. Neutralization of VSV-GPC however may not be whole story as VSV-GPC may have cryptic entry mechanisms other than using CCHFV glycoproteins in the same method as CCHFV. Due to technical issues, neutralization assays with CCHFV were not reported and the correlation between the VSV-GPC neutralization and CCHFV neutralization assays are unknown.

Following Ad vaccination T-cell responses were monitored for cytokine production following stimulation and changes in circulating T-cell populations. To assess the quality of effector cell populations, activated (defined as expressing the surface molecule CD44 or CD44+) and total cytotoxic T-cells (defined as T-cells expressing the surface markers CD8 or CD8+) were monitored for their ability to produce the cytokines IFNγ, TNFα and IL2 (or IFNγ+, TNFα+, IL2+ cells). Those cytotoxic T-cells producing at least one cytokine in response to stimulation were considered to be the effector T-cell phenotype. Following PMA/ionomycin stimulation, T-cell

populations of Ad vaccinated compared to mock vaccinated animals had a decreased percentage of activated cytotoxic T-cells (CD8+CD44+ cells), however, had a greater proportion of activated effector cytotoxic T-cells (CD8+CD44+IL2+, CD8+CD44+TNFα+, CD8+CD44+IFNγ+, CD8+CD44+IFNγ+TNFα+ CD8+CD44+IFNγ+ IL2+ and CD8+CD44+IFNγ+TNFα+IL2+, $p<0.01$ comparing Ad vs mock and $p<0.05$ Ad-NP/Ad-GPC vs mock) demonstrating a higher level of memory cells being activated to act by the chemical antigen following (Figure 45). As expected, there were no differences in activation pattern of T-cells between Ad vaccinated and Ad-NP/Ad-GPC vaccinated groups following PMA/ionomycin stimulation ($p>0.05$).

Following CCHFV stimulation no difference was observed between Ad vaccinated and Ad-NP/Ad-GPC vaccinated IFNAR$^{-/-}$ mice (Figure 46). This suggests that either the CCHFV stimulation failed or that vaccination does not induce T-cell memory, which expands to activated effector T-cells following CCHFV stimulation.

### 3.7 Transfer of immune cells and antibodies can partially protect naïve IFNAR$^{-/-}$ mice from lethal CCHFV challenge

To demonstrate the protective potential of each arm of the immune system, B-cells, T-cells, total splenocytes and total antibodies were isolated and pooled from the spleens (B-, T-cells and splenocytes) and sera (antibodies) of IFNAR$^{-/-}$ mice, which had been given a protective prime/boost vaccination with Ad-NP/Ad-GPC. Naïve IFNAR$^{-/-}$ mice were transferred total splenocytes with total antibodies; purified B-cells with total antibody; purified T-cells with total antibody; purified T-cells or total antibodies.

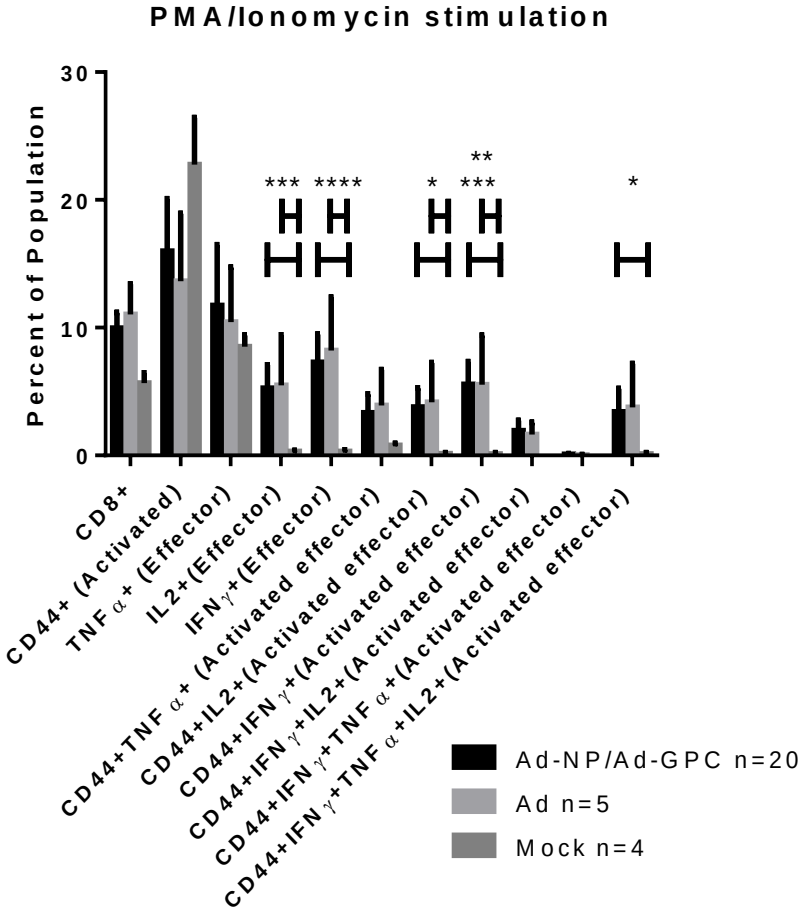


Figure 45. Chemical stimulation of T cells following vaccination. A group of 19 mice was vaccinated with Ad-NP/Ad-GPC. 56 days later the lymphocytes were isolated and stimulated with PMA/ionomycin for 6 hours. Cells were stained for surface markers for cytotoxic T-cells (CD8) and cell activation (CD44), and for effector function as measured by production of cytokines (tumor necrosis alpha [TNFα], interleukin-2 [IL2] and interferon gamma [IFNγ]). Ad and Ad-NP/Ad-GPC vaccinated groups had significantly higher percentage of effector T cells secreting IL2 ($p<0.001$ for both groups) or IFNγ ($p<0.0001$ for both groups); and activated effector T cells secreting IL2 ($p< 0.05$ for both groups), IFNγ ($p<0.01$ and $p<0.001$, respectively) or IL2, IFNγ and TNFα ($p<0.05$ for Ad-NP/Ad-GPC group only) compared to the mock vaccinated groups. No difference was detected between Ad and Ad-NP/Ad-GPC vaccinated groups.

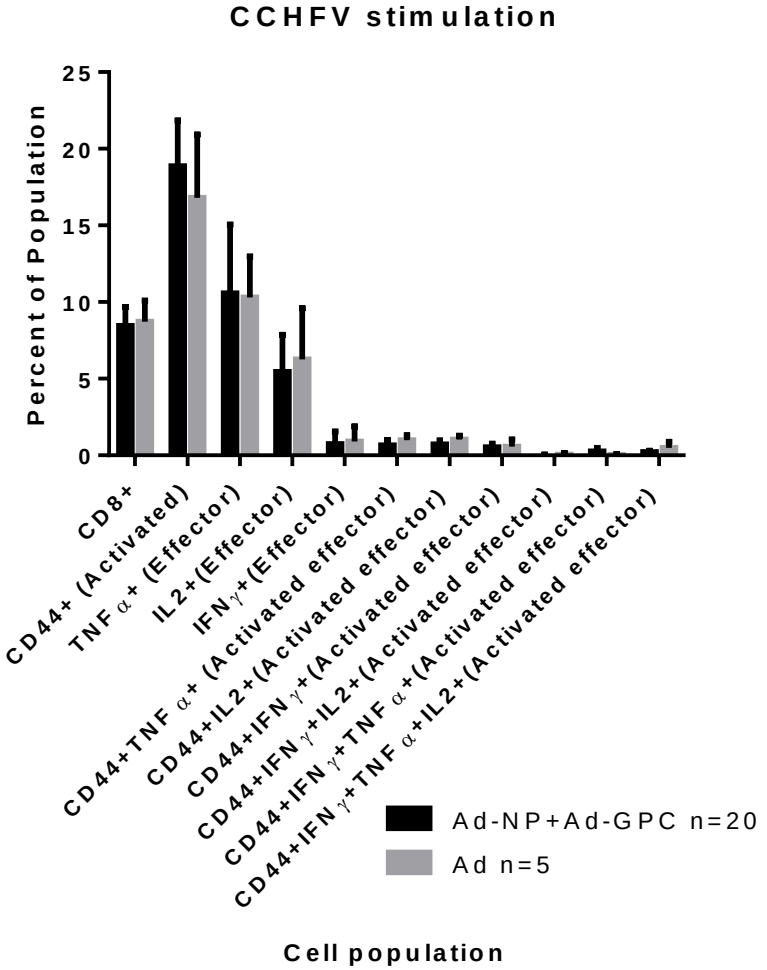


Figure 46. CCHFV antigen stimulation of T cells. A group of 20 IFNAR$^{-/-}$ mice was vaccinated with Ad-NP/Ad-GPC. 56 days later the lymphocytes were isolated and stimulated with PMA/ionomycin for 6 hours. Cells were stained for surface markers for cytotoxic T-cells (CD8) and cell activation (CD44), and for effector function as measured by production of cytokines (tumor necrosis alpha [TNFα], interleukin-2 [IL2] and interferon gamma [IFNγ]). Ad and Ad-NP/Ad-GPC vaccinated groups were not significantly different from each other ($p>0.05$).

Purity and viability of B-, T-cells and splenocytes were determined by flow analysis and live dead-staining. B-cell purity and viability were 97% and 90%, respectively; T-cell purity was 90% with a viability of 95%; total splenocytes consisted of 50% B-cells, 35% T-cells and 15% of other cell types. Following isolation and determination of purity, cells and/or total purified antibodies were transferred into naïve IFNAR$^{-/-}$ mice. The mice were mandibularly bled a day following transfer and the sera were analyzed by ELISA to confirm seroconversion of the naïve IFNAR$^{-/-}$

mice. Due to an inability to confirm the identity of T-cell populations in recipient mice no other assays were undertaken.

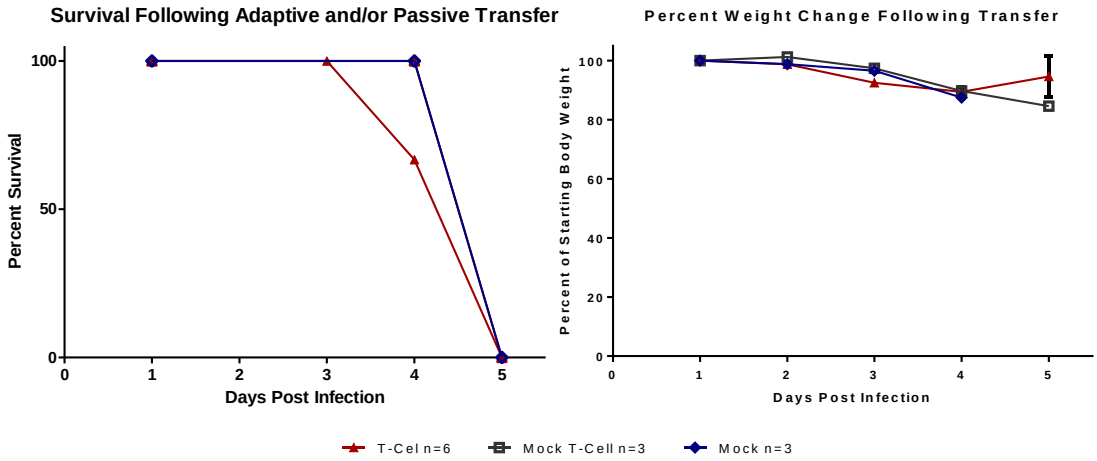


Figure 47. IFNAR$^{-/-}$ mouse survival following adoptive transfer and CCHFV challenge. A group of 6 naive IFNAR$^{-/-}$ mice received 3x10$^{7}$ total T-cells from mice vaccinated with Ad-NP/Ad-GPC; a group of 3 IFNAR$^{-/-}$ mice received 3x10$^{7}$ total T-cells from Ad-empty (mock) vaccinated IFNAR$^{-/-}$ mice. All cell suspensions were diluted in PBS-0.5% BSA and the transfers were delivered in a 200µL volume by the intraperitoneal route. IFNAR$^{-/-}$ mice were rested for 2 days following transfer and challenged with 1000LD$_{50}$ of CCHFV by the subcutaneous route. IFNAR$^{-/-}$ mice receiving the CCHFV vaccinated T-cells did not have any protective effect compared to IFNAR$^{-/-}$ mice receiving mock vaccinated T-cells or naive IFNAR$^{-/-}$ mice (p=0.8425).

Following confirmation of transfer, IFNAR$^{-/-}$ mice were challenge with 1000 MLD$_{50}$ (50TCID$_{50}$) of CCHFV and monitored for disease signs. Animals receiving only T-cells were not protected from lethal CCHFV infection, nor were the disease kinetics different between this group and mice, which received mock vaccinated T-cells (average survival time 5 days following transfer versus 5 days following transfer of mock vaccinated T-cells p=0.8425) (Figure 47). Transfer of antibodies alone did not protect naïve IFNAR$^{-/-}$ mice from lethal CCHFV challenge, however, there was a statistically significant increase in survival time (8 days versus 5 days for transfer of mock vaccinated antibodies, p<0.01) (Figure 48). Addition of T- or B-cells alone did not enhance the

protective efficacy nor did it extend the survival time beyond the effects seen with a transfer of only antibodies (average survival time of 8.5 days or 7 days, respectively compared to 8 days of the antibody transfer, p=0.4936) (Figure 48). Naïve IFNAR$^{-/-}$ mice, which received a transfer of both splenocytes and antibodies had almost identical infection kinetics as those receiving only antibodies (9.5 days vs 8 days, p=0.2718), but were partially protected (20%) from lethal CCHFV challenge; however, this result is not statistically significant (p=0.0759) (Figure 48).

### 3.8 Antibody responses are essential for protection from lethal CCHFV challenge following protective Ad vaccination

#### 3.8.1 Depletion removes circulating B-cells and/or T-cells and prevents seroconversion following vaccination

To assess which arm of the immune system is responsible for protection, IFNAR$^{-/-}$ mice were depleted of circulating B-cells with a depleting anti-CD20 monoclonal antibody. Following antibody treatment splenic and circulating B-cells were reduced by >98% compared to untreated and mock treated controls and IFNAR$^{-/-}$ mice depleted of B-cells did not seroconvert following Ad-NP/Ad-GPC vaccination (Figures 49 and 50). T-cell numbers were unaffected in IFNAR$^{-/-}$ mice following B-cell depletion. IFNAR$^{-/-}$ mice depleted of both B- and T-cells, had the same level of depletion of B-cells as the single treatment group and did not seroconvert following vaccination (Figure 49 and 50).

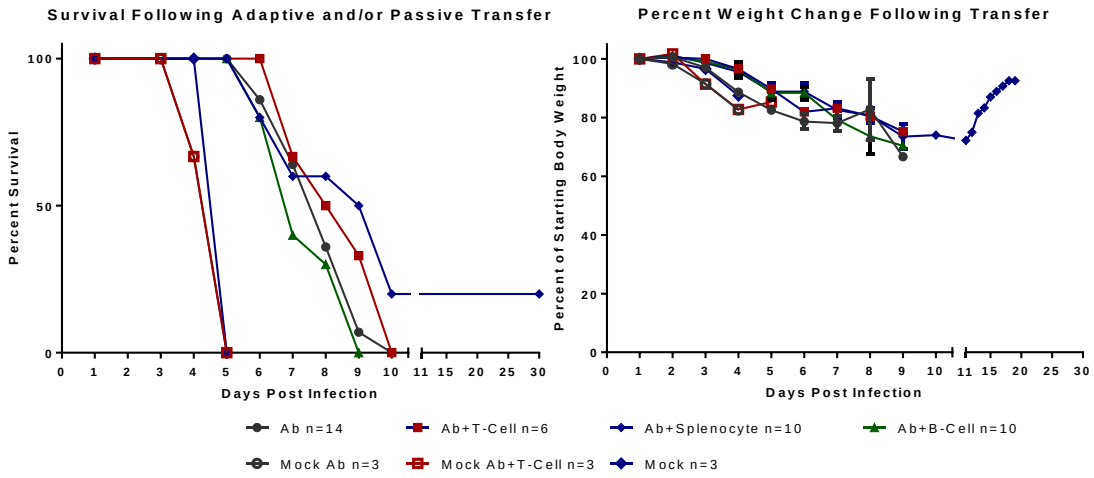


Figure 48. IFNAR$^{-/-}$ mouse survival following adoptive and/or passive transfer and CCHFV challenge. A group of 6 naive IFNAR$^{-/-}$ mice received 3x10$^{7}$ total T-cells and 1.2mg of total antibodies (Ab) from IFNAR$^{-/-}$ mice vaccinated with Ad-NP/Ad-GPC; a group of 14 naive IFNAR$^{-/-}$ mice received 1.2mg of total Ab from IFNAR$^{-/-}$ mice vaccinated with Ad-NP/Ad-GPC; a group of 10 naive IFNAR$^{-/-}$ mice received 4x10$^{7}$ total B-cells and 0.5mg total Ab from IFNAR$^{-/-}$ mice vaccinated with Ad-NP/Ad-GPC; a group of 10 naive IFNAR$^{-/-}$ mice received 1x10$^{8}$ total splenocytes and 0.5mg of total antibodies (Ab) from IFNAR$^{-/-}$ mice vaccinated with Ad-NP/Ad-GPC; a group of 3 IFNAR$^{-/-}$ mice received 3x10$^{7}$ total T-cells and 0.5mg of total Ab from Ad-empty (mock) vaccinated IFNAR$^{-/-}$ mice; and a group of 3 IFNAR$^{-/-}$ mice received 0.5mg of total Ab from mock vaccinated IFNAR$^{-/-}$ mice. All antibody and cell suspensions were diluted in PBS-0.5% BSA and the transfers were delivered in a 200µL volume by the intraperitoneal route. IFNAR$^{-/-}$ mice were rested for 2 days following transfer and challenged with 1000LD$_{50}$ of CCHFV by the subcutaneous route. IFNAR$^{-/-}$ mice receiving the CCHFV vaccinated antibodies were not protected compared to IFNAR$^{-/-}$ mice receiving mock antibodies or naive IFNAR$^{-/-}$ mice, however significant increases in survival times were seen in animals receiving antibodies ($p<0.01$). IFNAR$^{-/-}$ mice receiving the CCHFV vaccinated Ab and splenocytes were partially protected compared to naive IFNAR$^{-/-}$ mice (20% survival), however this result was not statistically significant ($p=0.0759$). IFNAR$^{-/-}$ mice receiving T-cell or B-cell in addition to total Ab were not protected from lethal disease and did not have a significantly changed disease course compared to mice receiving only Ab ($p=0.4936$).

Following antibody treatment, splenic and circulating T-cells were reduced by 94% compared to untreated and mock treated controls and IFNAR$^{-/-}$ mice depleted of T-cells seroconverted against CCHFV following Ad-NP/Ad-GPC vaccination (Figure 49). Circulating and splenic B-cell counts

increased by approximately 40% compared to untreated and mock treated IFNAR$^{-/-}$ mice following depletion suggesting some compensation by the immune system. Animals depleted of T-cells, but not B- cells, seroconverted similar to mock depleted and untreated vaccinated IFNAR$^{-/-}$ mice (Figure 50).

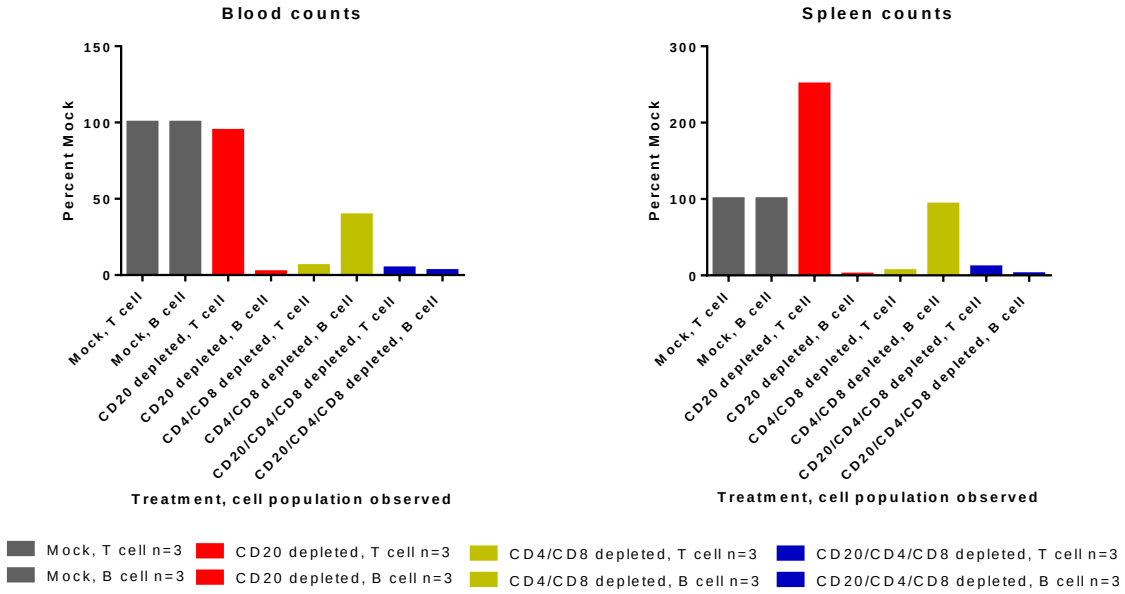


Figure 49. Levels of splenic and circulating lymphocytes following depletion. Groups of 18 IFNAR$^{-/-}$ mice were depleted of B-cells (CD20 depletion) prior to and/or depleted of T-cells (CD4/CD8 depletion) post vaccination with Ad-NP/Ad-GPC. 4 weeks post boost, the circulating blood lymphocytes and splenocytes of the vaccinated and depleted mice were analyzed for depletion efficacy. Mice that were depleted of B-cells prior to vaccination were depleted by 98-99% in both blood and spleen. Mice depleted of T-cells following vaccination were depleted by 94-95% in the spleen and blood. Circulating B-cells decreased to approximately 60% following T-cell depletion.

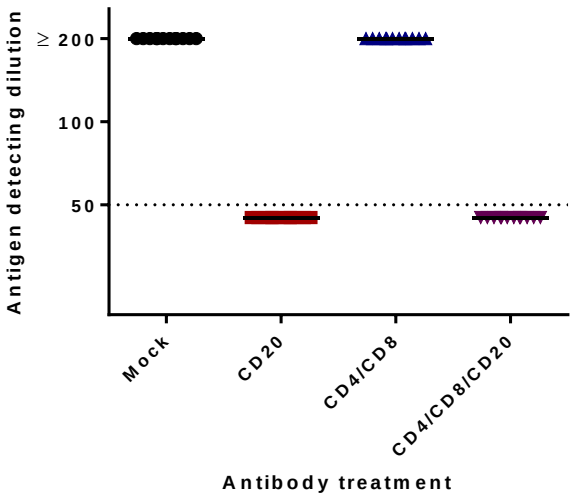


Figure 50. CCHFV antigen antibody development following depletion and vaccination. Groups of 6 analyzed IFNAR$^{-/-}$ mice were depleted of B-cells (CD20 depletion) prior to and/or depleted of T-cells (CD4/CD8 depletion) post vaccination with Ad-NP/Ad-GPC or mock depleted with purified Rat IgG prior to and post vaccination. 3 days prior to CCHFV challenge, the sera of the vaccinated and depleted mice was analyzed for seroconversion against CCHFV antigen. Mice which were depleted of B-cells prior to vaccination did not seroconvert against CCHFV regardless of whether T-cells were depleted. Mice depleted of T-cells following vaccination developed normal antibody levels compared to mock depleted animals. 1:100 primary sera dilution in 1% BSA-PBS, 1:1000 secondary HRP conjugated antisera dilution in 1%BSA-PBS. Signal was developed for 1 hour at room temperature following addition of substrate.

### 3.8.2 Antibody, but not T-cell, responses are essential for protection of IFNAR$^{-/-}$ mice against CCHFV

Following the protective vaccination regimen IFNAR$^{-/-}$ mice depleted of B-cells, with or without depletion of T-cells, were not protected from lethal CCHFV challenge but had a slightly increased survival time (median survival time of 6 days following challenge of B-cell or B- and T-cell depleted mice or vs 5 days in mock vaccinated mice, p= 0.0084 and p= 0.0208, respectively). In contrast, IFNAR$^{-/-}$ mice depleted of only T-cells were mostly protected (83% survival, p< 0.0001)

from lethal CCHFV challenge, with the mice that succumbed to disease surviving longer than unvaccinated, B-cell or B- and T-cell depleted mice (Figure 51).

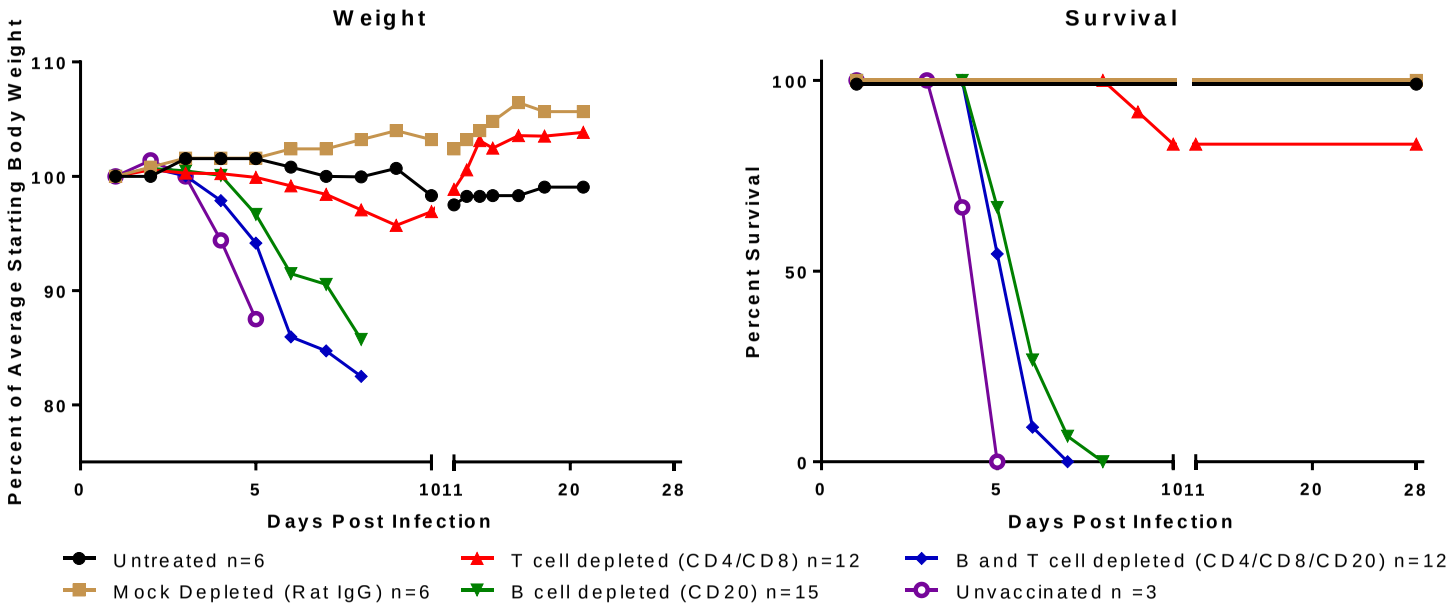


Figure 51: Survival following depletion, vaccination and CCHFV challenge. Groups of IFNAR$^{-/-}$ mice were depleted of B-cells (CD20 depleting antibody treated) prior to vaccination, depleted of T-cells (CD4/CD8 depleting antibody treated) post vaccination, depleted of B-cells prior to and of T-cells post vaccination (same antibodies as before), mock depleted (purified rat antibody treated) prior to and post vaccination or untreated. 4 weeks post full vaccination regimen with Ad-NP/Ad-GPC, IFNAR$^{-/-}$ mice were challenged with 1000 $MLD_{50}$ (50 $TCID_{50}$) of CCHFV and monitored for disease development and survival. Groups depleted of B-cells did not develop antibody responses following vaccination (Figure 3.8.2.1) and were not protected from lethal CCHFV challenge. Groups depleted of T-cells, mock depleted or untreated by antibodies were protected from lethal challenge with a survival rate of 83.3%, 100% and 100%, respectively. The disease course as measured by onset of weight loss was also delayed by 3 days in the T-cell depleted group. These results demonstrate the importance of antibodies in protection against lethal CCHFV challenge.

## 4. Discussion

CCHF is a widely distributed, but often sporadic, disease associated with high case fatality rates and without approved clinical countermeasures. With the increasing frequency of outbreaks and expansion of the CCHF endemic area there is an urgent need to develop strategies to combat this serious threat to public health. In order to develop and evaluate efficacious CCHF countermeasures the development of animal models is of the utmost importance. This dissertation work focused on the characterization of a lethal animal model, which has been a major hurdle in the study of CCHF, and the use of this animal model to evaluate potential vaccine candidates against CCHF as well as to elucidate the mechanisms of protection following vaccination. The characterization of the animal model, vaccine candidate and mechanisms of protection provides valuable data which allows other researchers to evaluate additional aspect of CCHF.

### 4.1 CCHFV tool development

In addition to a lack of animal models, general molecular tools to study CCHFV are not readily available. Therefore, in order to detect and characterize CCHFV and its proteins and anti-CCHFV immune responses significant effort had to be invested into development of specific CCHFV reagents.

During the course of this work expression plasmids of CCHFV NP and GPC were created (Figure 13). These 2 proteins have been successfully expressed previously for a number of purposes and are the primary genes of interest for vaccine development and detection [4-6, 8, 14, 17, 19, 25, 98, 112]. Unfortunately, no commercial or other antibodies were available during the course of this work and thus these antigens were detected with peptide antibodies derived from

vaccination with specific peptides or by sera from convalescent IFNAR$^{-/-}$ mice. Antipeptide antibodies targeting the NP worked well in both ELISA and Western blot, while those targeting GPC could not detect mature CCHFV glycoproteins. The GPC peptides (CCHFV GPC residues 528-540 [$G_N$], 600-611 [$G_N$], 1524-1534 [$G_C$] and 1631-1643 [$G_C$]) had previously been reported to generate antibody responses against CCHFV glycoproteins [8, 25, 113], however, those results could not be duplicated suggesting the need for alternate mechanisms of vaccination.

### 4.1.1 Construction of Ad expressing CCHFV antigens

Ad constructs containing CCHFV GPC, NP, mature $G_N$ and $G_C$ were made in the pAdenoX plasmid from Clontech. Cloning and virus rescue did not require significant optimization away from manufacturer's recommendations. The apparent ease of recombinant Ad construction is likely because Ad vectors are not reliant of CCHFV antigens for their life cycle. The propagation of Ad vectors expressing CCHFV antigens was efficient with the vectors all replicating to an approximately equivalent level, as determined by an Ad infectivity assay. The expression of CCHFV RNA was determined by mRNA specific amplification, followed by CCHFV gene specific amplification of DNase I treated whole cell RNA of Ad infected 293 cells (Figure 15). Expression of NP, GPC, $G_N$ and $G_C$ were confirmed by Western blot (Figure 16) and demonstrate that this vector can be used to efficiently deliver CCHFV antigens to cells. This is the first report of CCHFV antigens being successfully expressed from Ad vectors and validates Ad vectors as a potential vaccine platform against CCHFV. Due to the promise shown by Ad vectors, this platform was selected for use in IFNAR$^{-/-}$ mice as these Ad vectors are replication incompetent outside of a few cell lines expressing Ad E1 protein, such as 293 cells.

### 4.1.2 Construction of VSV expressing CCHFV GPC

As an alternative vaccine approach, CCHFV GPC was cloned into the pAK-VSVΔG vector and VSV-GPC was successfully rescued with minimal optimization for CCHFV compared to previous attempts [114-116]. While VSVΔG expressing a Bunyaviridae family member glycoproteins have been previously reported [117, 118], this is the first time a CCHFV glycoprotein has been expressed and used for entry into cells by VSV. However, in order to successfully rescue this construct the first ~70 aa of the GPC (the proposed signal peptide, which is neither conserved among CCHFV species nor present in processed CCHFV glycoproteins) had to be deleted in order to successfully rescue the VSV encoding CCHFV glycoproteins. This region of sequence was not replaced by other sequence. Why this deletion is necessary is unknown however; it is hypothesized that this deletion alters the cellular localization of $G_N$ away from the Golgi, as has been previously reported [25], and enables the VSV particle, which does not bud from the Golgi, to more easily incorporate this glycoprotein to bud from infected cells. The ability of VSV-GPC to infect subsequent cells suggests that the CCHFV GPC is functional to the degree to allow entry, however it may be altered in post-translational modification from authentic CCHFV. However, the analysis of how the GPC processing differs from authentic CCHFV GPC processing is beyond the scope of this research. While this construct may not be ideal for elucidating pathways of egress or CCHFV GPC processing, it is ideal as a tool to assess neutralization capacity of anti-CCHFV antibodies. The expression of CCHFV GPC was confirmed by ELISA (Figure 18) and demonstrated that this construct was antigenically similar to native CCHFV glycoproteins. The similarity in antigenicity suggests that this construct may also be utilized as a live, attenuated vaccine. However, since the goal of the project was to generate a platform which could be tested on $IFNAR^{-/-}$ mice, we chose the replication deficient Ad vaccines for efficacy evaluation in

immunocompromised IFNAR$^{-/-}$ mice rather than the replication competent VSV-GPC vaccine candidate.

### 4.2 IFNAR$^{-/-}$ mice challenged with CCHFV display a rapid, lethal disease which mimics hallmarks of human CCHF

Since CCHFV is an emerging threat to public health in a vast geographic area, development of appropriate countermeasures is of utmost importance. Research into CCHFV countermeasures has been significantly hampered by a lack of animal models, which manifest disease and therefore, no prophylactic vaccines or specific therapies have been developed against CCHFV. In order to evaluate the efficacy of vaccines or therapies, development and characterization of novel CCHF disease models is essential. The susceptibility of IFNAR$^{-/-}$ mice to lethal CCHFV challenge was reported shortly following the beginning of this work [85]. At the time this was the only adult animal disease model and so both prophylactic vaccination (which was the eventual intended purpose of this model) and therapeutic treatments could be assessed in this model, unlike in the suckling mouse model. The obvious disadvantage to this model is that it is an immuno-deficient animal, which is unresponsive to type I IFN signaling and in some cases has altered adaptive immune responses [119]. Furthermore, the IFNAR$^{-/-}$ mouse model was not characterized with respect to susceptibility to routes of infection, mouse 50% lethal dose, pathologic changes, kinetics of infection, and immune responses to infection. Therefore, to use this model to evaluate mechanisms of protection from lethal CCHFV challenge, the infection kinetics and immune responses of IFNAR$^{-/-}$ mice to CCHFV infection were characterized.

Humans are thought to be susceptible to CCHFV infection by multiple routes of infection [24, 50, 51]. Infection in humans is either quickly resolved or develops into a rapid, acute disease which is characterized by high fever, coagulopathies, and hemorrhagic symptoms. Following challenge with CCHFV IFNAR$^{-/-}$ mice develop disease signs similar to severe human CCHF.

IFNAR$^{-/-}$ are susceptible to CCHFV challenge by the i.m., i.n., i.p. and s.c. infection routes and develop disease both with high and low doses of CCHFV (Figure 19). In human CCHF outbreaks variable incubation times have been reported, with bloodborne transmission and higher inoculation doses often cited as resulting in more rapid disease manifestations and higher mortality [24, 50, 51]. Similarly, in IFNAR$^{-/-}$ mice the groups inoculated with a higher CCHFV dose developed disease more rapidly (Figure 19). In accordance with what has been suspected in human cases, the i.p. route of inoculation, which is thought to mimic bloodborne transmission, resulted in the shortest survival time while the i.n. route, which mimics large droplet transmission, resulted in the longest survival time, with mice surviving infection at the lower doses, while the i.m. and s.c. routes of infection resulted in intermediate survival periods (Figure 19). Since IFNAR$^{-/-}$ mice are susceptible to all tested challenge routes, the s.c. challenge route was chosen as it most closely mimics tick bite infection by targeting similar primary sites of replication, e.g. dermal dendritic cells, prior to being disseminated to other cell types. As the $MLD_{50}$ was undefined by this route of inoculation in IFNAR$^{-/-}$ mice, the $MLD_{50}$ was first determined to be 0.05 $TCID_{50}$. Therefore, these experiments demonstrate that IFNAR$^{-/-}$ mice are very sensitive to CCHFV challenge, which display differential susceptibility to routes of infection similar to what is hypothesized to occur in human CCHFV transmission.

To assess pathological, virological and immunological responses to infection a serial sacrifice study was undertaken. Soon after CCHFV challenge IFNAR$^{-/-}$ mice support high level of replication in all analyzed organs (Figure 21). The late appearance of viremia may be due to the route of inoculation and/or the IFNAR$^{-/-}$ mouse disease model and is in contrast to a related mouse model, STAT1$^{-/-}$ mice, which display immediate signs of viremia following i.p. challenge with CCHFV [84]. The limited time frame during which viremia is detectable is similar to the human clinical picture as CCHFV is often only detected in the blood for approximately 1 week

following symptom onset in clinical cases [24]. The lack of early viremia suggests the involvement of non-blood routes of dissemination in this model, such as lymphatic dissemination; however, the role of other dissemination systems was not investigated. IFNAR$^{-/-}$ mice develop highest organ CCHFV titers in liver, lung lymph node and spleens during the terminal disease stages (Figure 21) and virus isolation was accompanied by significant antigen staining in the same organs (Figure 22-24). The antigen staining and virus replication in IFNAR$^{-/-}$ mice mirrors the reports of CCHFV replication sites in humans [73]. Therefore, IFNAR$^{-/-}$ mice may be a good model to study the sites and kinetics of early CCHFV dissemination and accumulation of CCHFV antigen, in addition, is with the location of pathological changes in multiple organs.

Following onset of overt disease, IFNAR$^{-/-}$ mice developed significant organ pathology in the liver and progressive pathological changes within the lymphoid tissues (Figure 22-24). The pathologic changes in the liver appear as multifocal necrosis accompanied by infiltration of inflammatory cells, which eventually lead to destruction of hepatic architecture (Figure 22). Liver pathology and dysfunction is a hallmark of human CCHF and patients often develop multifocal necrosis accompanied by low grade infiltration of inflammatory cells of liver [73]. Since the highest level of virus replication, as measured by antigen staining (compare Figure 21 with 22), is associated with the greatest degree of pathological lesions (both in terms of frequency and severity of lesions), it can be inferred that uncontrolled CCHFV replication is directly or indirectly responsible for the pathological changes seen in IFNAR$^{-/-}$ mice and in human tissues. IFNAR$^{-/-}$ mouse lymphoid tissues all displayed lymphocytolysis and loss of lymphocytes with an overall loss of lymphoid architecture (Figure 23 and 24). In contrast, human CCHF patients uncommonly display pathologic changes of the spleen, however, in patients who display pathologic changes in the lymphoid tissues the pathologic patterns mimic the manifestations in IFNAR$^{-/-}$ mouse [73]. This suggests that the IFNAR$^{-/-}$ mouse lymphocytes are more sensitive to infection or support a

higher level of CCHFV replication than human lymphocytes. Once again the appearance of prominent pathological changes overlapped the highest level of virus replication which would suggest that uncontrolled virus replication is, directly or indirectly, responsible for pathological changes (compare Figures 22 with 23 and 24). Other IFNAR$^{-/-}$ mouse tissues (i.e. heart, lung, and kidney), while positive for antigen within embedded lymphocytes and endothelial cells, did not develop any pathologic abnormalities (Figure 25). The IFNAR$^{-/-}$ mouse model mimics the most common pathological changes observed in human CCHF patients and correlates to foci of CCHFV replication. Uncontrolled viral replication in IFNAR$^{-/-}$ mice leads to dysfunction of the most affected organs leading to liver and immune dysfunction.

The significant hepatic pathologic changes observed in IFNAR$^{-/-}$ mice challenged with CCHFV lead to liver dysfunction. At the onset of overt disease signs and liver pathology, IFNAR$^{-/-}$ mice develop substantial increases in both ALT and AST (Figure 26). Other markers of liver pathology (i.e. serum albumin, alkaline phosphatase, gamma-glutamyltransferase, total bilirubin, and total dissolved protein) are not altered throughout the disease suggesting that the significant liver pathology caused by CCHFV infection only induces partial liver failure as opposed to complete liver failure. Unsurprisingly, based on a lack of pathologic changes within the pancreas and kidneys, markers of pancreatic and kidney function are not altered during CCHFV infection of IFNAR$^{-/-}$ mice. The appearance of liver dysfunction in IFNAR$^{-/-}$ mice is in accordance with human CCHF, which usually involves significant increases in ALT and AST [24, 51, 54]. However, unlike in the IFNAR$^{-/-}$ mice increases in additional liver enzymes and some evidence of renal failure are also reported [24, 51, 54, 90].

In addition to liver dysfunction, hemorrhagic manifestations are the most consistent clinical parameters seen in severe CCHF patients and a disease model should recapitulate these

features. Much like human patients, IFNAR$^{-/-}$ mice develop severe thrombocytopenia and coagulopathies following infection with CCHFV. CCHFV infected IFNAR$^{-/-}$ mice display a substantial (~90% by the terminal stages of disease) and statistically significant decreases in circulating platelet counts (Figure 27). Human CCHF also usually includes severe thrombocytopenia with as much as a ~90% reduction in circulating platelets in severe cases [54, 69]. The drop in platelets results in marked coagulopathy in IFNAR$^{-/-}$ with a significantly increased APTT, but not PT (Figure 29). The increase in APTT but not PT may be an indicator of presence of antibodies to phospholipids, and/or depletion or inhibition of von Willenbrand factor or coagulations factors VIII, IX, XI, or XII[106]. This finding would suggest that the coagulopathy seen in IFNAR$^{-/-}$ mice may be reversible by infusion of platelets and phospholipids. The replacement of platelets and phospholipids is common practice and reportedly efficacious in treatment of human CCHF in the Turkish outbreaks [90, 94, 120-122] The accompanying increase in MPV, as seen in some severe human cases [123], suggests that platelet destruction or extensive coagulation are likely responsible for the decrease in platelets (Figure 27). The platelet destruction hypothesis, as opposed to extensive coagulation, is supported by an accumulation in serum fibrinogen during the disease course and a lack of organ fibrin deposition as detected by PTAH staining (Figure 28). Furthermore, neither evidence of vascular leakage nor tissue hemorrhages were detected by histologic analysis (Figures 22 to 25). This would suggest in contrast to some human patients, IFNAR$^{-/-}$ mice do not develop disseminated intravascular coagulopathy and suggests that platelet destruction is an innate function of CCHFV infection [73]. In addition, to platelet involvement several lymphocyte parameters are altered during CCHFV infection.

On day 2 p.i. IFNAR$^{-/-}$ mice develop a transient increase in total white blood cells, lymphocytes, neutrophils and monocytes (Figure 30). A rapid, transient increase in immune cells is a fairly

common observation in response to infection; [107] however, the increase appears with delayed kinetics in IFNAR$^{-/-}$ mice (2 days as opposed to typically 1 day p.i.) suggesting that IFNAR$^{-/-}$ mice fail to recognize CCHFV replication initially. By 2 days p.i. the majority of tissues are already infected with CCHFV, which is less affected by immune responses following infection than prior to infection [20, 124]. The lack of rapid immune cell activation suggests that in this model CCHFV infection is not detected during the early stages of infection, similar to what is thought to occur in the most severe cases of human CCHF [24]. This same observations also suggests that type I interferon signaling is important for detection and to limit the early replication of CCHFV *in vivo* suggesting that CCHFV has innate mechanisms to overcome human IFN signaling but not that of other species.

In contrast to white blood cell counts, red blood cell parameters are only affected during the last stages of disease. Red blood cell parameters are largely unaffected until day 5 p.i. and then significantly decrease (Figure 31). The drop in total numbers suggests that during the terminal stages of infection IFNAR$^{-/-}$ mice develop blood loss through sequestration or leakage, or red blood cell destruction [107]. The lack of coagulation in the organs of IFNAR$^{-/-}$ mice (Figures 22-25) suggests that IFNAR$^{-/-}$ mice develop mucosal hemorrhage, as occurs in severe human CCHFV infection, or undergo red blood cell destruction. The dysfunction that is seen in blood cell populations may be a direct result of CCHFV attachment or, as has been suggested for the drop in platelets, may be a result of an overactive inflammatory response due to uncontrolled CCHFV replication.

Strong inflammatory responses appear at the same time as appearance of significant pathologic changes within the tissues, viremia, thrombocytopenia and coagulopathy. Pro-inflammatory and chemotactic cytokines and chemokines are seen in the sera of IFNAR$^{-/-}$ mice a day following the

spike in circulating white blood cells and just prior to death/euthanasia. G-CSF, GM-CSF, IL -1α, -1β, -2, -6, -12p70, -13, -17, IFNγ, CXCL1, CXCL10, CCL2, CCL3, CCL5 and TNFα are significantly increased suggesting immune overstimulation (Figure 32). The lack of an early response, coupled with the delayed increases in lymphocytes, suggests that CCHFV is not detected until high levels of the CCHFV replication or a wide range of infected cells result in immunological overstimulation. The increases in serum pro-inflammatory cytokines in IFNAR$^{-/-}$ mice may represent an alternate, indirect mechanism of platelet destruction which is supported by the accumulation of plasma fibrinogen levels in CCHFV infected IFNAR$^{-/-}$ mice (Figure 27).

Taken together these data demonstrate that IFNAR$^{-/-}$ mice develop a rapid, lethal disease. The disease is characterized by uncontrolled viral replication leading to pathologic changes within the liver and lymphatic organs, alterations in hematology, coagulopathy, and strong inflammatory responses, which is similar to human CCHF progression, albeit in a shorter time frame (Figure 52). It is, however, important to note that IFNAR$^{-/-}$ mice are severely immunocompromised and therefore, in this model CCHFV does not have to subvert the innate immune response, unlike in humans. However, due to a lack of animal models, the IFNAR$^{-/-}$ mouse model is the most appropriate animal model for future studies. Therefore, this model represents a milestone for future work requiring animal testing such as antivirals, vaccines and correlates of protection.

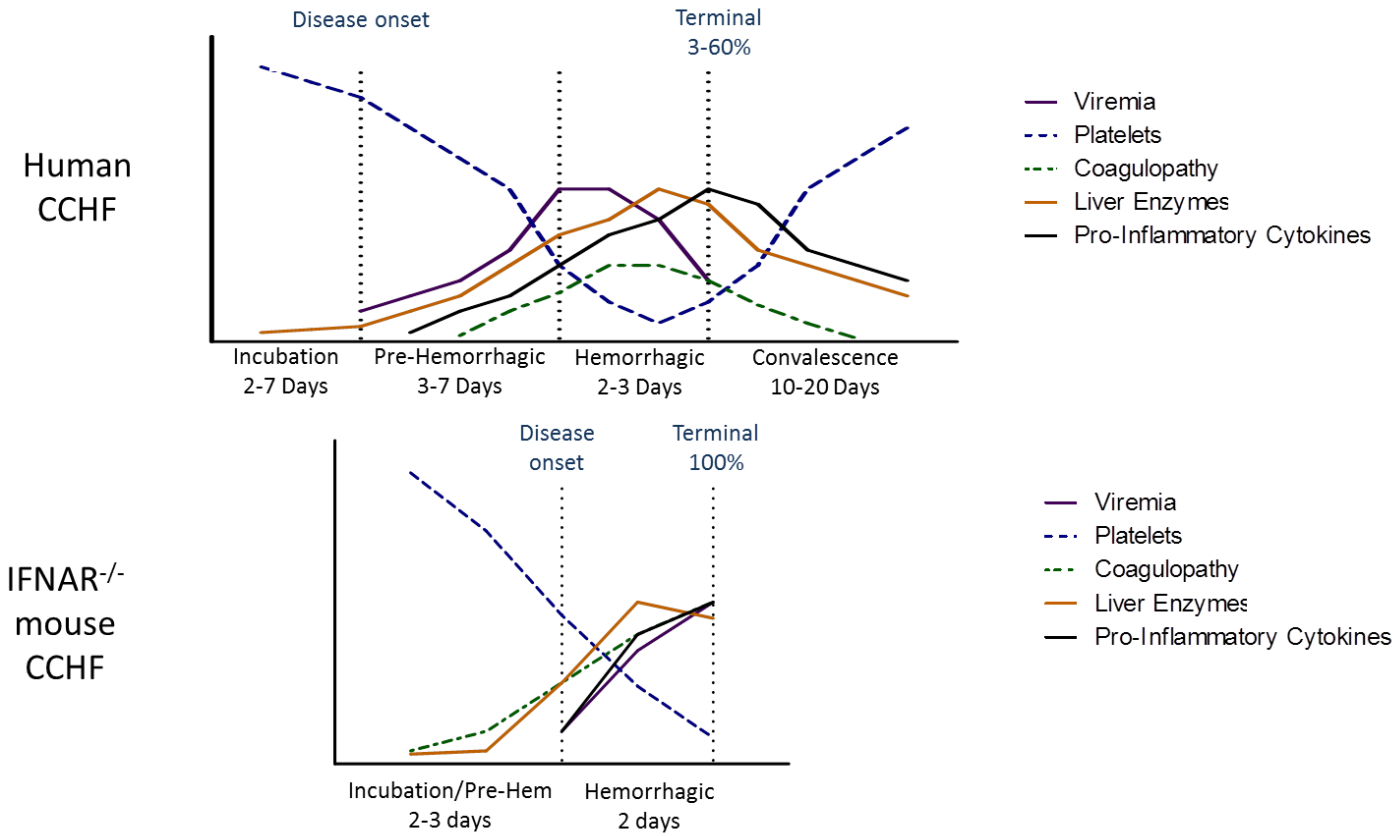


Figure 52. Comparison of IFNAR$^{-/-}$ and human CCHF. Human CCHF is split into 4 acute phases. Patients typically progress rapidly between phases and depending on the outbreak between 3-60% of patients succumb to infection. Human CCHF first manifests as flu like symptoms during which viremia is present, followed by a significant drops in platelet counts, development of coagulopathies, and increases in liver enzymes and pro-inflammatory cytokines. Most severe cases of human CCHF rapidly progress through the disease stages and those patients often succumb to disease. Following infection with CCHFV, IFNAR$^{-/-}$ mice develop a severe, rapid, lethal disease similar to the most severe human CCHF cases. IFNAR$^{-/-}$ mice rapidly progress from the incubation/pre-hemorrhagic phase, which manifests as weight loss and lethargy (i.e. non-specific disease signs), to the hemorrhagic phase characterized by high viremia, a significant drop in platelets, development of coagulopathy and increased liver enzymes and pro-inflammatory cytokines. Therefore, IFNAR$^{-/-}$ mice are an appropriate model to study human CCHF and should be utilized to study the development of CCHFV countermeasures.

### 4.3 Ad vaccines protect against lethal CCHFV challenge in IFNAR$^{-/-}$ mice

IFNAR$^{-/-}$ mice, due to insensitivity to type I interferon, are severely immunocompromised against intracellular pathogens such as viruses. Therefore, utilizing live attenuated viruses as vaccines, such as recombinant VSV, may result in severe disease in IFNAR$^{-/-}$ mice. To avoid the risks associated with replicating viruses, replication incompetent vectors were selected to evaluate the protective efficacy of vaccines in this model. Replication incompetent platforms are currently limited to inactivated whole virus, virus-like-particles, viral subunits, DNA plasmids and replication incompetent viruses. Due to safety (replication incompetent virus), immunogenicity, ease of manufacture, and quality of both cell mediated and humoral immune responses the replication incompetent Ad vector was selected as the vaccine platform against CCHFV in IFNAR$^{-/-}$ mice.

#### 4.3.1 IFNAR$^{-/-}$ mice are difficult to protect due to altered immune responses

The generation of effective immune responses to infection or vaccination with attenuated or inactivated viruses requires proper activation of subsets of immune cells and processing of antigen(s). Type I IFN was originally described to induce a non-specific antiviral state within cells [125, 126]; however, the immunomodulatory and, importantly, the immunostimulatory effects of type I IFN have been more recently recognized [127, 128]. Type I IFN signaling has a significant impact on activation and proliferation of both innate immune cell populations, such as dendritic cells, macrophages, and natural killer cells [129, 130], and adaptive immune cell populations such as B- and T-cell [131, 132]. Therefore, it is currently thought that type I IFN signaling is an important step in pathogen recognition and significantly impacts the development of a proper adaptive immune response. Pathogens have evolved mechanisms to

either prevent or antagonize type I IFN signaling [133-135]. IFNAR$^{-/-}$ mice, due to their inability to signal by the type I IFN pathway are less likely to effectively recognize pathogens and, therefore, more susceptible to severe disease in response to infection with pathogens including CCHFV [85, 136]. In addition to innate immunity dysfunction, the inability to signal by type I IFN may negatively impact the formation of adaptive immune responses to antigens, such as viruses, in IFNAR$^{-/-}$ mice; this is primarily mediated by inefficient priming of antigen specific T- and B-cells by antigen presenting cells and an inability to induce strong activation, survival or expansion of T- and B-cells [131, 132, 137-139]. Therefore, successful vaccination strategies in IFNAR$^{-/-}$ mice must overcome the lack of strong adaptive immune stimulation by the innate immune system in addition to being very safe. IFNAR$^{-/-}$ mice are a "high bar" due to the restrictions in usable vaccine platforms; however, other studies have successfully protected IFNAR$^{-/-}$ mice from lethal viral challenge [140, 141] making vaccine studies acceptable in this model.

### 4.3.2 Rationale for antigen selection

The mature CCHFV virion is thought to contain 3 major structural proteins: the mature glycoproteins $G_N$ and $G_C$, and the NP, encoded by the GPC gene and NP gene, respectively. Initially it was thought that induction of neutralizing antibodies would be the key to successfully protecting IFNAR$^{-/-}$ mice from lethal CCHFV challenge as lethal human CCHF is usually characterized by low or undetectable antibody responses [51, 142]. Therefore Ad expressing the complete GPC gene and the coding regions of the mature $G_N$ and $G_C$ were created. However, as antibody responses are primarily reported to be against the NP in CCHF survivors [90] and NP based vaccines have been successful with other Bunyavirus members [140, 143], Ad expressing NP was also created. All vaccine constructs were evaluated for protective efficacy in this model.

### 4.3.3 Immune response to NP is important for protection from lethal disease

Following a single vaccination, animals vaccinated only with Ad expressing GPC, $G_N$, $G_C$, or a combination of $G_N$ and $G_C$ failed to protect IFNAR$^{-/-}$ mice from lethal CCHFV challenge (Figure 33). This suggests that these antigens are not expressed to sufficiently high levels to induce an effective immune response; glycoprotein processing is not being correctly carried out and/or that glycoproteins as antigens do not induce a protective immune response. As the glycoprotein antigens appear to be expressed to the approximately the same degree as the NP antigen (Figure 15 and 16) this would suggest that expression is not the limiting factor and suggests that appropriate processing or incorrect immune responses are the reason why these vaccines fail to alter CCHFV disease course in IFNAR$^{-/-}$ mice.

In contrast, IFNAR$^{-/-}$ mice vaccinated with Ad expressing NP were partially protected following CCHFV challenge (Figure 33). Including Ad-GPC, but not combination of Ad-$G_N$ and Ad-$G_C$, along with Ad-NP enhanced the protective efficacy of vaccination significantly (78% compared to 33%) (Figure 34). The ability of Ad-GPC to enhance the protective efficacy of vaccination further suggests that poor expression is not a reason for why vaccination with Ad-GPC alone fails to protect IFNAR$^{-/-}$ mice. How the vaccine protects IFNAR$^{-/-}$ mice from lethal CCHF was further complicated by the viral burden in IFNAR$^{-/-}$ mice. Following the partially protective vaccination (i.e. Ad-NP, Ad-NP/Ad-GPC, and Ad-NP/Ad-$G_N$/Ad-$G_C$) IFNAR$^{-/-}$ mice did not develop CCHFV viremia at 3 days p.i. despite having significant organ viral loads (Figure 35). Presumably, the mice which succumbed to CCHFV challenge in the partially protected groups eventually developed viremia; however, the appearance of viremia at a later time point was not monitored. Interestingly, while IFNAR$^{-/-}$ mice in partially protected groups still develop high

tissue viral loads, pathological changes in the spleen and liver are significantly reduced compared to unprotected groups (Figure 36 and 37). The efficient level of CCHFV replication in the partially protected IFNAR$^{-/-}$ mouse group organs suggests that Ad vaccination does not simply affect initial viral replication, e.g. by neutralizing virus prior to infecting cells, but rather protects by another mechanism, e.g. by modulation of host immune responses. Furthermore, this result demonstrates that immune responses against NP can be protective and that the non-neutralizing anti-NP immune response seen in human CCHF survivors may be a major protective component.

### 4.3.4 Prime/boost strategy fully protects mice from lethal CCHFV challenge

Ad-NP/Ad-GPC vaccinated (highest level of protection following single vaccination), Ad-NP (intermediate level of protection following single vaccination) and Ad-GPC (no protection following single vaccination) were repeated with a prime/boost strategy to enhance the protective efficacy of vaccination. Following the full vaccination schedule the same trend was observed; i.e. Ad-NP/Ad-GPC had the highest level of protection (100%), Ad-NP had an intermediate level of protection (78%) and Ad-GPC had no protection (0%) against lethal CCHFV challenge (Figure 38). A later time point was also used to assess virology, pathology and hematology following CCHFV challenge. Unlike with the single vaccination schedule, CCHFV tissue loads were significantly reduced in the Ad-NP and Ad-NP/Ad-GPC groups (Figure 39) demonstrating that the higher dose of CCHFV vaccination or perhaps the i.n. vaccination route is better at stimulating effective adaptive immune responses as has been previously suggested [110]. Furthermore pathological changes were not apparent in Ad-NP and Ad-NP/Ad-GPC groups unlike the single vaccination schedule, which displayed pathological changes in the liver (compare Figure 40 to 22). In addition to the lack of pathological changes, Ad-NP/Ad-GPC

vaccinated IFNAR$^{-/-}$ mice did not display significant alterations in blood cell parameters following challenge unlike other vaccinated groups (Figure 42-44). The data suggest the homologous Ad boost either targets a wider range of immune cells and/or results in higher affinity immune responses capable of neutralizing CCHFV entry or replication more effectively and earlier in infection. Due to the appearance of low level of neutralizing antibodies against VSV-GPC following Ad-NP/Ad-GPC prime/boost, it is likely that development of neutralizing responses plays a role in the increased efficacy of protection; however, this cannot be the only mechanism of protection as mice vaccinated with Ad-NP (which do not develop a neutralizing response) also increase in degree of protection following the boost.

### 4.3.5 Ad vaccine conclusions

Vaccination with Ad based vaccines confers a protective adaptive immune response in IFNAR$^{-/-}$ mice. All 3 of the major structural proteins are required for an effective immune response against CCHFV, with NP being the crucial component in every vaccination schedule (Figure 53). It is surprising that GPC expressed on its own does not confer any protection from lethal CCHFV challenge. This could be for numerous reasons including insufficient post-translational processing or inducing incorrect immune responses, which are incapable of controlling CCHFV infection. An attractive hypothesis is that Ad-GPC fails to undergo correct antigen processing as this would suggest that NP is required in the CCHFV life cycle to properly process infectious surface glycoproteins, however, as the GPC alone is properly processed and yields infectious VSV-GPC in the absence of NP it suggests that the lack of protection with Ad-GPC is not due to incorrect processing but rather by incorrect immune responses generated by Ad-GPC. An explanation as to why Ad-NP/Ad-GPC provide a higher level of protection compared to Ad-NP or Ad-GPC alones is that NP, when overexpressed in mammalian cells, has been observed to

produce “virus-like-particles” (VLPs) which egress from the cell [16]. The production of VLPs, in addition to the intracellularly expressed NP from Ad expression, would stimulate both CD4 (antibody) and CD8 (cellular) adaptive immune responses by two mechanisms. There is no evidence that GPC is capable of producing VLPs by itself and, therefore, is predominantly recognized following intracellular expression by Ad. Therefore, animals vaccinated with only Ad-GPC may not display extracellular antigen induced immune response due to a lack of VLPs; while animals vaccinated with Ad-NP display both intracellular and intracellular NP helping to explain the difference in efficacy. However, in animals, vaccinated with both Ad-NP and Ad-GPC, it is possible that, in cells in which both GPC and NP are produced, VLPs containing surface $G_N$ and $G_C$ are produced which induce both a CD4 and CD8 adaptive immune responses against both the glycoproteins and the nucleoprotein. This dual CD4 and CD8 immune response against all major CCHFV structural proteins would be superior to vaccination with simply NP or GPC. This hypothesis would therefore suggest that immune responses against multiple CCHFV components are important for protection from CCHFV challenge (Figure 54). However to date no information directly supporting this hypothesis exists due to technical issues with obtaining sufficiently high levels of CCHFV VLP required for direct detection by the available assays.

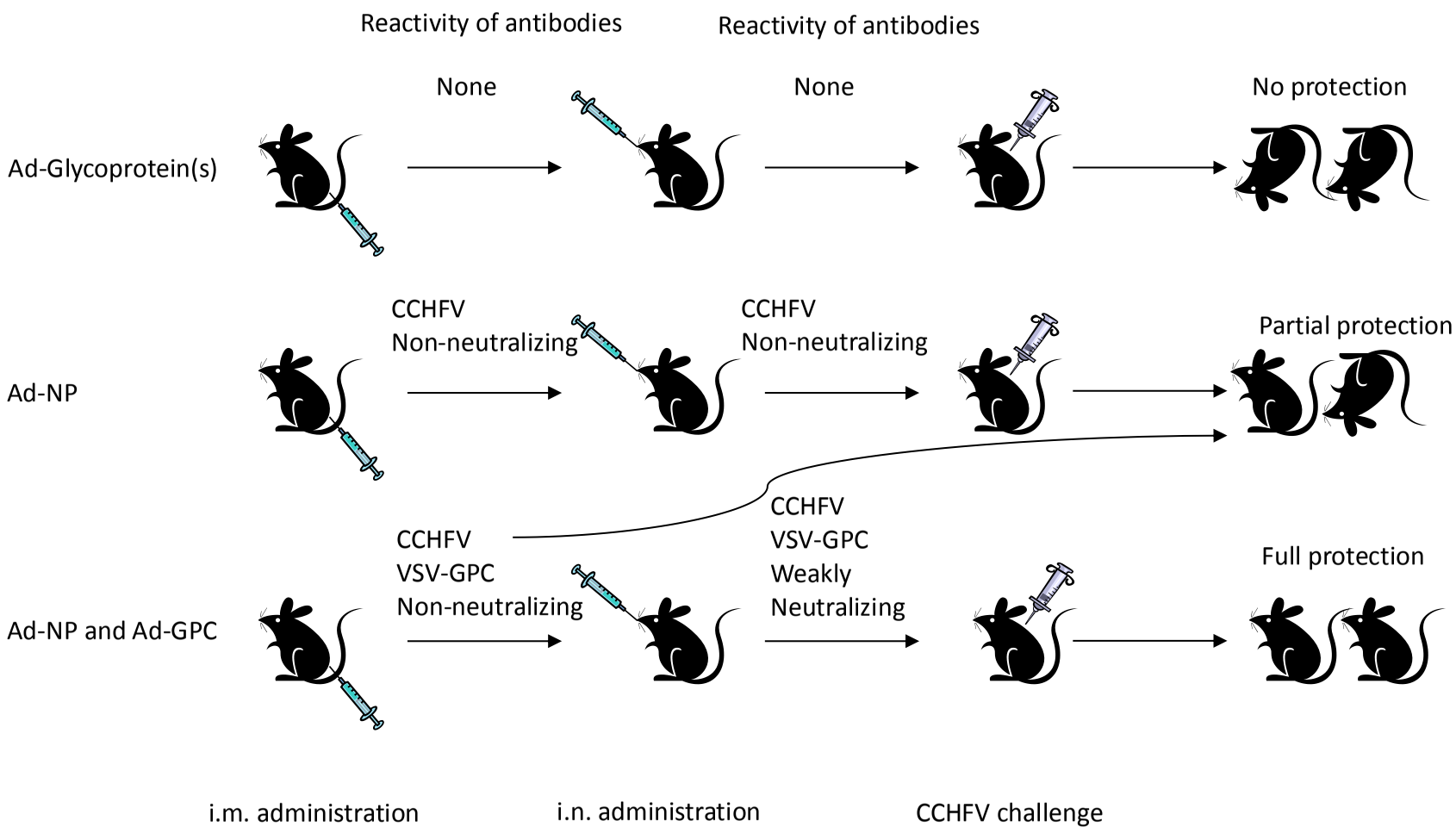




Figure 53. Schematic of outcome following Ad vaccination regimen and CCHFV challenge. IFNAR$^{-/-}$ mice vaccinated with Ad expressing only glycoprotein components are not protected from CCHFV challenge. In contrast, only some of the IFNAR$^{-/-}$ mice vaccinated and/or boosted with Ad-NP alone are protected from CCHFV challenge. Mice vaccinated and boosted with Ad expressing NP and Ad expressing GPC are fully protected from CCHFV challenge.

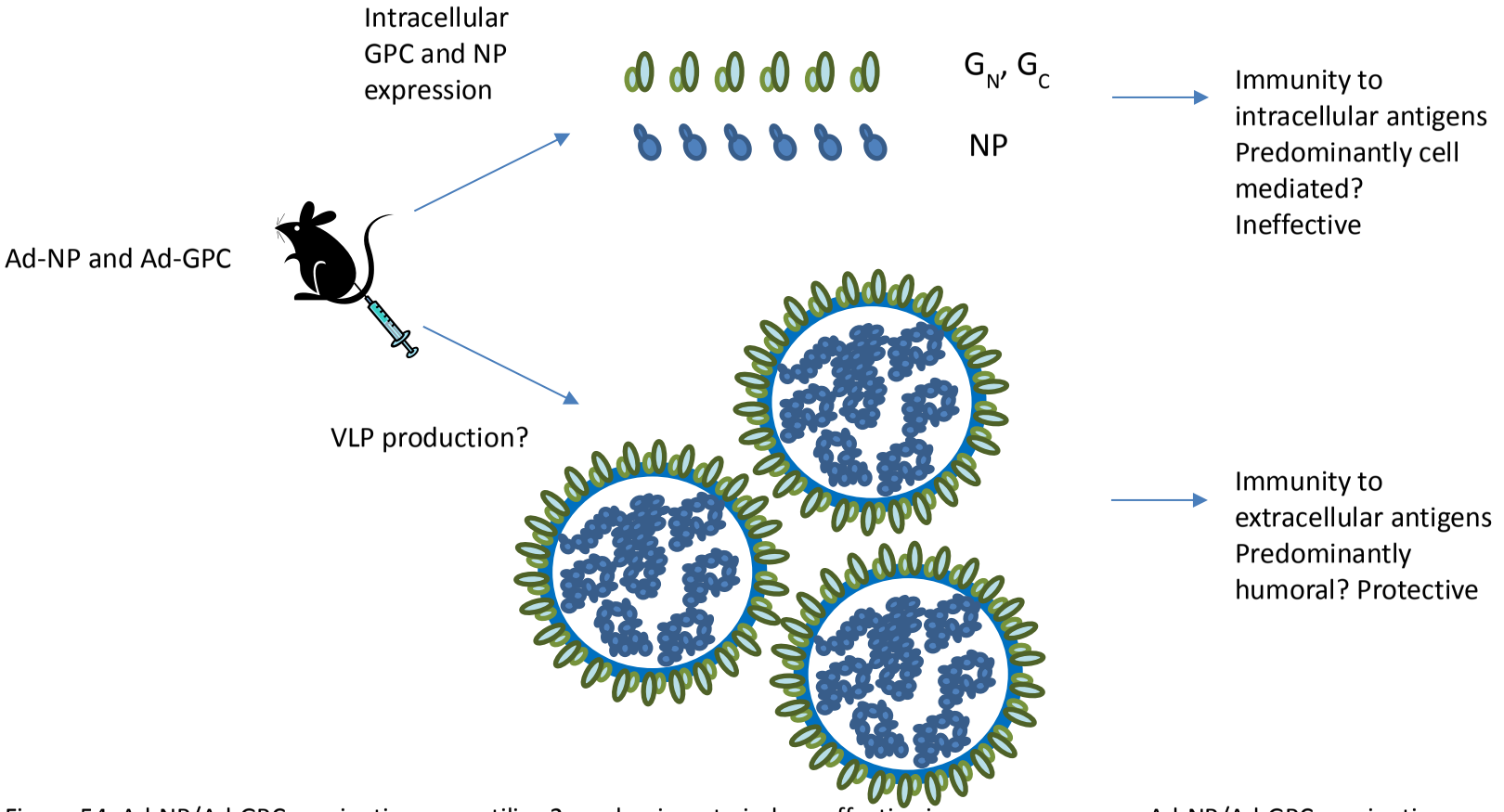


Figure 54. Ad-NP/Ad-GPC vaccination may utilize 2 mechanisms to induce effective immune responses. Ad-NP/Ad-GPC vaccination stimulates the immune system simply through direct production of virus components intracellularly. However, the combination of Ad-NP/Ad-GPC may also induce the formation of virus-like particles which may egress from Ad infected cells and stimulate the immune system as extra cellular immunogens.

### 4.4 Immune responses following Ad vaccination

To assess immune responses to Ad vaccination the fully protective vaccination schedule (Ad-NP/Ad-GPC prime/boost) was used. IFNAR$^{-/-}$ mice vaccinated on this schedule were monitored for seroconversion and T-cell responses following vaccination. Mice vaccinated with Ad-NP/Ad-GPC develop antibody responses starting at first vaccination and increasing post boost (Figure 18). T-cell responses develop in response to Ad vaccination, however due to limitations in available reagents stimulation failed to detect differences between effector T-cell stimulation in IFNAR$^{-/-}$ mice vaccinated with Ad compared to IFNAR$^{-/-}$ mice vaccinated with Ad-NP/Ad-GPC (Figure 45 and 46). To see which arm of the adaptive immune response was responsible for protection from lethal CCHFV challenge, gain of immunity and loss of immunity experiments following protective vaccination were undertaken. Gain of immunity experiments focused on adaptive and passive transfer of immune cells and antibodies, respectively. Total T- and B-cells, total splenocytes and antibodies were transferred from IFNAR$^{-/-}$ mice receiving the full protective regimen to naïve IFNAR$^{-/-}$ mice.

#### 4.4.1 Antibodies are important, but antibody transfer alone is insufficient to protect IFNAR$^{-/-}$ mice from CCHFV challenge

Following the complete prime/boost vaccination regimen IFNAR$^{-/-}$ mice were euthanized and their spleen and blood collected for isolation of immune cell subpopulations and antibodies, respectively. From the vaccinated mice total splenocytes, B- and T-cells, and total antibodies were purified and transferred to naïve recipient IFNAR$^{-/-}$ mice. Antibody recipient mice had a significantly increased time to disease onset; however, antibody transfer alone or in combination with either total T- or B-cells did not protect IFNAR$^{-/-}$ mice from lethal CCHFV challenge suggesting that antibodies are important for protection from CCHFV challenge (Figure

47 and 48). T-cell transfers, on the other hand, failed to alter disease course in IFNAR$^{-/-}$ mice suggesting that effector T-cell responses are not important or insufficient to protect from lethal CCHFV challenge in this model. Transfer of total splenocytes in addition to antibodies, resulted in low level (20%) of survival in naïve IFNAR$^{-/-}$ mice. The exact immune correlates in this model are unknown, but may include other cell types like memory natural killer (NK) cells or tissue specific immune cells, e.g. liver effector memory T-cells, which were absent or present in insufficient quantities from the spleen of vaccinated IFNAR$^{-/-}$ mice. Furthermore, due to a lack of a neutralizing antibody response even following challenge with lethal CCHFV, the role of antibodies may be not to neutralize CCHFV by preventing its entry into or release from cells, but rather to recruit or activate the correct immune cells to primary sites of CCHFV replication, e.g. the liver. To study these phenomena additional studies involving knock-down of IFNAR$^{-/-}$ B- and T-cells, were undertaken.

### 4.4.2 Antibody response is essential while T-cell response is dispensable for protection from lethal CCHFV challenge following vaccination with Ad vectors

To assess how IFNAR$^{-/-}$ mice are protected from lethal CCHFV challenge, depletion experiments targeted against mouse B- and/or T-cells were undertaken. IFNAR$^{-/-}$ mice vaccinated with a protective vaccine regimen were depleted of B-cell, T-cells or both and assessed for protection following lethal CCHFV challenge. All animals depleted of B-cells failed to seroconvert against CCHFV following vaccination (Figure 50) and uniformly succumbed to lethal CCHFV infection (Figure 51). In contrast, animals depleted of only T-cells demonstrated seroconversion against CCHFV and were predominantly protected (83.3%) from lethal CCHFV challenge. This result demonstrates that antibody responses are essential for the protection seen in the IFNAR$^{-/-}$ mouse CCHF model. Furthermore, while antibodies are essential for protection from CCHFV

challenge, IFNAR$^{-/-}$ mice do not develop high level neutralizing antibodies against CCHFV, even following CCHFV challenge, suggesting that the elicited antibody response functions through alternate pathways such as complement or opsonization of infected cells or virions. Elucidation of the mechanism of antibody mediated protection, while beyond the scope of this dissertation, merits further investigation as it may indicate the appropriate assay(s) to assess whether vaccinated subjects will be protected from disease following CCHFV infection.

**4.5 Summary**

CCHFV is an extensively distributed virus with limited information available on the immunological, pathological and virological parameters following human infection. In addition, animals, while susceptible to CCHFV infection, do not develop disease signs. IFNAR$^{-/-}$ mice are susceptible to lethal CCHFV disease; however, the disease progression in this model had not been thoroughly studied prior to these studies. To address questions regarding susceptibility of IFNAR$^{-/-}$ mice, as well as virological, pathological and immunological parameters following infection a thorough evaluation of the model was performed.

CCHFV infected IFNAR$^{-/-}$ mice develop a rapid, lethal disease. Similarly to humans, IFNAR$^{-/-}$ mice are susceptible to multiple routes of infection and doses, however, the routes and doses display differences in the timing of disease progression. The disease in IFNAR$^{-/-}$ is characterized by high level of CCHFV replication, pathological changes within the liver and lymphoid tissue, high inflammation, alterations to blood chemistry and blood cell composition, thrombocytopenia and coagulopathy. Overall, the parameters overlap fairly well with human CCHF cases; however, it is important to note that, due to a lack of type I IFN signaling in this model, the mechanisms of immune evasion are probably different from human infection. To further investigate the role of

the immune system in this model vaccine candidates were designed and used to protect IFNAR$^{-/-}$ mice from lethal CCHFV challenge.

CCHFV structural proteins were successfully cloned into expression vectors and expressed both *in vitro* and *in vivo*. IFNAR$^{-/-}$ mice vaccinated with Ad constructs expressing nucleoprotein and the surface glycoproteins (components or complete glycoproteins precursor) demonstrated partial protection from lethal challenge, while those vaccinated with only the surface glycoproteins failed to protect IFNAR$^{-/-}$ mice from lethal challenge. Additional vaccination increased the efficacy of the vaccines to 100% and provided the foundation from which segments of the protective immune could be dissected and characterized.

Immune responses of IFNAR$^{-/-}$ mice following Ad vaccination were monitored until challenge and demonstrate development of an antibody response against CCHFV with an undefined cell mediated response. The affinity of antibody response to CCHFV increases over the course of the vaccination regimen; however, only weak neutralizing antibody responses were detected in IFNAR$^{-/-}$ mice vaccinated with Ad-NP/Ad-GPC and those of survivors of CCHFV challenge. However, neutralizing antibodies are not needed in this model as mice vaccinated with Ad-NP alone are also partially protected from CCHFV challenge. This is in accordance with human CCHF patients as development of NP specific antibodies have been primarily detected in CCHF survivors but not in patients succumbing to disease [90]. T-cell responses are less clear than antibody responses and there does not seem to be a significant CCHFV specific T-cell and T-cell memory response above what was observed in animals vaccinated with Adenovirus alone. To determine if T-cell or antibody responses could protect IFNAR$^{-/-}$ mice, transfer and depletion experiments were undertaken.

T-cell transfer did not show any protective efficacy in naïve IFNAR$^{-/-}$ mice challenge with CCHFV; while antibody transfer delayed disease onset, no protection was observed; coupling antibodies with T-cells did not enhance the effect of antibodies alone; and transfer of whole splenocytes (T-cells, B-cells, NK cells, DCs, etc) along with antibodies demonstrated a low level of protection along with a delayed disease onset.

Corroborating the transfer results depletion of T-cells did not significantly alter the protective efficacy of vaccination with Ad-NP/Ad-GPC, while depletion of B-cells, with or without depletion of T-cells, completely abolished the protective efficacy of vaccination. Together these data demonstrate that protection in IFNAR$^{-/-}$ mice is mediated by non-neutralizing antibody responses, without significant involvement of cytotoxic T-cells.

### 4.6 Future directions

#### 4.6.1 Further immunological parameters of protection

The current data demonstrates that adaptive antibody responses are essential for protection against CCHFV. Due to the trial and error nature of immune transfer studies additional work into elucidating the correct dosing and subtype composition of the transferred antibodies and timing of transfer should be considered. The future of this project should be to determine which humoral responses are essential for protection against lethal CCHFV challenge e.g. purified IgG, whole serum etc and the latest time point at which intervention can successfully protect IFNAR$^{-/-}$ mice from lethal challenge. These experiments are important as establishment of the mechanisms of protection can suggest which other vaccine platforms should be considered for protection from disease e.g. vaccines that are cheaper and/or easier to produce than Ad and up to which phase of disease treatments/prophylactic treatment may be considered.

### 4.6.2 Development of vaccines against CCHFV

The IFNAR$^{-/-}$ mouse model is the first reported adult animal model of CCHF. As such, it has many potential uses in novel experiments, which have been up until now impossible or unethical to perform in human CCHF patients. The experiments outlined in this dissertation demonstrate the protective efficacy of Ad vaccination against lethal CCHFV challenge with a homologous CCHFV strain (i.e. the vaccine is based on the CCHFV challenge strain). In nature, multiple strains, and often different genetic clades, of CCHFV circulate within an endemic region [28, 144]. Therefore, it is likely that people will get infected by heterologous strains compared to the vaccine strain. Therefore, a successful vaccine candidate, in addition to being safe, must be efficacious in protecting individuals from disease caused by homologous and heterologous CCHFV strains. This would be an ideal set of experiments to perform using the IFNAR$^{-/-}$ mouse model. IFNAR$^{-/-}$ mice would first need to be evaluated for susceptibility to other strains of CCHFV, ideally with more contemporary strains and human isolates. Following establishment of the susceptibility of IFNAR$^{-/-}$ mice to alternate CCHFV strains, the IFNAR$^{-/-}$ mice should be vaccinated with the protective regimen of Ad based vaccines, challenged with other strains of CCHFV and monitored for protection from disease. Should the vaccines fail to protect from heterologous challenge, additional work would need to be conducted to decipher which antigens are both conserved between and capable of conferring protection against challenge again several strains of CCHFV.

### 4.6.3 Post exposure treatment of CCHFV in this model

In addition to prophylactic vaccines, post exposure treatments are of high importance for development against this pathogen. The IFNAR$^{-/-}$ model offers an ideal way to test direct antivirals against CCHFV in an *in vivo* model. Direct CCHFV entry, replication or egress inhibitors may be tested using this model, while therapeutics which primarily affect the host immune

system may be difficult to test within this model due to the difference between immune responses in humans and IFNAR$^{-/-}$ mice. Furthermore, testing of post exposure vaccines, such as a further attenuated VSV which has been shown as protective against Ebola and Marburg viruses [118, 145], are promising venues of further research in this system.

### 4.6.4 Development of additional animal models of CCHFV

CCHFV is transmitted to humans often through interaction with agricultural animals. Therefore, the establishment of agricultural animal models, such as sheep or goats, of CCHFV would allow us to study level of viremia in more natural animals and would allow for most realistic transmission experiments. Furthermore, these experiments could be utilized to assess whether or not vaccination with the vaccines developed in these studies, prevents transmission to susceptible hosts. Prevention of transmission from animals to humans would be a major step forward in reducing incidence in endemic areas and, from a regulatory point of view, vaccination of agricultural animals is easier to facilitate than vaccination of human populations.

### 4.6.5 Future direction conclusions

The IFNAR$^{-/-}$ mouse model of CCHFV can provide the CCHFV research community with invaluable insight in pathogenesis of CCHFV as well discovery and development of effective countermeasures. The work presented in this dissertation initiates the first in a long line of research, which will, hopefully, ultimately culminate in the development of inexpensive, safe and effective prophylactic and treatment options for people, and possibly agricultural animals, living in endemic areas of the world.

REFERENCES


1. Hoogstraal, H., *The epidemiology of tick-borne Crimean-Congo hemorrhagic fever in Asia, Europe, and Africa.* J Med Entomol, 1979. **15**(4): p. 307-417.
2. Tignor, G.H., et al., *Close relationship of Crimean hemorrhagic fever-Congo (CHF-C) virus strains by neutralizing antibody assays.* Am J Trop Med Hyg, 1980. **29**(4): p. 676-85.
3. Casals, J., *Antigenic similarity between the virus causing Crimean hemorrhagic fever and Congo virus.* Proc Soc Exp Biol Med, 1969. **131**(1): p. 233-6.
4. Sanchez, A.J., et al., *Crimean-congo hemorrhagic fever virus glycoprotein precursor is cleaved by Furin-like and SKI-1 proteases to generate a novel 38-kilodalton glycoprotein.* J Virol, 2006. **80**(1): p. 514-25.
5. Sanchez, A.J., M.J. Vincent, and S.T. Nichol, *Characterization of the glycoproteins of Crimean-Congo hemorrhagic fever virus.* J Virol, 2002. **76**(14): p. 7263-75.
6. Bergeron, E., M.J. Vincent, and S.T. Nichol, *Crimean-Congo hemorrhagic fever virus glycoprotein processing by the endoprotease SKI-1/S1P is critical for virus infectivity.* J Virol, 2007. **81**(23): p. 13271-6.
7. Altamura, L.A., et al., *Identification of a novel C-terminal cleavage of Crimean-Congo hemorrhagic fever virus PreGN that leads to generation of an NSM protein.* J Virol, 2007. **81**(12): p. 6632-42.
8. Bertolotti-Ciarlet, A., et al., *Cellular localization and antigenic characterization of crimean-congo hemorrhagic fever virus glycoproteins.* J Virol, 2005. **79**(10): p. 6152-61.
9. Mir, M.A. and A.T. Panganiban, *Characterization of the RNA chaperone activity of hantavirus nucleocapsid protein.* J Virol, 2006. **80**(13): p. 6276-85.
10. Mir, M.A. and A.T. Panganiban, *The hantavirus nucleocapsid protein recognizes specific features of the viral RNA panhandle and is altered in conformation upon RNA binding.* J Virol, 2005. **79**(3): p. 1824-35.
11. Mir, M.A. and A.T. Panganiban, *The triplet repeats of the Sin Nombre hantavirus 5' untranslated region are sufficient in cis for nucleocapsid-mediated translation initiation.* J Virol, 2010. **84**(17): p. 8937-44.
12. Cheng, E. and M.A. Mir, *Signatures of host mRNA 5' terminus for efficient hantavirus cap snatching.* J Virol, 2012. **86**(18): p. 10173-85.
13. Guo, Y., et al., *Crimean-Congo hemorrhagic fever virus nucleoprotein reveals endonuclease activity in bunyaviruses.* Proc Natl Acad Sci U S A, 2012. **109**(13): p. 5046-51.
14. Andersson, I., et al., *Role of actin filaments in targeting of Crimean Congo hemorrhagic fever virus nucleocapsid protein to perinuclear regions of mammalian cells.* J Med Virol, 2004. **72**(1): p. 83-93.
15. Carter, S.D., J.N. Barr, and T.A. Edwards, *Expression, purification and crystallization of the Crimean-Congo haemorrhagic fever virus nucleocapsid protein.* Acta Crystallogr Sect F Struct Biol Cryst Commun, 2012. **68**(Pt 5): p. 569-73.
16. Ma, B., et al., *[Use of a novel baculovirus vector to express nucleoprotein gene of Crimean-Congo hemorrhagic fever virus in both insect and mammalian cells].* Zhonghua Shi Yan He Lin Chuang Bing Du Xue Za Zhi, 2002. **16**(3): p. 249-52.
17. Garcia, S., et al., *Evaluation of a Crimean-Congo hemorrhagic fever virus recombinant antigen expressed by Semliki Forest suicide virus for IgM and IgG antibody detection in human and animal sera collected in Iran.* J Clin Virol, 2006. **35**(2): p. 154-9.

18. Vanhomwegen, J., et al., *Diagnostic assays for crimean-congo hemorrhagic fever.* Emerg Infect Dis, 2012. **18**(12): p. 1958-65.
19. Samudzi, R.R., et al., *Bacterial expression of Crimean-Congo hemorrhagic fever virus nucleoprotein and its evaluation as a diagnostic reagent in an indirect ELISA.* J Virol Methods, 2012. **179**(1): p. 70-6.
20. Andersson, I., et al., *Type I interferon inhibits Crimean-Congo hemorrhagic fever virus in human target cells.* J Med Virol, 2006. **78**(2): p. 216-22.
21. Andersson, I., et al., *Human MxA protein inhibits the replication of Crimean-Congo hemorrhagic fever virus.* J Virol, 2004. **78**(8): p. 4323-9.
22. Wang, Y., et al., *Structure of Crimean-Congo hemorrhagic fever virus nucleoprotein: superhelical homo-oligomers and the role of caspase-3 cleavage.* J Virol, 2012. **86**(22): p. 12294-303.
23. Karlberg, H., Y.J. Tan, and A. Mirazimi, *Induction of caspase activation and cleavage of the viral nucleocapsid protein in different cell types during Crimean-Congo hemorrhagic fever virus infection.* J Biol Chem, 2011. **286**(5): p. 3227-34.
24. Ergonul, O., *Crimean-Congo haemorrhagic fever.* Lancet Infect Dis, 2006. **6**(4): p. 203-14.
25. Erickson, B.R., et al., *N-linked glycosylation of Gn (but not Gc) is important for Crimean Congo hemorrhagic fever virus glycoprotein localization and transport.* Virology, 2007. **361**(2): p. 348-55.
26. Knipe, D.M., et al., *Field's Virology*. 5th ed, ed. D.M. Knipe. 2007.
27. Xiao, X., et al., *Identification of a putative Crimean-Congo hemorrhagic fever virus entry factor.* Biochem Biophys Res Commun, 2011. **411**(2): p. 253-8.
28. Chinikar, S., et al., *New circulating genomic variant of Crimean-Congo hemorrhagic fever virus in Iran.* Arch Virol, 2012.
29. Seregin, S.V., et al., *[Genomic S segment of Crimean-Congo hemorrhagic fever virus circulating in Russia and Bulgaria].* Vopr Virusol, 2006. **51**(3): p. 25-32.
30. Tumanova, I., et al., *[Genetic monitoring of the Crimean-Congo Hemorrhagic Fever virus in Kazakhstan and Tajikistan in 2001-2003].* Mol Gen Mikrobiol Virusol, 2006(2): p. 36-41.
31. Gargili, A., et al., *Crimean-Congo hemorrhagic fever in European part of Turkey: genetic analysis of the virus strains from ticks and a seroepidemiological study in humans.* Vector Borne Zoonotic Dis, 2011. **11**(6): p. 747-52.
32. Morikawa, S., M. Saijo, and I. Kurane, *Recent progress in molecular biology of Crimean-Congo hemorrhagic fever.* Comp Immunol Microbiol Infect Dis, 2007. **30**(5-6): p. 375-89.
33. Chen, S., *Molecular evolution of Crimean-Congo hemorrhagic fever virus based on complete genomes.* J Gen Virol, 2013. **94**(Pt 4): p. 843-50.
34. Anagnostou, V. and A. Papa, *Evolution of Crimean-Congo Hemorrhagic Fever virus.* Infect Genet Evol, 2009. **9**(5): p. 948-54.
35. Estrada-Pena, A., et al., *Unraveling the ecological complexities of tick-associated Crimean-Congo hemorrhagic fever virus transmission: a gap analysis for the western Palearctic.* Vector Borne Zoonotic Dis, 2012. **12**(9): p. 743-52.
36. Gonzalez, J.P., et al., *Sexual and transovarian transmission of Crimean-Congo haemorrhagic fever virus in Hyalomma truncatum ticks.* Res Virol, 1992. **143**(1): p. 23-8.
37. Shepherd, A.J., et al., *Viraemic transmission of Crimean-Congo haemorrhagic fever virus to ticks.* Epidemiol Infect, 1991. **106**(2): p. 373-82.
38. Dohm, D.J., et al., *Transmission of Crimean-Congo hemorrhagic fever virus by Hyalomma impeltatum (Acari:Ixodidae) after experimental infection.* J Med Entomol, 1996. **33**(5): p. 848-51.

39. Logan, T.M., et al., *Experimental transmission of Crimean-Congo hemorrhagic fever virus by Hyalomma truncatum Koch.* Am J Trop Med Hyg, 1989. **40**(2): p. 207-12.
40. Okorie, T.G., *Comparative studies on the vector capacity of the different stages of Amblyomma variegatum Fabricius and Hyalomma rufipes Koch for Congo virus, after intracoelomic inoculation.* Vet Parasitol, 1991. **38**(2-3): p. 215-23.
41. Gordon, S.W., K.J. Linthicum, and J.R. Moulton, *Transmission of Crimean-Congo hemorrhagic fever virus in two species of Hyalomma ticks from infected adults to cofeeding immature forms.* Am J Trop Med Hyg, 1993. **48**(4): p. 576-80.
42. Walker A.R., et al., *Ticks of Domestic Animals in Africa: a Guide to Identification of Species*, 2013, Bioscience Reports: Edinburgh, Scotland, U.K. p. 227.
43. Shepherd, A.J., et al., *Antibody to Crimean-Congo hemorrhagic fever virus in wild mammals from southern Africa.* Am J Trop Med Hyg, 1987. **36**(1): p. 133-42.
44. Saidi, S., J. Casals, and M.A. Faghih, *Crimean hemorrhagic fever-Congo (CHF-C) virus antibodies in man, and in domestic and small mammals, in Iran.* Am J Trop Med Hyg, 1975. **24**(2): p. 353-7.
45. Zeller, H.G., J.P. Cornet, and J.L. Camicas, *Experimental transmission of Crimean-Congo hemorrhagic fever virus by west African wild ground-feeding birds to Hyalomma marginatum rufipes ticks.* Am J Trop Med Hyg, 1994. **50**(6): p. 676-81.
46. Zeller, H.G., J.P. Cornet, and J.L. Camicas, *Crimean-Congo haemorrhagic fever virus infection in birds: field investigations in Senegal.* Res Virol, 1994. **145**(2): p. 105-9.
47. Swanepoel, R., et al., *Experimental infection of ostriches with Crimean-Congo haemorrhagic fever virus.* Epidemiol Infect, 1998. **121**(2): p. 427-32.
48. Shepherd, A.J., et al., *Field and laboratory investigation of Crimean-Congo haemorrhagic fever virus (Nairovirus, family Bunyaviridae) infection in birds.* Trans R Soc Trop Med Hyg, 1987. **81**(6): p. 1004-7.
49. Shepherd, A.J., P.A. Leman, and R. Swanepoel, *Viremia and antibody response of small African and laboratory animals to Crimean-Congo hemorrhagic fever virus infection.* Am J Trop Med Hyg, 1989. **40**(5): p. 541-7.
50. Vorou, R., I.N. Pierroutsakos, and H.C. Maltezou, *Crimean-Congo hemorrhagic fever.* Curr Opin Infect Dis, 2007. **20**(5): p. 495-500.
51. Whitehouse, C.A., *Crimean-Congo hemorrhagic fever.* Antiviral Res, 2004. **64**(3): p. 145-60.
52. Brumshtein, M.S. and E.V. Leshchinskaia, *[Clinical-anatomical aspects of Crimean hemorrhagic fever].* Arkh Patol, 1968. **30**(10): p. 57-62.
53. Leshchinskaia, E.V., *[Clinical aspects of Crimean hemorrhagic fever].* Sov Med, 1967. **30**(12): p. 74-8.
54. Cevik, M.A., et al., *Clinical and laboratory features of Crimean-Congo hemorrhagic fever: predictors of fatality.* Int J Infect Dis, 2008. **12**(4): p. 374-9.
55. Onguru, P., et al., *Coagulopathy parameters in patients with Crimean-Congo hemorrhagic fever and its relation with mortality.* J Clin Lab Anal, 2010. **24**(3): p. 163-6.
56. Weber, F. and A. Mirazimi, *Interferon and cytokine responses to Crimean Congo hemorrhagic fever virus; an emerging and neglected viral zonoosis.* Cytokine Growth Factor Rev, 2008. **19**(5-6): p. 395-404.
57. Saksida, A., et al., *Interacting roles of immune mechanisms and viral load in the pathogenesis of crimean-congo hemorrhagic fever.* Clin Vaccine Immunol, 2010. **17**(7): p. 1086-93.
58. Yesilyurt, M., et al., *The early prediction of fatality in Crimean Congo hemorrhagic fever patients.* Saudi Med J, 2011. **32**(7): p. 742-3.

59. Yilmaz, G., et al., *The effectiveness of routine laboratory findings in determining disease severity in patients with Crimean-Congo hemorrhagic fever: severity prediction criteria.* J Clin Virol, 2010. **47**(4): p. 361-5.
60. Ergonul, O., et al., *Analysis of risk-factors among patients with Crimean-Congo haemorrhagic fever virus infection: severity criteria revisited.* Clin Microbiol Infect, 2006. **12**(6): p. 551-4.
61. Papa, A., et al., *Cytokine levels in Crimean-Congo hemorrhagic fever.* J Clin Virol, 2006. **36**(4): p. 272-6.
62. Duh, D., et al., *Viral load as predictor of Crimean-Congo hemorrhagic fever outcome.* Emerg Infect Dis, 2007. **13**(11): p. 1769-72.
63. Wolfel, R., et al., *Virus detection and monitoring of viral load in Crimean-Congo hemorrhagic fever virus patients.* Emerg Infect Dis, 2007. **13**(7): p. 1097-100.
64. Papa, A., et al., *Viral load and Crimean-Congo hemorrhagic fever.* Emerg Infect Dis, 2007. **13**(5): p. 805-6.
65. Ergonul, O., et al., *Evaluation of serum levels of interleukin (IL)-6, IL-10, and tumor necrosis factor-alpha in patients with Crimean-Congo hemorrhagic fever.* J Infect Dis, 2006. **193**(7): p. 941-4.
66. Cevik, M.A., et al., *Viral load as a predictor of outcome in Crimean-Congo hemorrhagic fever.* Clin Infect Dis, 2007. **45**(7): p. e96-100.
67. Tasdelen Fisgin, N., et al., *Crimean-Congo hemorrhagic fever: five patients with hemophagocytic syndrome.* Am J Hematol, 2008. **83**(1): p. 73-6.
68. Kubar, A., et al., *Prompt administration of Crimean-Congo hemorrhagic fever (CCHF) virus hyperimmunoglobulin in patients diagnosed with CCHF and viral load monitorization by reverse transcriptase-PCR.* Jpn J Infect Dis, 2011. **64**(5): p. 439-43.
69. Ozturk, B., et al., *Evaluation of factors predictive of the prognosis in Crimean-Congo hemorrhagic fever: new suggestions.* Int J Infect Dis, 2012. **16**(2): p. e89-93.
70. Ozturk, B., et al., *Evaluation of the association of serum levels of hyaluronic acid, sICAM-1, sVCAM-1, and VEGF-A with mortality and prognosis in patients with Crimean-Congo hemorrhagic fever.* J Clin Virol, 2010. **47**(2): p. 115-9.
71. Bodur, H., et al., *Evidence of vascular endothelial damage in Crimean-Congo hemorrhagic fever.* Int J Infect Dis, 2010. **14**(8): p. e704-7.
72. Tezer, H., et al., *Crimean-Congo hemorrhagic fever in children.* J Clin Virol, 2010. **48**(3): p. 184-6.
73. Burt, F.J., et al., *Immunohistochemical and in situ localization of Crimean-Congo hemorrhagic fever (CCHF) virus in human tissues and implications for CCHF pathogenesis.* Arch Pathol Lab Med, 1997. **121**(8): p. 839-46.
74. Peyrefitte, C.N., et al., *Differential activation profiles of Crimean-Congo hemorrhagic fever virus- and Dugbe virus-infected antigen-presenting cells.* J Gen Virol, 2010. **91**(Pt 1): p. 189-98.
75. Flick, R. and C.A. Whitehouse, *Crimean-Congo hemorrhagic fever virus.* Curr Mol Med, 2005. **5**(8): p. 753-60.
76. Schwarz, T.F., H. Nsanze, and A.M. Ameen, *Clinical features of Crimean-Congo haemorrhagic fever in the United Arab Emirates.* Infection, 1997. **25**(6): p. 364-7.
77. Rodriguez, L.L., et al., *Molecular investigation of a multisource outbreak of Crimean-Congo hemorrhagic fever in the United Arab Emirates.* Am J Trop Med Hyg, 1997. **57**(5): p. 512-8.

78. Schwarz, T.F., et al., *Polymerase chain reaction for diagnosis and identification of distinct variants of Crimean-Congo hemorrhagic fever virus in the United Arab Emirates.* Am J Trop Med Hyg, 1996. **55**(2): p. 190-6.
79. Khan, A.S., et al., *An outbreak of Crimean-Congo hemorrhagic fever in the United Arab Emirates, 1994-1995.* Am J Trop Med Hyg, 1997. **57**(5): p. 519-25.
80. Bodur, H., et al., *Subclinical infections with Crimean-Congo hemorrhagic fever virus, Turkey.* Emerg Infect Dis, 2012. **18**(4): p. 640-2.
81. Smirnova, S.E., *A comparative study of the Crimean hemorrhagic fever-Congo group of viruses.* Arch Virol, 1979. **62**(2): p. 137-43.
82. Fagbami, A.H., et al., *Experimantal Congo virus (Ib -AN 7620) infection in primates.* Virologie, 1975. **26**(1): p. 33-7.
83. Tignor, G.H. and C.A. Hanham, *Ribavirin efficacy in an in vivo model of Crimean-Congo hemorrhagic fever virus (CCHF) infection.* Antiviral Res, 1993. **22**(4): p. 309-25.
84. Bente, D.A., et al., *Pathogenesis and immune response of Crimean-Congo hemorrhagic fever virus in a STAT-1 knockout mouse model.* J Virol, 2010. **84**(21): p. 11089-100.
85. Bereczky, S., et al., *Crimean-Congo hemorrhagic fever virus infection is lethal for adult type I interferon receptor-knockout mice.* J Gen Virol, 2010. **91**(Pt 6): p. 1473-7.
86. Blagoveshchenskaya N. M., et al., *Experimental infection of horses with Crimean hemorrhagic fever virus. Report 2. Virological and serological observations.* Nauchp Sesso Insto Polioo Virus. Ents, 1969. **2**: p. 126-127.
87. Freudenberg, M.A., et al., *Cutting edge: a murine, IL-12-independent pathway of IFN-gamma induction by gram-negative bacteria based on STAT4 activation by Type I IFN and IL-18 signaling.* J Immunol, 2002. **169**(4): p. 1665-8.
88. Prevention, C.f.D.C.a. *CDC ticks*. 2012 [cited July 26, 2012; Available from: http://www.cdc.gov/ticks/.
89. Athar, M.N., et al., *Short report: Crimean-Congo hemorrhagic fever outbreak in Rawalpindi, Pakistan, February 2002.* Am J Trop Med Hyg, 2003. **69**(3): p. 284-7.
90. Ergonul, O., *Crimean-Congo hemorrhagic fever virus: new outbreaks, new discoveries.* Curr Opin Virol, 2012. **2**(2): p. 215-20.
91. Bodur, H., et al., *Effect of oral ribavirin treatment on the viral load and disease progression in Crimean-Congo hemorrhagic fever.* Int J Infect Dis, 2011. **15**(1): p. e44-7.
92. Koksal, I., et al., *The efficacy of ribavirin in the treatment of Crimean-Congo hemorrhagic fever in Eastern Black Sea region in Turkey.* J Clin Virol, 2010. **47**(1): p. 65-8.
93. Soares-Weiser, K., et al., *Ribavirin for Crimean-Congo hemorrhagic fever: systematic review and meta-analysis.* BMC Infect Dis, 2010. **10**: p. 207.
94. Mardani, M., M. Rahnavardi, and B. Sharifi-Mood, *Current treatment of Crimean-Congo hemorrhagic fever in children.* Expert Rev Anti Infect Ther, 2010. **8**(8): p. 911-8.
95. Papa, A., E. Papadimitriou, and I. Christova, *The Bulgarian vaccine Crimean-Congo haemorrhagic fever virus strain.* Scand J Infect Dis, 2011. **43**(3): p. 225-9.
96. Mousavi-Jazi, M., et al., *Healthy individuals' immune response to the Bulgarian Crimean-Congo hemorrhagic fever virus vaccine.* Vaccine, 2012. **30**(44): p. 6225-9.
97. Spik, K., et al., *Immunogenicity of combination DNA vaccines for Rift Valley fever virus, tick-borne encephalitis virus, Hantaan virus, and Crimean Congo hemorrhagic fever virus.* Vaccine, 2006. **24**(21): p. 4657-66.
98. Ghiasi, S.M., et al., *Mice orally immunized with a transgenic plant expressing the glycoprotein of Crimean-Congo hemorrhagic fever virus.* Clin Vaccine Immunol, 2011. **18**(12): p. 2031-7.

99. de Gruijl, T.D. and R. van de Ven, *Chapter six--Adenovirus-based immunotherapy of cancer: promises to keep.* Adv Cancer Res, 2012. **115**: p. 147-220.
100. Brave, A., et al., *Vaccine delivery methods using viral vectors.* Mol Pharm, 2007. **4**(1): p. 18-32.
101. Khare, R., et al., *Advances and future challenges in adenoviral vector pharmacology and targeting.* Curr Gene Ther, 2011. **11**(4): p. 241-58.
102. Nemerow, G.R., et al., *Insights into adenovirus host cell interactions from structural studies.* Virology, 2009. **384**(2): p. 380-8.
103. L. J. Reed and H. Muench, *A simple method of estimating fifty percent endpoints.* American Journal of Epidemiology, 1938. **27**(3): p. 4323-4329.
104. Robertson, S.J., et al., *Suppression of acute anti-friend virus CD8+ T-cell responses by coinfection with lactate dehydrogenase-elevating virus.* J Virol, 2008. **82**(1): p. 408-18.
105. Ergonul, O., et al., *Characteristics of patients with Crimean-Congo hemorrhagic fever in a recent outbreak in Turkey and impact of oral ribavirin therapy.* Clin Infect Dis, 2004. **39**(2): p. 284-7.
106. Drews, R.E., *Critical issues in hematology: anemia, thrombocytopenia, coagulopathy, and blood product transfusions in critically ill patients.* Clin Chest Med, 2003. **24**(4): p. 607-22.
107. Dugdale D.C. and D. Zieve. *Complete Blood Count*. A.D.A.M. Encyclopedia 2012 3/19/2012 [cited 2013; Available from: www.nlm.nih.gov/medlineplus/ency/article/003642.htm.
108. Richardson, J.S., et al., *Airway delivery of an adenovirus-based Ebola virus vaccine bypasses existing immunity to homologous adenovirus in nonhuman primates.* J Virol, 2013. **87**(7): p. 3668-77.
109. Richardson, J.S., et al., *Impact of systemic or mucosal immunity to adenovirus on Ad-based Ebola virus vaccine efficacy in guinea pigs.* J Infect Dis, 2011. **204 Suppl 3**: p. S1032-42.
110. Patel, A., et al., *Mucosal delivery of adenovirus-based vaccine protects against Ebola virus infection in mice.* J Infect Dis, 2007. **196 Suppl 2**: p. S413-20.
111. Croyle, M.A., et al., *Nasal delivery of an adenovirus-based vaccine bypasses pre-existing immunity to the vaccine carrier and improves the immune response in mice.* PLoS One, 2008. **3**(10): p. e3548.
112. Escadafal, C., et al., *First international external quality assessment of molecular detection of Crimean-Congo hemorrhagic fever virus.* PLoS Negl Trop Dis, 2012. **6**(6): p. e1706.
113. Haferkamp, S., et al., *Intracellular localization of Crimean-Congo Hemorrhagic Fever (CCHF) virus glycoproteins.* Virol J, 2005. **2**: p. 42.
114. Schnell, M.J., et al., *Foreign glycoproteins expressed from recombinant vesicular stomatitis viruses are incorporated efficiently into virus particles.* Proc Natl Acad Sci U S A, 1996. **93**(21): p. 11359-65.
115. Takada, A., et al., *Identification of protective epitopes on ebola virus glycoprotein at the single amino acid level by using recombinant vesicular stomatitis viruses.* J Virol, 2003. **77**(2): p. 1069-74.
116. Garbutt, M., et al., *Properties of replication-competent vesicular stomatitis virus vectors expressing glycoproteins of filoviruses and arenaviruses.* J Virol, 2004. **78**(10): p. 5458-65.
117. Brown, K.S., et al., *Vesicular stomatitis virus-based vaccine protects hamsters against lethal challenge with Andes virus.* J Virol, 2011. **85**(23): p. 12781-91.

118. Tsuda, Y., et al., *Protective efficacy of a bivalent recombinant vesicular stomatitis virus vaccine in the Syrian hamster model of lethal Ebola virus infection.* J Infect Dis, 2011. **204 Suppl 3**: p. S1090-7.
119. Frenz, T., et al., *Concomitant type I IFN receptor-triggering of T cells and of DC is required to promote maximal modified vaccinia virus Ankara-induced T-cell expansion.* Eur J Immunol, 2010. **40**(10): p. 2769-77.
120. Ergonul, O., *Treatment of Crimean-Congo hemorrhagic fever.* Antiviral Res, 2008. **78**(1): p. 125-31.
121. Elaldi, N., et al., *Efficacy of oral ribavirin treatment in Crimean-Congo haemorrhagic fever: a quasi-experimental study from Turkey.* J Infect, 2009. **58**(3): p. 238-44.
122. Leblebicioglu, H., et al., *Case management and supportive treatment for patients with Crimean-Congo hemorrhagic fever.* Vector Borne Zoonotic Dis, 2012. **12**(9): p. 805-11.
123. Ekiz, F., et al., *Mean platelet volume in the diagnosis and prognosis of crimean-congo hemorrhagic Fever.* Clin Appl Thromb Hemost, 2013. **19**(4): p. 441-4.
124. Andersson, I., et al., *Crimean-Congo hemorrhagic fever virus delays activation of the innate immune response.* J Med Virol, 2008. **80**(8): p. 1397-404.
125. Isaacs, A., J. Lindenmann, and R.C. Valentine, *Virus interference. II. Some properties of interferon.* Proc R Soc Lond B Biol Sci, 1957. **147**(927): p. 268-73.
126. Isaacs, A. and J. Lindenmann, *Virus interference. I. The interferon.* Proc R Soc Lond B Biol Sci, 1957. **147**(927): p. 258-67.
127. Biron, C.A., *Interferons alpha and beta as immune regulators--a new look.* Immunity, 2001. **14**(6): p. 661-4.
128. Doughty, L., et al., *A role for IFN-alpha beta in virus infection-induced sensitization to endotoxin.* J Immunol, 2001. **166**(4): p. 2658-64.
129. Medzhitov, R., *Recognition of microorganisms and activation of the immune response.* Nature, 2007. **449**(7164): p. 819-26.
130. Akira, S., S. Uematsu, and O. Takeuchi, *Pathogen recognition and innate immunity.* Cell, 2006. **124**(4): p. 783-801.
131. Le Bon, A., et al., *Direct stimulation of T cells by type I IFN enhances the CD8+ T cell response during cross-priming.* J Immunol, 2006. **176**(8): p. 4682-9.
132. Le Bon, A., et al., *Cutting edge: enhancement of antibody responses through direct stimulation of B and T cells by type I IFN.* J Immunol, 2006. **176**(4): p. 2074-8.
133. Valmas, C. and C.F. Basler, *Marburg virus VP40 antagonizes interferon signaling in a species-specific manner.* J Virol, 2011. **85**(9): p. 4309-17.
134. Thakar, J., et al., *Overcoming NS1-Mediated Immune Antagonism Involves Both Interferon-Dependent and Independent Mechanisms.* J Interferon Cytokine Res, 2013.
135. Shi, X., et al., *The Zinc-Finger Domain Was Essential for Porcine Reproductive and Respiratory Syndrome Virus Nonstructural Protein-1alpha to Inhibit the Production of Interferon-beta.* J Interferon Cytokine Res, 2013. **33**(6): p. 328-34.
136. Zivcec, M., et al., *Lethal Crimean-Congo Hemorrhagic Fever Virus Infection in Interferon alpha/beta Receptor Knockout Mice Is Associated With High Viral Loads, Proinflammatory Responses, and Coagulopathy.* J Infect Dis, 2013.
137. Thompson, L.J., et al., *Innate inflammatory signals induced by various pathogens differentially dictate the IFN-I dependence of CD8 T cells for clonal expansion and memory formation.* J Immunol, 2006. **177**(3): p. 1746-54.
138. Walters, K.A., et al., *Host-specific response to HCV infection in the chimeric SCID-beige/Alb-uPA mouse model: role of the innate antiviral immune response.* PLoS Pathog, 2006. **2**(6): p. e59.

139. Curtsinger, J.M., et al., *Type I IFNs provide a third signal to CD8 T cells to stimulate clonal expansion and differentiation.* J Immunol, 2005. **174**(8): p. 4465-9.
140. Boshra, H., et al., *A DNA vaccine encoding ubiquitinated Rift Valley fever virus nucleoprotein provides consistent immunity and protects IFNAR(-/-) mice upon lethal virus challenge.* Vaccine, 2011. **29**(27): p. 4469-75.
141. Calvo-Pinilla, E., et al., *Multiserotype protection elicited by a combinatorial prime-boost vaccination strategy against bluetongue virus.* PLoS One, 2012. **7**(4): p. e34735.
142. Mardani, M. and M. Keshtkar-Jahromi, *Crimean-Congo hemorrhagic fever.* Arch Iran Med, 2007. **10**(2): p. 204-14.
143. Safronetz, D., et al., *Adenovirus vectors expressing hantavirus proteins protect hamsters against lethal challenge with andes virus.* J Virol, 2009. **83**(14): p. 7285-95.
144. Chinikar, S., et al., *Crimean-Congo hemorrhagic fever in Iran and neighboring countries.* J Clin Virol, 2010. **47**(2): p. 110-4.
145. Feldmann, H. and T.W. Geisbert, *Ebola haemorrhagic fever.* Lancet, 2011. **377**(9768): p. 849-62.